Deborah Susan Schenberger
June 2006
Biological Systems Engineering

Design of MEMS Sensor System to Measure Spinal Fusion

Abstract

Being able to determine the formation of a solid, spinal fusion after lumbar surgery continues to be one of the most difficult issues facing spinal surgeons today. Patients are fitted with a spinal brace for three to twelve months after surgery, even though the spinal implant provides internal fixation. Such a brace is not only inconvenient, as it completely immobilizes the patient, but not in the patient's long term interest. Studies have shown that immobility leads to muscle atrophy in the spine; therefore, the best option is to minimize the amount of time for bracing. Currently, surgeons rely on radiographs to view the fusion mass. Fusions are inherently difficult to view, as the spine's transverse processes and the spinal hardware lie within the fusion region. Thus, surgeons use their best judgment and their professional experience to decide when a fusion is solid and the patient may remove their brace. According to one study, fusion actually occurs between eight and twelve weeks in sheep, as much as eight weeks before it was indicated in their radiographs. Radiographs are delayed because they can only determine fusion when the trabecular bone of the fusion has mineralized, which occurs after the fusion

agglomeration has reached full size and stabilization and can bear mechanical load.

Immobilization causes another cost to the patient and society. While wearing the brace, the patient cannot return to work, drive, or perform everyday activities that constitute a good quality of life. Long term disability insurance costs are thus dramatically increases, making spinal fusion surgery the most costly orthopaedic procedure. With over 300,000 predicted spinal surgeries in 2005 in a market calculated at $2.4 to $3.1 billion dollars, and at an average cost of $34,000 per surgery, plus $20,000 for professional surgeon fees, and because worker disability payments are averaging 1% of the gross domestic product, major steps need to be taken to reduce overall costs where possible. Serious progress toward the goal of controlling costs could be made by reducing the cost of disability, mainly by allowing patients to return to work sooner.

Because of the importance of allowing early patient mobility to avoid muscle atrophy, and because of the equal importance of reducing costs of spinal fusion, the goal of this research is to develop a more accurate and earlier means of detecting spinal fusion. This study has developed a better diagnostic tool for surgeons based on strain to address the problems associated with the current method of bracing and radiographs. As it is known from the literature that the amount of time for fusion is significantly less than it is indicated by radiographs, and patient outcomes would be

improved if a superior diagnostic method were developed, this study has designed and submitted a patent application to measure strain in vivo using a capacitive sensor and a transponder to send the signal via radio frequency to an external receiver. A handheld unit would be brought into proximity of the sensor and an initial strain level would be recorded. Then, during routine office visits, the handheld sensor would again be brought into proximity of the sensor to get additional strain level recordings. Over time, the level of strain should decrease and eventually plateau at a lower level. The hypothesis was that this would occur within eight to twelve weeks following surgery, at which time the fusion could be proclaimed solid and the patient's external bracing removed.

The report outlines the evolution of a design to measure the onset of spinal fusion using a battery-free, interdigitated capacitive strain sensor that will use supplied radio frequency power from an external, handheld receiver to activate the sensor. The output data will be subsequently analyzed on a computer.

Design of MEMS Sensor System to Measure Spinal Fusion

By

DEBORAH SUSAN SCHENBERGER
B.S. (University of the Pacific, Stockton, CA) 1989
M.S. (Stanford University, Palo Alto, CA) 1995

DISSERTATION

Submitted in partial satisfaction of the requirements for the degree of

DOCTOR OF ENGINEERING

in

Biological Systems Engineering

in the

OFFICE OF GRADUATE STUDIES

of the

UNIVERSITY OF CALIFORNIA

DAVIS

Approved:

_____
Fadi Fathallah, Committee Chair

_____
Munish Gupta, Committee Member

_____
Norman Tien, Committee Member

Committee in Charge

2006

TABLE OF CONTENTS

ABSTRACT

Being able to determine the formation of a solid, spinal fusion after lumbar surgery continues to be one of the most difficult issues facing spinal surgeons today. Patients are fitted with a spinal brace for three to twelve months after surgery, even though the spinal implant provides internal fixation. Such a brace is not only inconvenient, as it completely immobilizes the patient, but not in the patient's long term interest. Studies have shown that immobility leads to muscle atrophy in the spine; therefore, the best option is to minimize the amount of time for bracing. Currently, surgeons rely on radiographs to view the fusion mass. Fusions are inherently difficult to view, as the spine's transverse processes and the spinal hardware lie within the fusion region. Thus, surgeons use their best judgment and their professional experience to decide when a fusion is solid and the patient may remove their brace. According to one study, fusion actually occurs between eight and twelve weeks in sheep, as much as eight weeks before it was indicated in their radiographs. Radiographs are delayed because they can only determine fusion when the trabecular bone of the fusion has mineralized, which occurs after the fusion agglomeration has reached full size and stabilization and can bear mechanical load.

Immobilization causes another cost to the patient and society. While wearing the brace, the patient cannot return to work, drive, or perform

everyday activities that constitute a good quality of life. Long term disability insurance costs are thus dramatically increased, making spinal fusion surgery the most costly orthopaedic procedure. With over 300,000 predicted spinal surgeries in 2005 in a market calculated at $2.4 to $3.1 billion dollars, and at an average cost of $34,000 per surgery, plus $20,000 for professional surgeon fees, and because worker disability payments are averaging 1% of the gross domestic product, major steps need to be taken to reduce overall costs where possible. Serious progress toward the goal of controlling costs could be made by reducing the cost of disability, mainly by allowing patients to return to work sooner.

Because of the importance of allowing early patient mobility to avoid muscle atrophy, and because of the equal importance of reducing costs of spinal fusion, the goal of this research is to develop a more accurate and earlier means of detecting spinal fusion. This study has developed a better diagnostic tool for surgeons based on strain to address the problems associated with the current method of bracing and radiographs. As it is known from the literature that the amount of time for fusion is significantly less than it is indicated by radiographs, and patient outcomes would be improved if a superior diagnostic method were developed, this study has designed and submitted a patent application to measure strain in vivo using a capacitive sensor and a transponder to send the signal via radio frequency to an external receiver. A handheld unit would be brought into

proximity of the sensor and an initial strain level would be recorded. Then, during routine office visits, the handheld sensor would again be brought into proximity of the sensor to get additional strain level recordings. Over time, the level of strain should decrease and eventually plateau at a lower level. The hypothesis was that this would occur within eight to twelve weeks following surgery, at which time the fusion could be proclaimed solid and the patient's external bracing removed.

The report outlines the evolution of a design to measure the onset of spinal fusion using a battery-free, interdigitated capacitive strain sensor, that will use supplied radio frequency power from an external, handheld receiver to activate the sensor. The output data will be subsequently analyzed on a computer.

ACKNOWLEDGEMENTS

I would like to thank all the faculty that helped me to research and analyze this design, including Dr. Fadi Fathallah for serving as my major professor, Dr. Munish Gupta for providing the idea for this research project and performing all the sheep surgeries, Dr. Norman Tien for teaching me microfabrication and serving as the third committee member on my dissertation, Dr. David Horsley for helping me with electric circuit design and microfabrication, and Dr. Michael Delwiche for teaching me bioinstrumentation and helping me focus my research topic.

I would also like to thank DePuy Acromed Spine, a Johnson & Johnson company, for their generous financial support and continued supply of spinal instrumentation for my various research activities. I would especially like to thank Eric Hamilton, our local DePuy Spine sales representative for his prompt and courteous support, and Dr. Hassan Serhan for supporting this research, allowing two time extensions, and considering further funding.

CHAPTER 1

Introduction and Literature Review

I. INTRODUCTION

Being able to determine the formation of a solid, spinal fusion after lumbar surgery continues to be one of the most difficult issues facing spinal surgeons today. Patients are fitted with a spinal brace for three to twelve months after surgery, even though the spinal implant provides internal fixation. Such a brace is not only inconvenient, as it completely immobilizes the patient, but not in the patient's long term interest. Several studies have shown that immobility leads to muscle atrophy in other areas of the skeleton, such as the medial collateral ligament, resulting in inferior strength after healing. Disuse atrophy occurs in the spine as well; therefore, the best option is to minimize the amount of time for bracing [1]. Currently, surgeons rely on radiographs, otherwise known as x-rays, to view the fusion mass. Fusions are inherently difficult to view, as the spine's transverse processes and the spinal hardware lie within the fusion region. Thus, surgeons use their best judgment and their professional experience to decide when a fusion is solid and the patient may safely remove their brace. Radiographs are also delayed relative to the state of the fusion mass, because they can only indicate fusion when the trabecular bone of

the fusion has mineralized, which occurs after the fusion agglomeration has reached full size and stabilization and can bear mechanical load. According to one landmark study, fusion actually occurs between eight and twelve weeks in sheep, as much as eight weeks before it was indicated in their radiographs [2].

Immobilization causes another cost to the patient and our society. While wearing the brace, the patient cannot return to work, drive, or perform everyday activities that constitute a good quality of life. Our long term disability insurance costs are thus dramatically increased, making spinal fusion surgery the most costly orthopaedic procedure. With over 300,000 predicted spinal surgeries in 2005 in a market calculated at $2.4 to $3.1 billion dollars, and at an average cost of $34,000 per surgery, plus $20,000 for professional surgeon fees, and because worker disability payments are averaging 1% of our gross domestic product, major steps need to be taken to reduce overall costs where possible [3-7]. All of this cost ends up affecting society through higher and higher medical and disability insurance premiums. Although the cost of surgery cannot be regulated in this economy, serious progress in controlling costs is possible by reducing the cost of disability, mainly by allowing patients to return to work sooner. Because of the importance of allowing patient mobility as early as possible after surgery to avoid permanent muscle atrophy, and because of the equal importance of reducing societal costs of spinal fusion

disability, the goal of this research is to develop a more accurate and earlier means of detecting spinal fusion.

II. LITERATURE REVIEW

A. Lumbar Spine Anatomy and Function

The human spine is comprised of seven cervical vertebrae, twelve thoracic vertebrae, five lumbar vertebrae, and a fused sacrum and coccyx [8]. Each vertebra is separated by an intervertebral disc made of a fibrous outer ring, called the annulus fibrosus and a gelatinous core, called the nucleus pulposus. The lumbar region of the spine is designed to support the body's weight during upright posture, thus the vertebral bodies are large and squat with thick cortical endplates. All of the vertebrae also articulate with each other through the articular facets on small pads of articular cartilage. As shown in Figure 1, the spine allows the human upper torso to move through a complex series of motions. A sideways bend is called lateral motion. Forward motion is called flexion, and backwards motion from an upright posture is called extension. A twist or rotation is called torsion and constitutes motion around the long axis of the spine. Lumbar fusion is one of the fastest growing areas of orthopaedic surgery. Although many devices have been designed to minimize the incidence of work-related back injury, as a society we still participate in many activities that lead to back injury. Most frequently, inappropriate lifting of objects,

pulling or lifting objects from awkward angles, and fatigue lead to injury of the lower back region [9-12]. If the level of injury is severe enough, the muscles and ligaments of the lumbar spine cannot withstand the load applied, and the intervertebral disc will become herniated from the anterior side of the spine. This is often called a herniated or ruptured disc. In addition, the vertebrae of the spine articulate with each other through the transverse and spinous processes located on the posterior aspect of the vertebrae. In between the processes, there are small pads of cartilage on the articular facets of the vertebrae that can become damaged with a back injury [13-15].

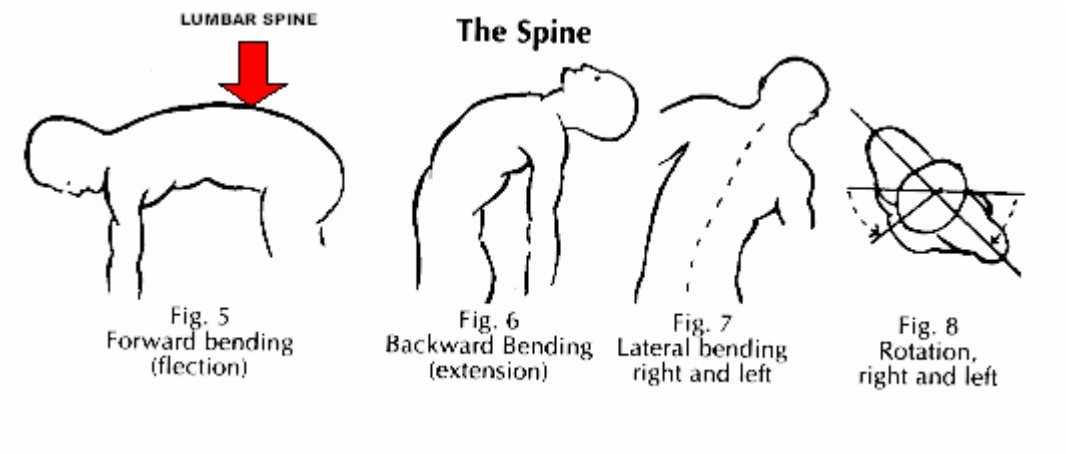

Figure 1, Back Motions

http://www.dwd.state.wi.us/dwd/publications/wc/images/f5-8.gif

The vast majority of spinal fusion surgeries, however, are performed for idiopathic pain in the lower back with no clear explanation as to the cause of that pain [16]. Many theories have been developed over the

years, such as facet pain on the vertebrae or muscle laxity, but these theories account for less than a quarter of all cases of pain [17]. As it is extremely important to determine the cause of pain in order to have a higher success rate in spinal fusion surgery, there have been numerous studies that have worked to determine the cause [2, 9-12, 18-24].

Regardless of cause, to eliminate the pain, a lumbar fusion is performed. An incision is made over the lumbar region of the spine and metal bracing is applied bilaterally to the posterior of the verterbrae in what is called a posterolateral fusion. Other methods are possible, such as anterior and lateral approaches, but posterolateral is the most common procedure. The metal bracing provides initial mechanical stiffness until bone growth, stimulated by a bone growth factor, encapsulates the metal bracing and eliminates motion between the two lumbar vertebrae. Surgeons have many choices for the metal bracing, called spinal implants or spinal instrumentation, which can be used to create the initial fixation. In general, a pedicle screw is screwed from the posterior of the vertebrae through the pedicle bony bridge and into the wall the vertebral body (Figure 2). This procedure is repeated for the neighboring vertebrae and bilaterally on the opposite side of the posterior spine. Once all four pedicle screws are in place, a rod or plate is placed over the posts on two of the pedicle screws. The rod or plate is then held down with locking nuts that screw onto the posts (Figure 2). A slurry of bone and bone graft is applied

over the spinal implant and transverse processes of the vertebrae, and the incision is closed.

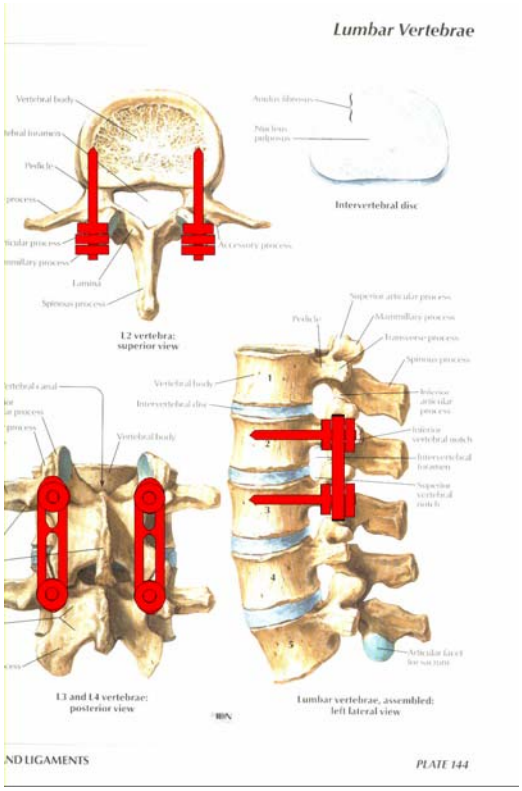

Figure 2, Lumbar Spine with Implant Hardware [25]

After lumbar fusion surgery, rehabilitation takes several months. The patient is immobilized with a brace that extends from beneath the arms to midline of the hips and is instructed not to perform any strenuous physical activity. No lifting, driving, running or bending at the waist is allowed. Any kind of activity that involves impact is also prohibited, such as jumping or roller coasters. The patient must wear the brace until fusion is visible on an x-ray radiograph. Depending on the age of the patient and their particular health, this can be anywhere from four months to a year after surgery [2,

26, 27]. Because of this extended period of immobility, the muscles of the spine and abdomen atrophy from disuse. The brace also contributes to stress shielding, meaning the brace is carrying some of the spinal load, resulting in an inferior strength lumbar fusion [28, 29].

As discussed earlier, however, fusion occurs much sooner than is predicted by radiographs [2, 30, 31]. No studies have been performed in humans, but it appears that a solid fusion could occur as early as eight weeks (two months) after surgery. The bone that initially grows around the spinal instrumentation is trabecular bone, and although it is strong and dense, it is not radiographically opaque. Thus, it cannot be seen on an x-ray until it infuses itself with minerals from the bone slurry, such as calcium and apatite. If researchers could develop a new method to detect a solid fusion without the need for radiographic verification, the amount of time patients would need to be in a brace could be cut by 50% or more.

The biological process of fusion itself is as yet poorly understood in large vertebrate animals and humans. Boden performed numerous spinal fusion studies in rabbit models, which appear to follow a long-bone fracture healing model [32], the same model used in humans to heal arm or leg fractures. In a long bone, when the fracture line is clean and relatively immobilized, the disruption of the marrow causes a hematoma to initially fuse the endosteal surfaces together. The marrow also instigates a chain of events that causes existing mesenchymal cells to differentiate into

osteoblasts and create a periosteal callus. Over time, this periosteal callus is converted from a woven trabecular bone into lamellar bone through remodeling and mineralization. The size of the callus decreases as the bone is mineralized and is eventually resorbed by the body, leaving almost no trace. This process is called endochondral ossification [33]. If the fracture line is not clean or if a large gap exists along the fracture line, a cartilaginous pseudoarthrosis may occur. When the marrow is initially disrupted, the mesenchymal cells differentiate into chondroblasts and thus form cartilage rather than trabecular bone. Cartilage can also be converted into lamellar bone through a process called intramembranous bone formation, similar to the process used in a developing child's body for creating flat bones, such as the skull [33]. In his paper using a sheep model to study spinal fusion, Foster states that intramembranous bone formation, contrary to what had previously been believed, is the process used by the sheep to form a bony spinal fusion, because the gap between vertebrae is too large to bridge even with the applied bone growth factor to achieve endochondral ossification. He discovered that large vertebrate animals must use a cartilaginous pseudoarthrosis, relying on the intervening cartilaginous phase of healing. This finding is interesting because unlike the long bone fracture healing model often used to study bony fusion, in spinal fusion, the site preferably forms cartilage rather than trabecular bone. It appears that the amount of cartilage formed controls the

amount of cortical bone that is finally formed. Resorption does not occur after spinal fusion, for reasons that Foster did not discuss in his paper [34]. The final fusion mass appears to not be remodeled over time, probably because the body never initiates the fracture healing process.

Radiographs are the most widely used means of determining fusion, and even though they cannot reveal early fusion, they are still the best tool available to surgeons because of their low cost and ready accessibility [2]. Other effective alternatives, such as computed tomography (CT) scans are used in rare cases when a fusion cannot be viewed with plane radiographs.

B. Methods in Use for Studying Bone Properties

To address the need to detect spinal fusion more rapidly, this study discusses the design of an electronic solution for detecting spinal fusion. The hypothesis was that the spinal instrumentation would not be rigid when initially implanted. There would be minor gaps between the pedicle screws and spinal plate that would allow for some movement. The screws would also move slightly until bone grew into the threads to hold them rigidly fixed. However, the anterior sides of the vertebrae are never rigid. Because the two vertebrae are separated by the cushioning intervertebral disc, the hypothesis was that there would always be some movement from this source. This design study shows that the spinal plate anchored by the two pedicle screws acts like a beam with a moment applied at both ends.

The moment induces bending in the spinal plate that can be measured as a strain.

Numerous studies show that strain is a reliable measure of motion in biomechanical experiments of bone, but most studies have been short-lived due to moisture problems [30, 35-45]. Bessman developed a numerical method to compare *in vivo* and *in vitro* rosette strain gages to see if transverse strains were negligible. For bending moments along the length of long bone, he found that the transverse strains were essentially zero and could be ignored [36]. Butterman used bone staples penetrating the tibia from the exterior to measure strain in facet joints of the spine. Using this method, he was able to extend the life of his studies from a few days to several weeks by avoiding moisture problems [37]. This concept was of particular interest to this research, as the researcher hypothesized that the spinal hardware would be load sharing with the bone and that strain in the hardware could thus be used to measure the strain in the surrounding bone. Other researchers have tried using extensometers to circumvent the problems associated with *in vivo* conditions, but extensometers must be precisely aligned in order to function properly and thus are not commonly used for *in vivo* studies of the spine [39, 41, 46]. This design study extended the use of strain gages from measurement of a change in strain to use of strain as a diagnostic tool. The prediction was that the strain in the spinal plate would initially be large, but it would

decrease over time as the bone in-growth provided additional fixation. After some period of time, the strain would minimize at a lower value and remain relatively constant. By periodically sampling the strain electronically, a curve might be generated, showing the onset of rigid fixation and thus a solid bony fusion. A similar system was developed by Szivek for scoliosis instrumentation, although he bonded coated strain gages to the bone itself. Because scoliosis involves the entire thoracic region of the spine, Szivek found torsion to be his most reliable measurement of strain in a telemetered signal [31]. Although the devices remained implanted for up to 15 months, Szivek noted that moisture began to affect his signal integrity after only eight weeks.

In some previous studies on fusion, strain gages have been mounted to the bone, complicating these studies by introducing moisture both surrounding and beneath the strain gages [30, 43]. Extensive research has gone into coating strain gages to extend their useful life, using hydroxyapatite, calcium phosphate ceramic, and polymethylmethacrylate (PMMA) [30, 31, 41, 44, 45, 47]. Szivek simulated fusion with polymethylmethacrylate in three cadaver spines. The spines were fully instrumented with strain gages mounted on the posterior lamina of the vertebrae, then tested in flexion, extension, and torsion. In addition, the study used a subminiature radio transmitter to compare wireless transmission with their direct hard-wired system [31]. The results were

mixed due to the lack of constraints on the spines' movements, but the radio transmitter results correlated well with those from the hard-wired direct system.

C. Methods for Measuring "Strain" Properties

Although strain has been the transducer of choice for most studies on bone, because of the uniquely accessible and shallow location of the lumbar spine, this design study had other potential methods for measuring properties in the spinal hardware. Loosely, this study refers to all methods considered as "strain" measurement for convenience, even though the exact mechanism employed for the measurement may be vastly different. These options included harmonic strings or ribbons with ultrasonic excitation, change of frequency in the implant itself, optical fringe patterns with a photolithographic layer on the implant, tensioned wire, capacitance changes, and permanent radiographically opaque markers used with computer analysis. For all of these options, a microelectronic measurement system (MEMS) device can be used to microfabricate the sensor at a minute size.

Harmonics of a string or ribbon, such as one fabricated to be a sensor using MEMS technology, could be excited ultrasonically. Initially, the resonant frequency could be low, but as the system became stiffer, the string would become tighter or looser and change the frequency. This sensing method would have inherent difficulties with mounting, because

the behavior of the string would be highly sensitive to its perception of the loading changes in the implant. Alternatively, the entire spinal plate could be resonated and measured for its “ring down” frequency. This would also be difficult because the spinal plate is extremely stiff and any additional stiffness added from the fusion would be difficult to measure. However, combining these two ideas, the spinal plate could be made with an integral, encapsulated “string” that would vibrate at a known frequency. Shifts in this frequency with changes in stiffness could be modeled in the laboratory to characterize the effects of a spinal fusion. Figure 3 below is one example of the frequencies found in a generic aluminum rod. Interestingly, other aluminum rods of the same dimensions have the same resonance pattern within 5% [48], illustrating that a string would have a repeatable measurement of high reliability.

A very similar means of measuring a change in strain would be with a tensioned wire. Acting in the same manner as a strain gage, the resistance of the wire would change with a change in load or strain. Some type of temperature compensation scheme might be necessary if the range of human body temperatures were too large for proper operation. Using either a tensioned or harmonic wire would greatly simplify the manufacture and installation, making it more feasible than creating a MEMS harmonic string within the implant. This researcher envisions drilling a small hole through an encapsulated pocket, inserting the wire across the pocket, and

soldering both ends to secure the wire within the pocket. The wire could be ultrasonically excited and the instrumentation could then listen to the “ring down” of the signal or periodically sample for a change in resistance.

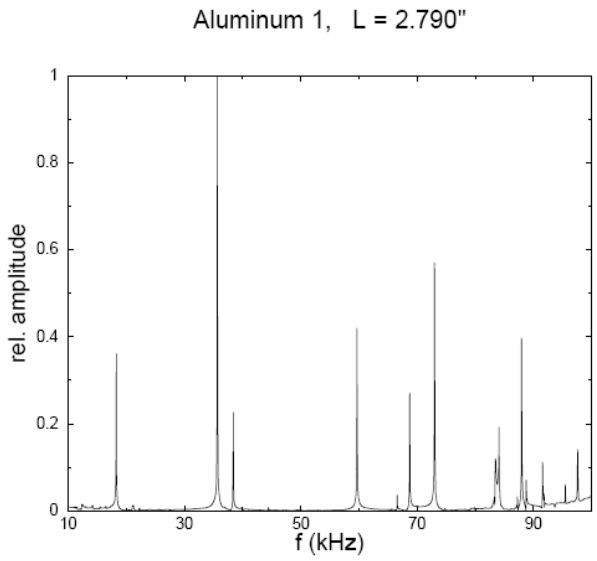

Figure 3, Example Frequency Response in Aluminum

Image from Zadler’s Dissertation [48]

Optical fringe patterns are also a possible means of measuring strain in our spinal plate. By coating the spinal plate with a photolithographic material (or attaching a silicon chip with a grate pattern), a red wavelength of light passed through the tissue of the body would produce an interference pattern on the spinal plate. As the strain in the spinal plate changed, the spacing of the interference fringe pattern would also change, giving a highly accurate measure of the strain [49]. Alternatively, an image

of the entire spinal plate could be recreated holographically in three dimensions to compare the shape before and after spinal fusion, but the preload may be too high for any changes from spinal fusion to be observed.

Another optical method would be to add radiographically opaque markers to the spine itself, such as small stainless steel balls. The patient could then be asked to perform a series of set motions, and radiographs could be taken. By knowing the diameter of the balls, computer software could determine the relative motion occurring between the balls. By performing multiple clinical trials, the amount of motion after complete bony fusion could be characterized.

Also, a photoelectric strain gage could be made using wavelengths of light that penetrate tissue and are safe for humans. In this case, the light itself would provide the power for the strain gage operation through a translucent window in or on the spinal implant. According to Greenmed of Japan, red wavelengths of 780nm, 830nm, and particularly 904nm are safe, invisible wavelengths that penetrate tissue and are approved for use in the United States. These infrared lengths would eventually heat tissue, so long-period exposure would need to be avoided in a sensor application [50].

Finally, rather than using resistance as a measured value, capacitance could be used for measuring strain. Capacitive sensors are

commonly used to measure rotational and translational motions and sounds, and according to Doebelin, capacitive sensors give very high resolution output even at extremely low current or voltage levels. The actual design of the capacitor could be done in either one of two ways, either by varying the spacing between the capacitive plates or by varying the overlapped area of the two plates. Overlapped area variation capacitive sensors have two advantages over space varying capactive sensors. First, the relationship between current and area of overlap is linear, and second, the signal strength of the output can be increased by employing the well-know interdigitated capacitor design that uses multiple fingers to increase the area [51-53]. In a bridge configuration, one system can measure strain with a sensing resolution of 0.09 με over a 10 kHz bandwidth and consumes only 1.5 mA from a 3 V supply when active [54]. Alternatively, a unique approach from the University of Wisconsin, Madison, outlines a method for making a single-plate capacitive sensor based on changes in the electrical properties of the dielectric material itself. This property, called electrostiction, is an easily measured property for strain, and has the advantage of being cheaply applied to an electrode-covered surface with no alignment issues [55]. The surface of the spinal plate could be sputter-coated with an electrode material and then with a dielectric film. With a time-varying applied voltage, the capacitance would change depending on the strain in the dielectric material.

Compared to capacitive strain gages, resistive strain gages dissipate a fair amount of power due to the resistance (Power=I^2*R). Also, resistive strain gages are temperature dependent, and a temperature dependent sensor could possibly lead to a less reliable measurement. The main advantages of capacitance, therefore, are the absence of temperature dependence and the minimized power consumption [53]. Because capacitive sensors can also be more sensitive than resistive sensors [56], one could expect a design based on a change in capacitance due to a change in strain to result in a more accurate measurement.

D. Sheep as a Model for Human Lumbar Spine

As discussed by F. McLain and H.J. Wilke, sheep are representative models for the human lumbar spine because the vertebral bodies are of similar size, sheep being larger, and the range of motion for all directions is biomechanically the same [57, 58]. McLain compared the use of several large vertebrate animals, including mature canines, immature pigs, mature micropigs, mature dairy goats, and mature sheep. Of these, canines did not have defined pedicles, and immature pigs and dairy goats had very small pedicles. All animal models have steeper angles for their pedicles than humans, and sheep and goats both have longer vertebral bodies. Overall, McLain found sheep to be a good model for gross lumbar fusion and implant studies. For this study, pigs and calves were excluded because they would continue to grow rapidly throughout the study.

Usually, pigs and calves are only used for short term studies, in vitro tests, or intervertebral disc tests as these discs are larger in diameter than sheep vertebrae [59-62]. Also, calves have a significantly larger transverse process spacing than humans, which would affect the biological process of fusion [59]. Small animals, particularly rabbits, have been used as models of spinal fusion [32, 39, 63-65]; however, Foster's recent study clearly demonstrates that because of the smaller spacing of the transverse processes, the biologic process of fusion occurs differently [34]. Goats can be used, but their tendency to head butt may adversely affect the process of spinal fusion. Although one study did evaluate the use of deer as a model for the human spine, sheep are docile, domesticated animals and are readily obtainable for studies and thus were selected as the animal model for this research.

E. Loading Changes in Spine After Spinal Fusion

Several studies have recently been performed to determine *in vivo* spinal loads [66, 67]. Although *in vivo* interbody spinal loading is a different objective than this study, the implantation and telemetry techniques are similar. Rohlmann and Wilke found that for *in vivo* and in vitro loading of an internal spinal fixator, a telemeterized spinal fixator can be implanted in lieu of an ordinary spinal fixator allowing signals to be transmitted to the surface of the skin. After implantation, they found that muscular loading, often ignored in cadaver studies, caused high loading on the fixators. They

therefore concluded that pedicle screw breakage or other types of failure more than half a year after surgery did not necessarily imply that fusion had not occurred. From these studies and others, it is apparent that the loading in the lumbar spine changes after spinal fusion surgery [14, 66, 68-76]. Some of these changes are due to distraction forces used during surgery and muscle damage during surgery [73, 75, 77, 78], but other changes appear to be caused by the stiffness of the fusion itself and how that affects the endplates of the adjacent vertebrae [72, 74, 79, 80]. In spite of the large volume of research done in this area, only a few studies have been done in instrumented large vertebrate animal models and none of them were used to study posterolateral fusion [30, 31, 37, 66, 67, 81]. This study recognized a need to study the time-dependent process of spinal fusion more carefully as part of its research objectives.

F. Muscle Injury and Repair After Spinal Fusion

Because muscle is considered a self-healing tissue, no accommodations are made for the optimal recovery of skeletal muscle of the spine or how its recovery will influence the eventual functional outcome for the patient. However, one of the objectives of this research is to safely decrease the amount of time spent in bracing and thus the costs of long term disability, so an understanding of muscle is important. Structural and functional recovery of skeletal muscle is possible, but is dependent on multiple factors, including extent of the induced injuries from laceration,

disruption of the vascular supply, muscle stretching, duration of the surgery, techniques used for suturing, duration of immobilization, and rehabilitation employed. Many of these fundamental principles for optimal muscle recovery are not considered by today's orthopaedic surgeons.

In general, muscle injury will trigger a consistent repair process, beginning with the release of endogenous protease enzymes from the ribosomes within the multinucleated muscle cells. In addition, macrophages from white blood cells circulating in the blood supply will be released. In a spine surgical procedure, the vascular supply will be affected, but the major vessels are usually undamaged, so mainly the macrophages from the bloodstream will be present to help repair the muscle injury. Macrophages invoke satellite cells, and laceration of many muscle cell membranes also invokes satellite cells to respond. The satellite cells create myoblasts that become myotubes that then become randomly oriented contractile proteins. Over time, the proteins at the site of the laceration and retraction become realigned and reinnervated [82]. Thus, within several weeks, the muscle is again structurally intact, but may not have achieved full functional recovery.

Functional recovery after muscle laceration is possible, but the muscle does not regain its full strength or range of motion quickly. In rabbit studies with completely and partially lacerated muscles, even after 12 weeks, ability to produce tension was only 50% and 60% of normal,

respectively. The muscle's ability to shorten was normal in the partially lacerated muscle and 80% of normal in the completely lacerated muscle, but both muscles showed distal fiber atrophy, increased fibrosis, and fiber arrangement suggestive of denervation [83]. The healing process appears to be highly dependent on the ability of the muscle to have "ingrowth of vascularity and regeneration of the intramuscular nerve branches" [84]. Healing is therefore dependent on the extent of the trauma. However, in a surgical injury, vascular and nerve trauma is minimal, so function recovery will be better than what is predicted by these rabbit studies.

Experiments with electromyography, magnetic resonance imaging, and histology in lacerated rat gastrocnemus muscles have also been employed to help understand the process of muscle repair. Electrical conductivity is fully restored in lacerated muscles within eight weeks of surgery, so the necessary signaling is obviously present. Histological examination of these same fibers shows a continuous, gradual regeneration of muscle fibers that is also fully restored after the eight weeks. Tension, however, lags behind with only 60% restored after six weeks. After six months, this tension level remained constant at 60% of control [85]. This is an unusual finding that requires further investigation and corroboration. Magnetic resonance imaging techniques in rats enhance understanding of surgically-induced injury by studying the effect of retraction duration. During orthopaedic surgery, the muscles are retracted to either side and held in a

stretched configuration for significant amounts of time, usually more than two hours. In a rat study by Gejo, sham, one hour, and two hour retraction groups were compared 21 days after surgery. Magnetic resonance imaging revealed that the 2-hour retraction group still had small diameter muscle fibers and large extracellular fluid spaces even 21 days after surgery, indicative of continued muscle regeneration [86]. This would have been more informative if extended to the more common eight week time frame.

In addition to the functional recovery of muscle are loading and mobilization that enhance the muscle repair process. In the last century, it has become clear that controlled, early resumption of activity of an injured extremity muscle will promote healing, and prolonged bed rest will not only delay recovery, but adversely affect the muscle tissues. It appears that immature muscle tissue is more sensitive to cyclic loading than normal tissue, and thus responds well to early, resumed activity. On the other hand, if the loading or motion is prematurely excessive, the immature repair tissue can be damaged and the repair process will be inhibited or stopped [87]. Thus, it is with extreme caution that a spine surgery patient should be rehabilitated. Upon further study, it may well prove to be true that some period of bracing, perhaps longer than what is needed for bony fusion, may be needed to help the spinal muscles heal. Early mobilization coupled with prolonged, low-level stress helps prevent muscular adhesions

in the hands. Adhesions to neighboring tendons can prevent the patient from regaining full range of motion of their hands [88]. Extrapolating to spine, scar tissue and fibrous adhesions of the bony facets may be minimized by early mobilization. A recent study by Menetry, et al., developed a laceration model in mice gastrocnemus muscles. Tetanus strength was 81% of normal in sutured muscles with free movement after surgery, 35% of normal in lacerated but unrepaired muscles with free movement, and yet only 18% for immobilized unrepaired muscles, showing the importance of mobility and suturing in the repair process [89]. Again, this study would have been better if they had included an immobilized, sutured group for comparison. This would have more closely mimicked surgical conditions. Immobilization during repair also alters the regenerating muscle's repair by stimulating an atrophic process. Myogenesis is dependent on the apparent needs of the muscle, which are minimal for immobilization, thus decreasing the number and influencing the type of cells that are created by the repair process [90].

Surgical techniques, such as stretching and suturing, will also influence the muscle's repair. Suturing is always one of the orthopaedic surgical techniques employed, and it is an effective method to enhance muscle repair and minimize fibrous scar tissue [89]. An early study by Phillips suggests that the type of suturing performed may be dependent upon the depth and location of the laceration. Although suturing through

the full thickness of the laceration and the dermal layer of the skin will obtain full closure, it provides no structural support to the underlying muscle. Thus, a layered suturing technique, beginning with the deepest muscles, is important rather than attempting a full-thickness suture [91]. The method of suturing used also affects the long term recovery of lacerated muscle. In a study on rabbit tibialis anterior muscles with a 12 week healing period, researchers divided the rabbits into three groups, cast immobilized for one week, cast immobilized for four weeks, and freely mobile, with three different suturing techniques, simple suture, modified Kessler, and simple suture with tendon graft. Muscles were then compared for physiologic muscle tension, contractile length and histologic staining pattern. Tension force regained was purely a function of immobilization time and not suture technique; however, contractile shortening length of the muscle was dependent only on suture technique and was not affected by immobilization time. From their data, the researchers concluded that the best overall result was obtained when a modified Kessler suturing technique was used without any immobilization time [92]. Although the suturing technique evokes no controversy, using no immobilization time directly contradicts the current method for spine surgery rehabilitation in human patients, who are immobilized continuously for four months.

In addition to suturing, as discussed above, surgery also induces an extreme passive stretch of the muscle fibers due to retraction to gain

access to the underlying bony structures. Forcible lengthening of a muscle is usually defined as an eccentric contraction, but this definition might be extended to include the effects of extreme passive stretching of the fibers to the point of injury, causing delayed onset muscle stiffness and soreness after surgery due to damage of the muscle fibers. Excessively stretched fibers display all the classic symptoms of an eccentric injury to the muscle, including a decrease in obtainable specific tension, shift in optimal length for active tension, and rise in passive tension. These conditions indicate sarcomere disruption as the cause of muscle fiber damage from the stretching [93]. Perhaps surgical retraction that involves stretching a muscle beyond its optimal length induces sarcomere "popping" from inconsistencies in length between neighboring sarcomeres [94].

G. Objective Evaluation of Human Subjects

Like muscle tissue injury, surgeons have largely ignored the functional recovery of patients after spinal fusion. As long as the fusion mass is of adequate size and opacity, the patient is allowed to return to work and their normal activities. Unfortunately, the patient's perception of their strength rarely matches their actual strength from objective evaluations. Marras and Ferguson have studied low back pain extensively over the past decade [10-12, 95-103]. Their methods make use of a noninvasive device they designed that is mounted to the posterior surface of the spine. It has a shoulder harness and a waist belt that allows them to

measure the three dimensional kinematics sense of the lumbar spine. Using this in combination with electromyography and known lifting forces or motions, they can accurately measure the muscle force and trunk orientation used by each patient. Patients with chronic low back pain often return to work only to be reinjured by their normal workplace tasks. In an effort to better understand the physiology of this phenomenon, Marras and Ferguson compared the physiologic status of their muscle strength against their perceived recovery. They found that fourteen weeks after injury, 80% of the patients felt fully recovered. In actuality, only 68% of them showed normal muscle strength and trunk motion patterns. Although this study found little research in the area of long-term effects of spinal fusion for patients returning to the workforce, an older study by Mayer suggests that trunk strengths in scoliosis surgery patients may be decreased by as much as 50% compared to normative samples [104]. Other researchers have also considered muscle impairment after spinal surgery or prolonged flexion and have also found that muscle strength decreases [73, 77, 78, 105-109]. Subjective measures of patient recovery, such as questionnaires and interviews may not be adequate measures of the patient's actual strength.

Researchers have also found that patients with chronic low back pain tend to recruit more muscles, require more muscle strength, and engage in less ideal trunk motions for normal lifting tasks [12, 101-103,

110, 111]. Thus, surgeons need a physiologic measure of return to normal strength and range of motion for their patients. As the patients are usually in severe, chronic pain prior to surgery, and because spinal fusion surgery relieves the pain, the patient may be wholly unaware of their impaired function. Because of this misperception, any outcome of this research for the completion of the spinal fusion process must be tempered by the physiologic condition of the muscles after immobilization. Other biosensors or follow-up tests may be necessary to determine if the muscles are also back to full strength.

H. Analysis of Previous Fusion Strain Studies

In an extensive study using twenty four mature sheep, Kanayama performed single-level spinal fusion on all animals, with one fusion location randomly receiving bone slurry from the iliac crest and the other serving as a control [2]. At four, eight, twelve, and sixteen weeks, he harvested the spines from six sheep and performed mechanical testing on the strength of the fusion mass. The mechanical testing was done with and without spinal hardware instrumented with strain gages. He found that bending stress decreased significantly after eight weeks, even though histological inspection showed the bony mass was almost entirely woven, trabecular bone. Since the stress in the spinal rods decreased (Figure 4), it makes sense that he also found that the strain in the rods decreased over the duration of the study (Figure 5).

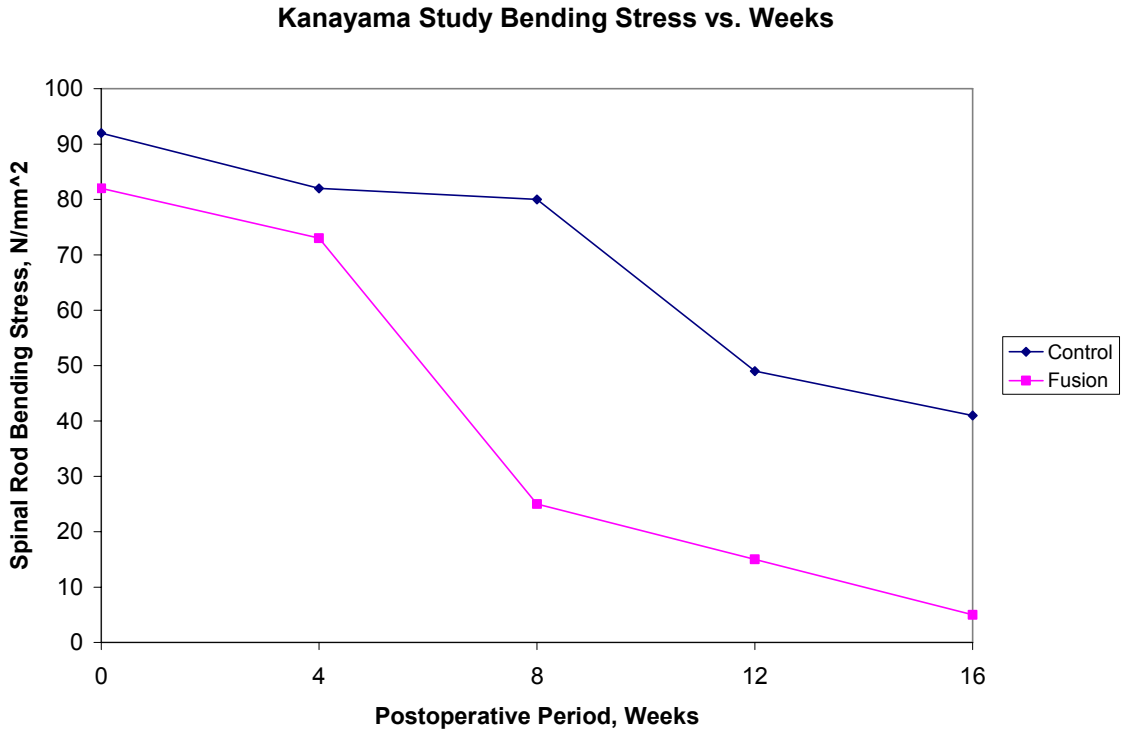

Figure 4, Spinal Rod Bending Stress vs. Weeks [2]

Kanayama also determined the stiffness of the fusion mass, showing that the bony mass increased in stiffness significantly after eight weeks as shown below (Figure 6). His study actually measured lateral bending stiffness and a function of degrees rotation, but the general trend should be the same for flexion, with the stiffness gradually increasing as the fusion obtains mechanical stiffness and thus offloads the spinal hardware.

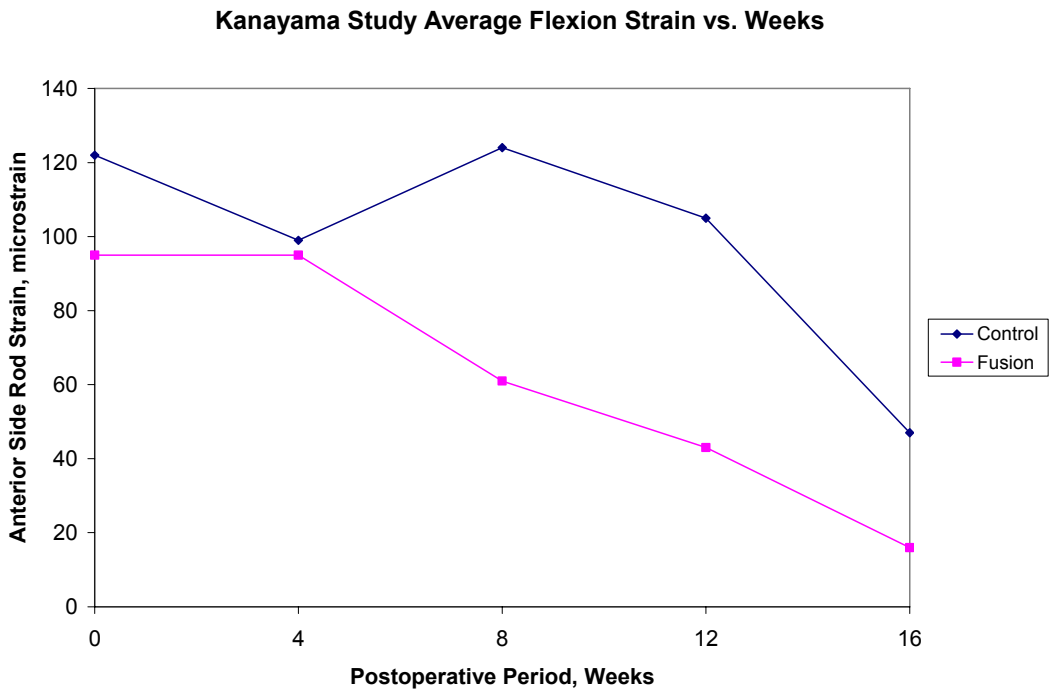

Figure 5, Rod Strain versus Weeks [2]

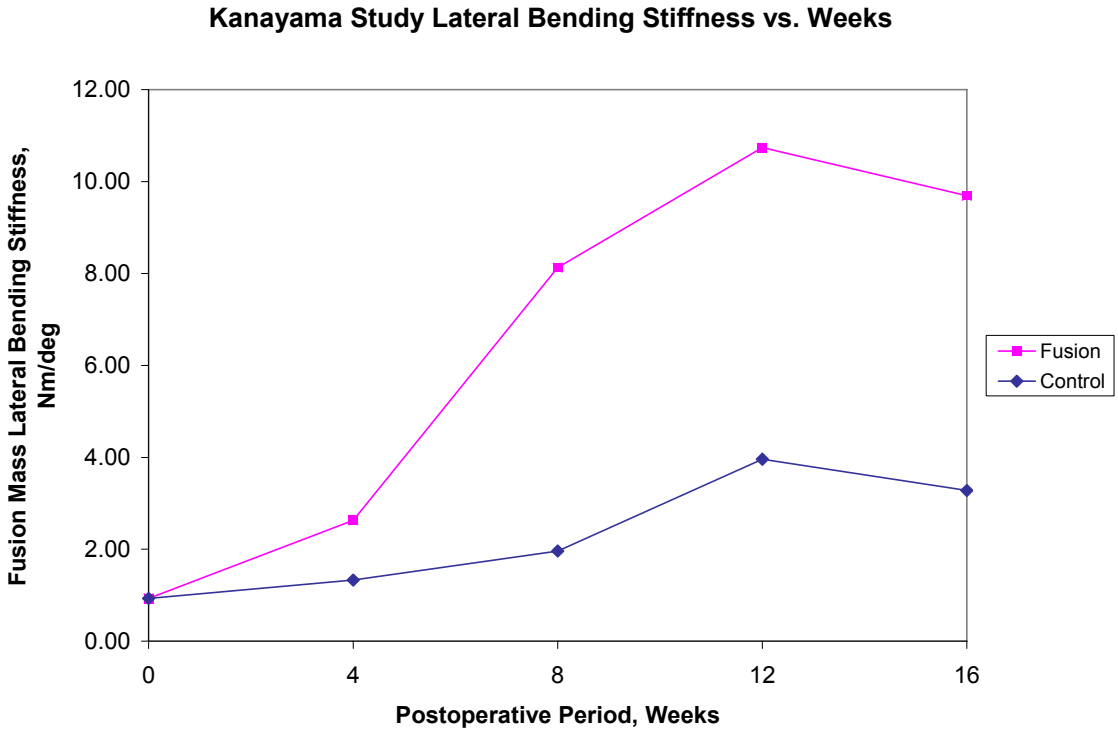

Figure 6, Fusion Mass Stiffness vs. Weeks [2]

H. Patent Review

Currently, there are several patented methods for measuring the movement or strain in the human spine. All involve collecting an electronic signal and transmitting it to an external receiver. In patent 6,433,629 [112], the inventors use a Wheatstone bridge and a timing circuit to measure the displacement (strain) in an orthopaedic knee implant. The unique feature of their strain measurement device is that it has no internal power source. A magnetic coil brought in close proximity to the Wheatstone bridge provides the power. This activates the circuit for the duration of the measurement.

In patent 5,935,086 [113], the inventors measure the relative angles between two or more joints and use a force transducer to simultaneously measure the applied force in the joint. This is similar to patent 5,995,879 [114], which also measures the angle between two freely movable points. The difference between these two patents is in the application. The first patent tries to determine the joint spacing and pressures in an artificial knee, whereas the second patent tries to determine the orientation of a second spinal vertebrate relative to a first vertebrate.

Patent 6,432,050 [115] uses audible acoustic feedback to monitor an *in vivo* sensor or device. By applying an acoustic query to the implanted device, the operator can audibly determine if the device is functioning

properly. This has wide reaching applications, from heart surgery stents, to intervertebral disc implants.

In patent 6,223,138 [116], the inventors have again used a Wheatstone bridge to measure their strain displacement, but they have amplified the signal and added it to a carrier frequency. By adding it to a secondary frequency, they avoid losing the small signal in the background noise. Patent application 2002/0050174 [117] also uses strain gages in a Wheatstone bridge, but the inventors have adapted the device to successfully measure strains on the micron scale.

Patent application 2002/0024450 [118] is a data collection apparatus designed to store data *in vivo* for future retrieval via radio telemetry. The advantage of internal storage is two-fold. First, the power requirements of the battery are greatly reduced, as the data collection system can be placed in a sleep mode until triggered to transmit, and second, the data collection apparatus is protected from damage that might occur from being left exposed to the animals for an extended period of time.

Patent application 2004/001137 [119] is most closely related to this research, as it utilizes strain to measure the presence of spinal fusion in a scoliosis spinal rod system. It also utilizes telemetry, and is thus in conflict with the patent application above. Because these are applications and have yet to be challenged by the U.S. Patent and Trademark Office, it is unknown which of the claims will be denied.

The researchers involved with this design study have also submitted a patent application to measure strain *in vivo* using an interdigitated capacitive sensor and a transponder to send the signal via radio frequency to an external receiver. Considering that the design for this study's device does not use a standard strain gage and the intended application is diagnostic, and because it includes considerable depth and detail lacking in the other applications, the university's patent attorney felt the claim was strong enough to warrant protection. The application was filed July 8, 2005. Details of the patent are discussed in a later chapter.

I. Significance of Current Research

Based on the literature review, this study has identified several voids in the current knowledge that will be addressed in this research study. First, lumbar fusion is routinely performed in the United States, with 300,000 surgeries per year in 2004 [3, 4]. In spite of the frequency for lumbar spinal fusion, the methodology for postoperative care has changed very little in the past two decades. Patients are still fitted with braces, even though their effectiveness is minimal in preventing adverse motions [5, 120], and they are known to cause muscle atrophy and stress shielding in the patient, resulting in an inferior outcome. In addition, x-ray radiographs are still the diagnostic tool used by most surgeons to determine spinal fusion [6]. Although some researchers are investigating the use of strain to measure torsional strength in scoliosis fusion, facet loading, or

intervertebral disc loading, as yet no one has used strain to measure spinal fusion. The objective of this study was to design a better diagnostic tool for surgeons based on strain to address the problems associated with the current method of bracing and diagnostic radiographs. It was hypothesized that the amount of time for fusion is significantly less than it is indicated by radiographs, and patient outcomes would be improved if a superior diagnostic method were developed.

III. HYPOTHESIS AND GOALS

The hypothesis is that strain is related to the onset of spinal fusion. This study will test this hypothesis and then develop an implantable diagnostic strain system for humans to detect when spinal fusion has occurred. To achieve these goals this study proceeded as follows:

1. Tested the hypothesis using an *in vivo* sheep model for a period of seventeen weeks.
2. Designed a sensor to detect strain in spinal hardware and develop a method to transmit that information through the body to an external receiver.
3. Prototyped the designed sensor and tested its performance.
4. Patented the intellectual property for later use in starting a business.
5. Developed a rudimentary business plan to begin seeking funding for this enterprise.

IV. DISCUSSION

It is apparent from reviewing the literature that there is a need for a better diagnostic tool for orthopaedic surgeons and researchers. Although much research has already gone into studying spinal fusion properties, as yet no one has generally characterized these properties and applied them to the larger problem of patient outcome. With hundreds of thousands of patients involved, the need for a solution is paramount.

The goal of this research is to fill that void by providing a simple, complete means for surgeons or researchers to determine the status of a spinal fusion postoperatively. Benefiting from this timely information, the patient will be able to remove their bracing sooner and thus return to work sooner and with less muscle weakness.

CHAPTER 2

Preliminary Research

I. Introduction

A. Sheep Pilot Study

i. Goals of study

The goal of the sheep pilot study was to validate this study's hypothesis that strain is related to the onset of fusion. As this had never been attempted in an *in vivo* study, the researchers decided to test the entire concept for feasibility on two sheep. Thus, the use of strain as a diagnostic tool, encapsulation of ordinary strain gages into existing implant hardware, and wireless data transmission were all included in this seventeen week study.

ii. Summary of seventeen week pilot study

In an animal protocol approved by the Institutional Animal Care and Use Committee (Protocol #10159), two sheep were used as a model for the human lumbar spine. This study's researchers implanted a DePuy Monarch Spine system, consisting of two spinal plates, four pedicle screws, and four nuts into each sheep (Sheep 324 and 325). During surgery, one of the spinal plates was replaced with an electronically instrumented spinal plate (Figure 7). The strain gages in the instrumented spinal plate were hardwired to a transponder built by MicroStrain on behalf of the research team. Using a laptop (Figure 8), the strain data stored in

the transponder were downloaded to a software program for analysis, AgileLink by MicroStrain, Inc. As stated previously, it was hypothesized that the level of strain would decrease and eventually plateau at a lower level. This electronic data would be corroborated by x-ray radiographs that were taken weekly, CT scans that were taken in the latter months, and mechanical testing to be performed in the laboratory.

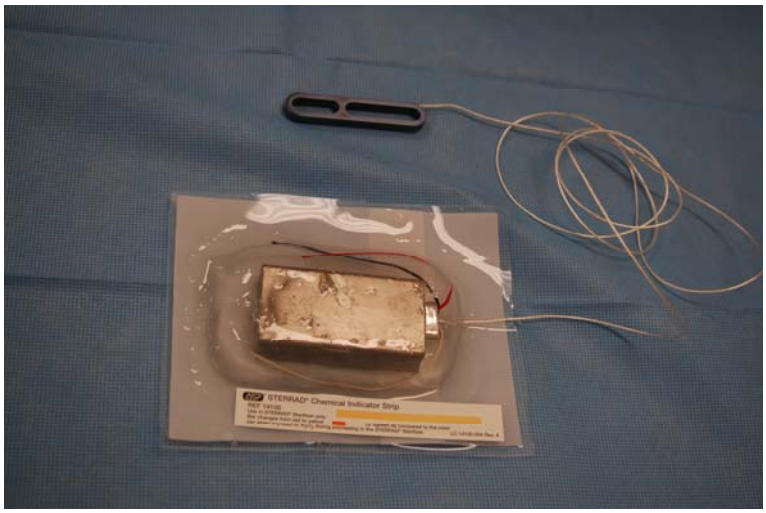

Figure 7, Instrumented Spinal Plate and Transponder

Figure 8, Laptop with Antenna and Both Transponder Units

The surgeries performed on the sheep proceeded with no issues. The plates fit cleanly over the pedicle screws, and the transponders were placed subcutaneously along the sheep's side. After harvest, the researchers learned that the wires to the instrumented spinal plate should have been enclosed in a silastic pouch to prevent the scar tissue mass from forming around the wires. This made removal of the spines more difficult upon harvest (Figures 9-12).

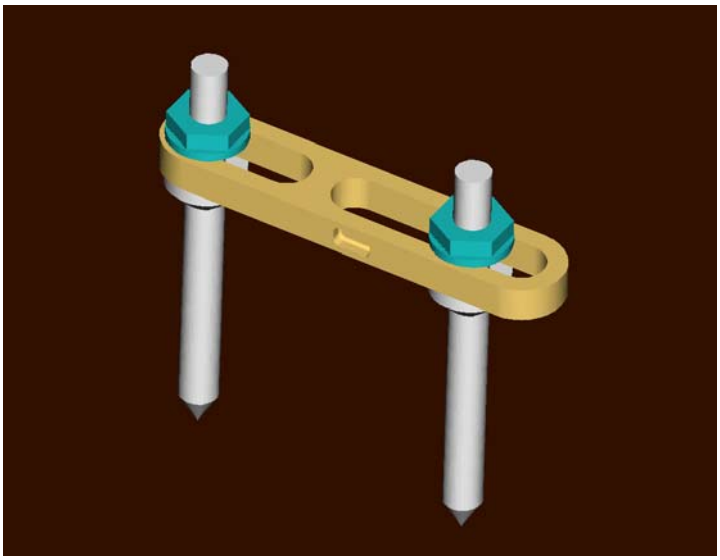

Figure 9: DePuy Monarch Spinal System Modeled in Pro/Engineer (showing machined pocket), by D. Schenberger

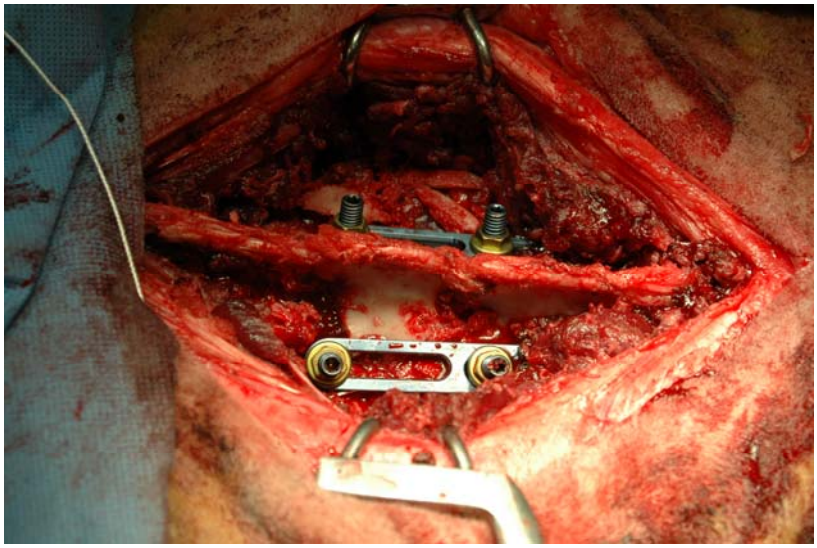

Figure 10, DePuy Monarch Spine System at Implantation

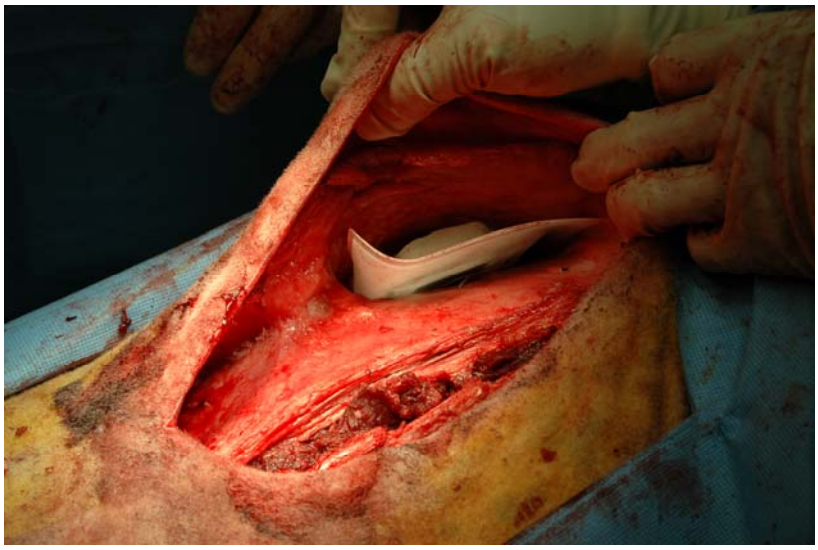

Figure 11, Transponder in Subcutaneous Pouch at Implantation

Figure 12, Spine & Transponder at Harvest with Wires in Tissue Mass

From the pilot study, the researchers obtained radiographs and CT scans. The radiographs, as expected showed no definitive fusion mass until after twelve weeks, but the CT scans detected a fusion mass at the ten week time frame. Figures 13 and 14 are three-dimensional reconstructions of the CT scans for Sheep 325 at the ten week and seventeen week time frames. Fusion was confirmed by manual manipulation at harvest.

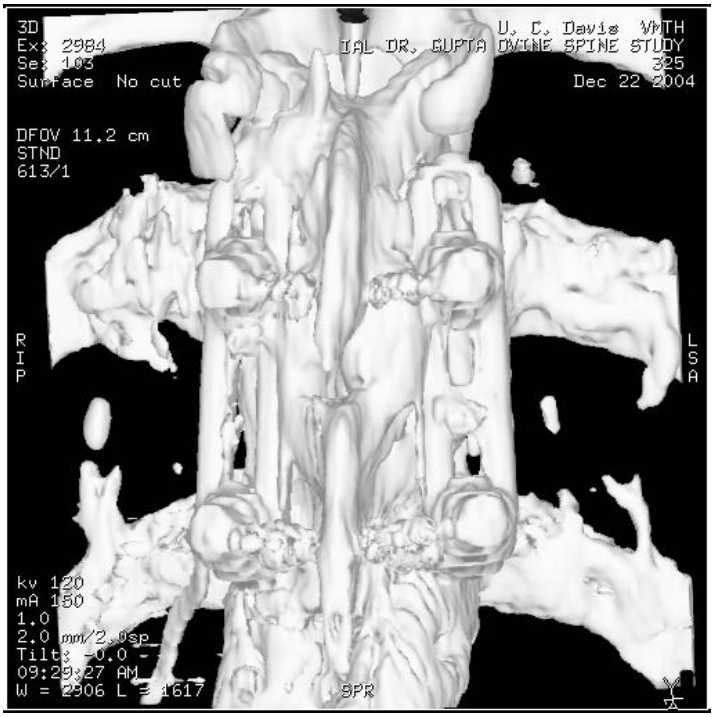

Figure 13, Sheep 325 at Ten Weeks with Bone Beneath Spinal Plates

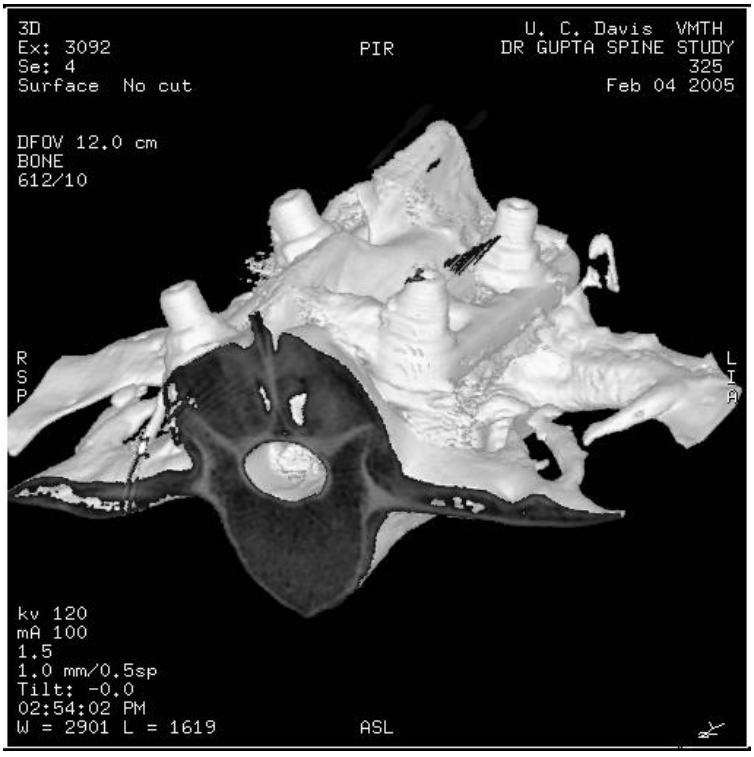

Figure 14, Sheep 325 at 17 Weeks Shows Bony Fusion at Spinal Plate

Although spinal fusion was achieved in both sheep and the strain did vary as the fusion progressed in both sheep, there was not enough of a trend to draw any conclusions because both strain gages failed due to moisture prior to the conclusion of the study. Also, as the sheep showed two different trends in the early weeks of strain measurement (one remaining constant the other initially decreasing before remaining constant), more sheep would be necessary to better understand the overall trend of the strain over the entire population. A minimum of seven sheep would be needed for statistical significance for a minimum of sixteen weeks.

iii. Issues encountered in pilot study

Although the MicroStrain devices performed as expected when manually pressed on the bench top just prior to implantation, problems became apparent after implantation. The MicroStrain transponders contained a two-level amplification system to allow for adjustment due to initial preload during implantation of the spinal plates. This was a good feature, as the spinal plates are subjected to an unknown amount of strain preload depending on the anatomy of the spine, the orientation of the pedicle screws, and the separation of the pedicle screws. Once the preload “offset” was set, the devices worked within a range of microstrain dependent on the preset gain of the transponders. Unfortunately, this gain was set too narrow to give greater sensitivity, and the overall range of the

transponders was thus too small, a mere 20 microstrain. Thus, every time the strain decreased or increased by more than 20 microstrain, the data output saturated and no strain was recorded beyond the offset value (Figure 15).

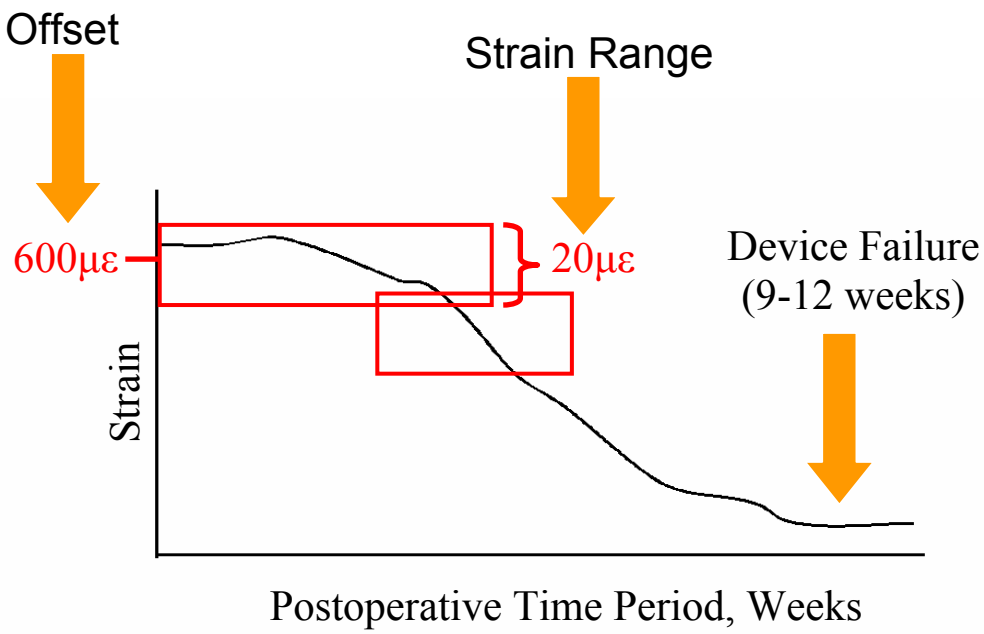

Figure 15, Graphical Illustration of Strain Range Problem

To correct for this problem during the sheep study, MicroStrain taught the researcher how to adjust the offset value. Theoretically, this should have allowed the adjustment of the base amount of strain up or down until the transponders were once again within range. Unfortunately, adjusting the offset introduced an unexplainable step into the output. Instead of simply moving the base strain location, the offset value relocated all of the strain values to a new base strain location, making it

impossible to compare data collected at one offset value with data from another offset value. The equation provided by MicroStrain is given below:

Strain = (BitsOut-VbitsZero)*StrainSlope +(OffsetValue-InitOffsetValue)*OffsetStrainSlope

Where the values for each variable are:

BitsOut = Measured value of strain in bits from sensor (i.e. 2000)

VbitsZero = Value read on sensor prior to implanting (591)

StrainSlope = 200/4096 in microstrain/bit

OffsetValue = Value at which sensor offset is currently set (i.e. 600)

InitOffsetValue = Value at which sensor offset was set when received from MicroStrain (575 on Sheep 324 Node 12)

OffsetStrainSlope = (4096 bits/InitOffsetValue)*StrainSlope

For example:

Strain = (2000-591)*(1/20.48)+(600-575)*(7.12/20.48)

Strain = 68.80 (from strain gages) + 8.69 (from offset)

Actual experience with the devices, however, indicates that the offset value, and not the strain gages, had about a tenfold greater effect on the output strain. To test the effect of the offset value, the researchers created a parallel test with two new spinal plates, as discussed later in this report.

In addition, after the first eight weeks in one device and the first twelve weeks in the other device, just as the strain levels were beginning

to consistently decrease as expected, the transponders stopped transmitting the strain portion of the data. The transponders kept functioning, leading to the conclusion that all was well, but in fact the output was only a function of the offset value. This was verified after harvest by cutting the leads to the strain gages on the spinal plate. The output was unaltered, and thus confirmed that the transponders had failed at a crucial point of spinal fusion, eight to twelve weeks, and no conclusions could thus be made about changes in strain due to fusion. Also, one spinal plate appears to have been loaded initially in flexion as expected (Sheep 324), but the other was loaded initially in extension (Sheep 325). The transponder in Sheep 325 was also extremely noisy, making the results virtually unusable. Regions where the graphs are horizontal lines indicate output was out of range or did not contain any contribution from the strain gages. The graphs for Sheep 324 and Sheep 325 are shown below (Figures 16 and 17).

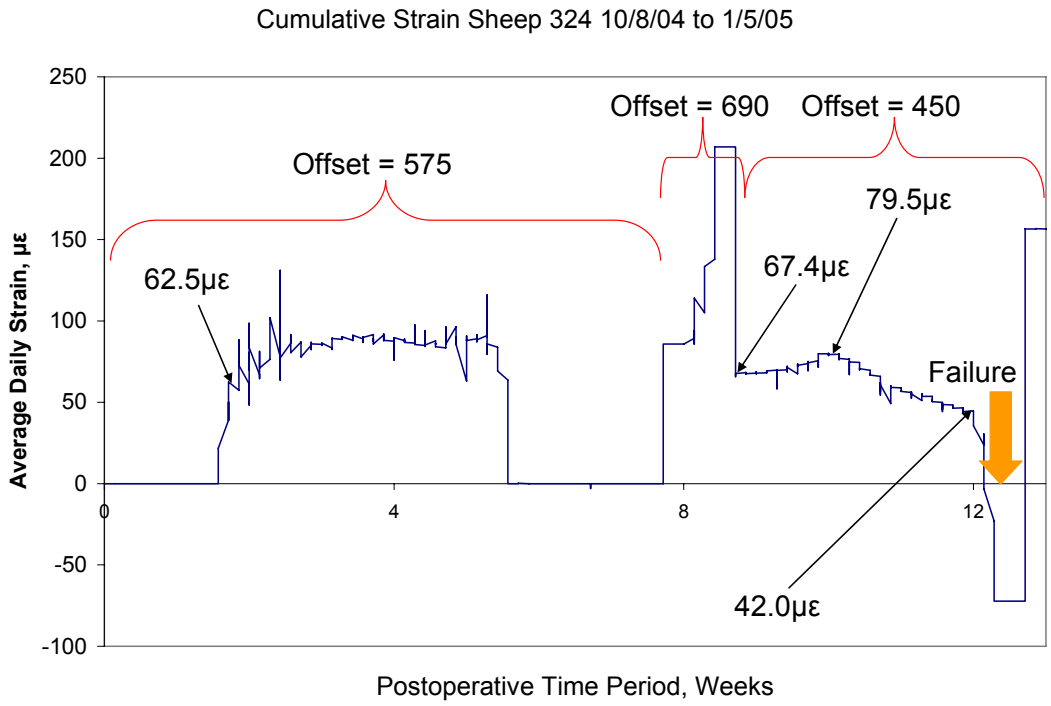

Figure 16, Cumulative Strain Data for Sheep 324 (Spine in Flexion Initially)

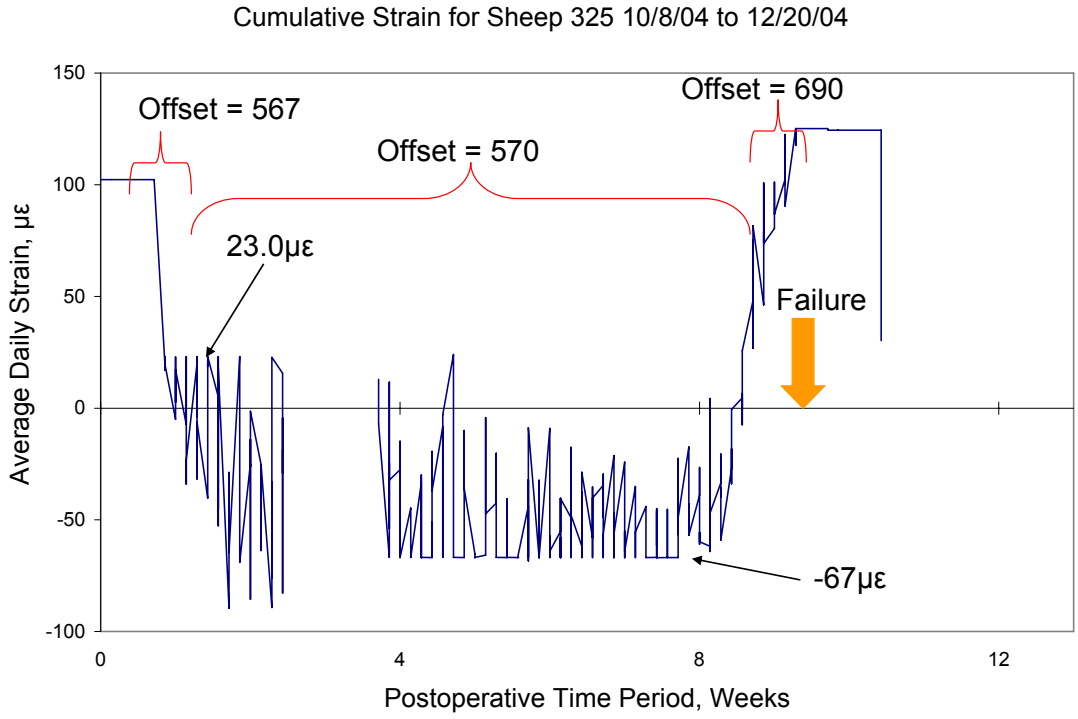

Figure 17, Cumulative Data for Sheep 325 (Spine in Extension Initially)

This study went to great lengths to resolve the offset problem for Sheep 324, as is discussed below. The goal was to determine the exact amount of influence of the offset value on the output to create a calibration equation.

iv. Subsequent research to account for issues

After much deliberation, the researchers decided to perform a parallel study to accurately measure the actual strain versus the output from the MicroStrain transponder system. This study thus obtained two new spinal plates and instrumented each of them with two copper foil strain gages configured in a half bridge. The strain gaged spinal plates were then mounted in a test stand (Figures 18-19), and the outputs were compared for amplified strain in millivolts versus MicroStrain databits at each offset value. The researchers received advice on the pin-out from MicroStrain and wired the strain gages to the transponder of Sheep 324 as shown (Figure 20). The pin out information also allowed this study to recharge the batteries for this experiment. The spinal plate was first manipulated manually in the lab, and the researchers confirmed it was communicating with the transponder. The transponder, however, did have issues that could not be predicted. First, the researchers had to query the transponder up to five times between each successful data stream or offset value adjustment. This was a bug in the software that could not be eliminated. Second, the range of acceptable strain was so small that the

researchers had to constantly adjust the offset value to get within a valid range. Basically, the device saturate at 4098 or 0 databits if the offset value was completely out of range. Otherwise, it gave an output relative to the offset value in databits. If the strain fell within the window of the second transponder amplifier, the data stream gave a time-varying output of ±200 databits. Thus, the data collected below give small regions of usable data, depending on the load applied, which the researchers varied between zero and 30lbs in two pound increments to simulate at zero to 6Nm physiologic moment (based on geometry of the test stand with a lever arm of 1.875 inches). The MicroStrain transponder had a narrower range of load it responded to of ±18lbs.

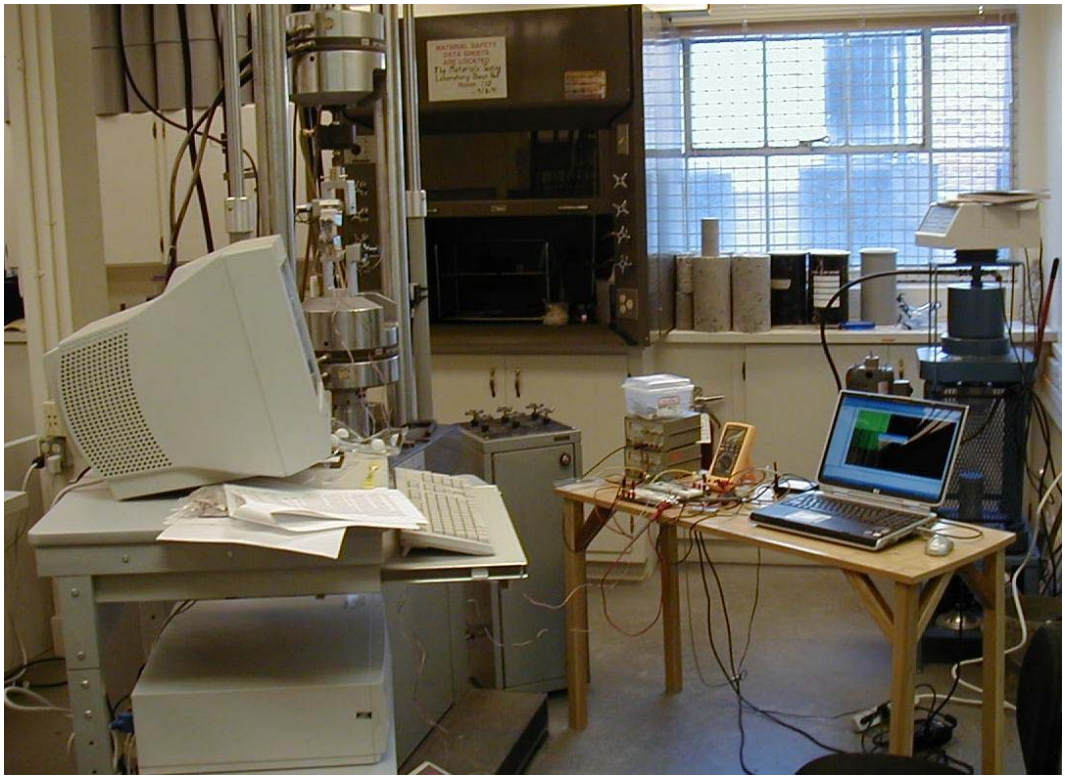

Figure 18, Overview of MicroStrain Transponder Testing

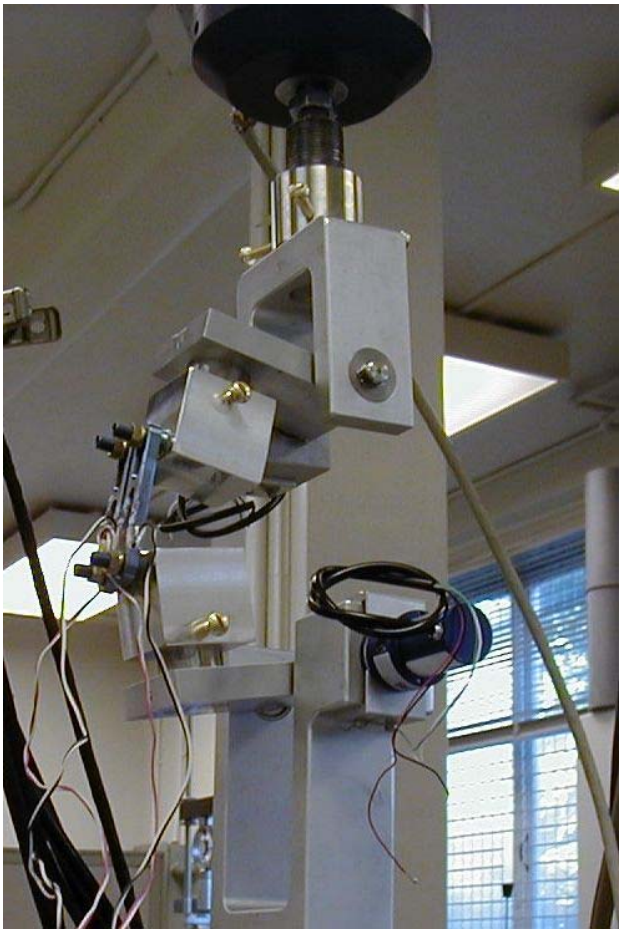

Figure 19, Closeup of Instrumented Spinal Plates on Test Stand

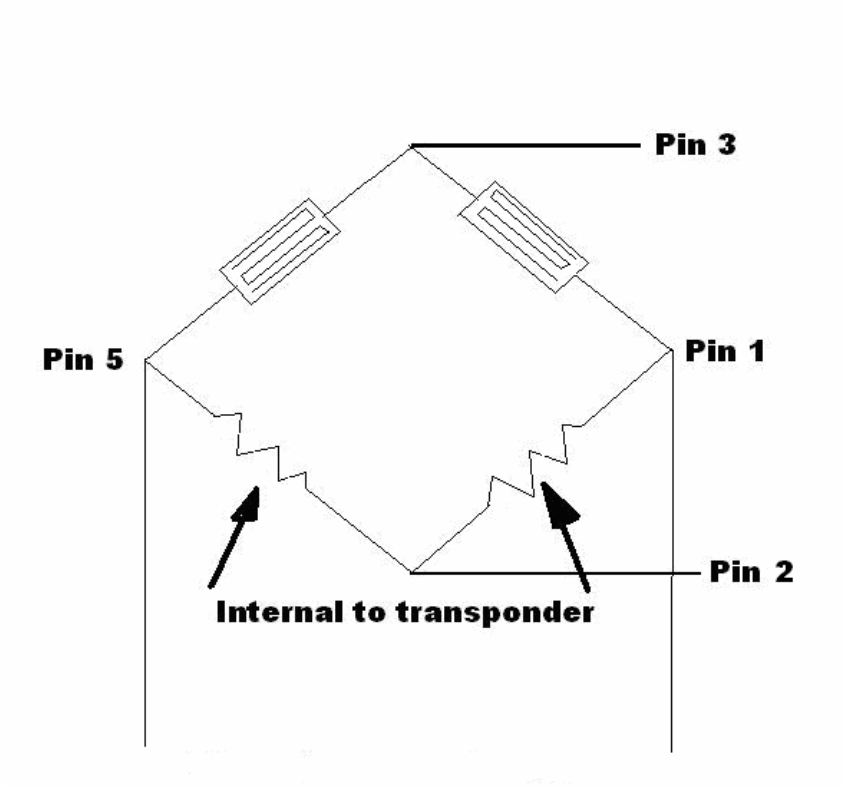

Figure 20, Pin Attachments on MicroStrain Transponder

For the second spinal plate, the researchers built and used an instrumentation amplifier to obtain a gain of ten and completed the bridge with resistors in a Wheatstone bridge configuration. These two spinal plates were then mounted on an aluminum test plate and attached to the test stand. To minimize error, one instrumented spinal plate was first attached to the MicroStrain transponder and subsequently attached to the instrumentation amplifier for each load level. This was then repeated for the second instrumented spinal plate to make sure the results were repeatable. The resulting graphs show how the MicroStrain transponder

and a direct strain measurement varied relative to the same load (Figures 21-22). At first glance, the two curves are linear and appear to be relatively similar, but by plotting the correction factor, a ratio of databits per millivolt, against the load, a much different result becomes apparent. The MicroStrain transponder behaved much differently for flexion versus extension and the number of databits changed linearly depending on applied moment per the equations shown on the graph (Figure 23). Also, this slope varied relative to the offset value, making it impossible to interpret the results from the pilot sheep study.

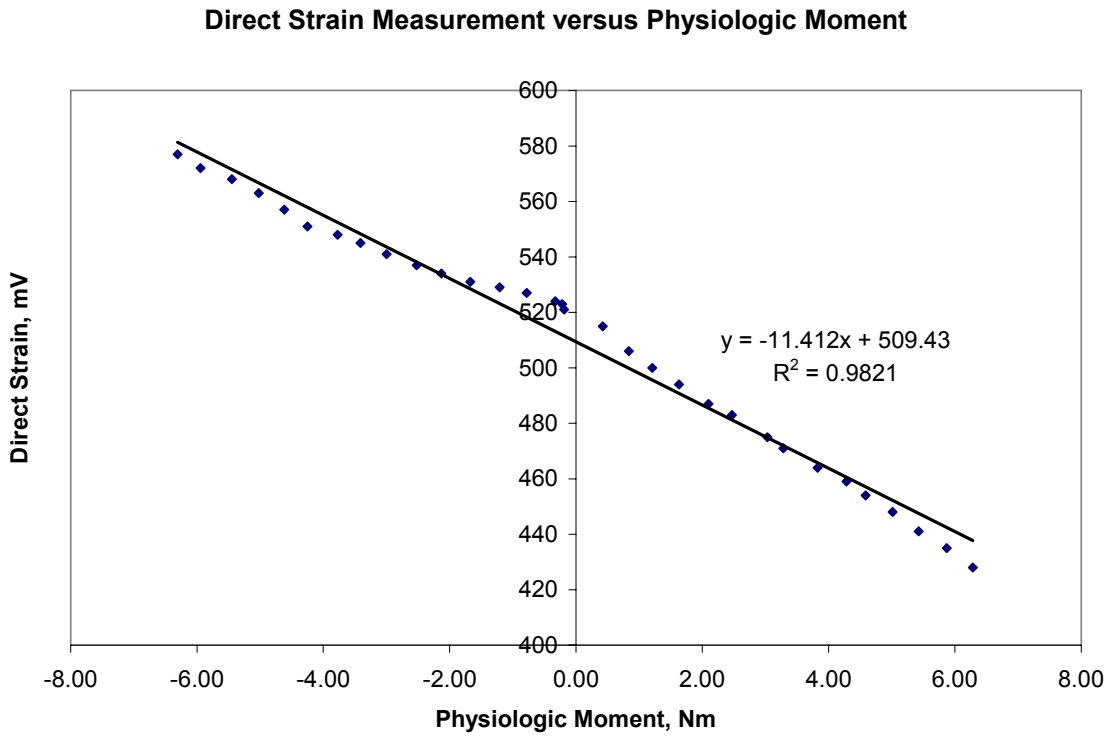

Figure 21, Direct Strain Measurement vs. Physiologic Moment

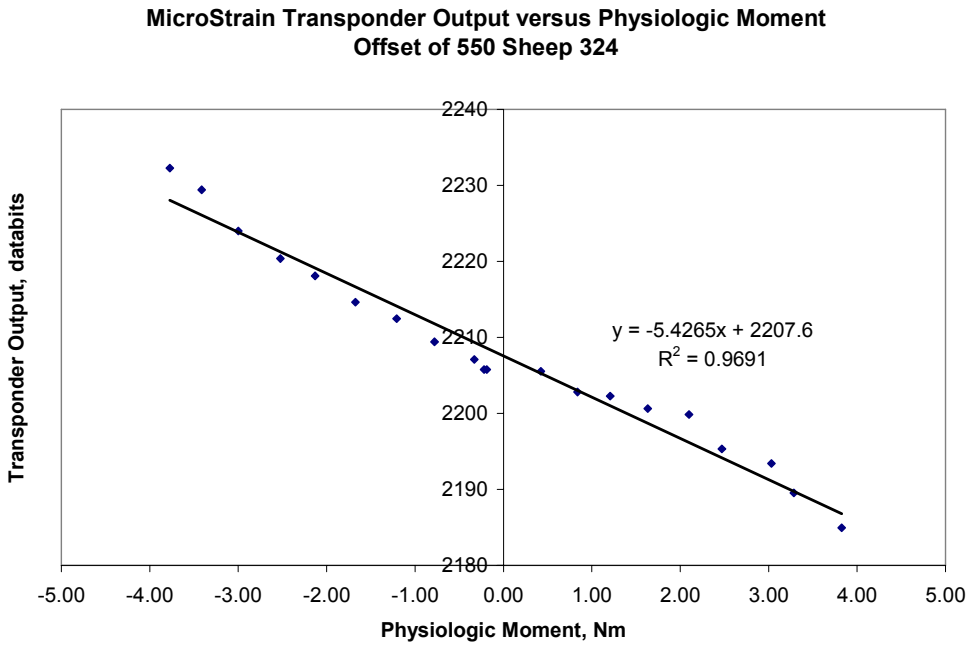

Figure 22, MicroStrain Transponder Output vs. Moment

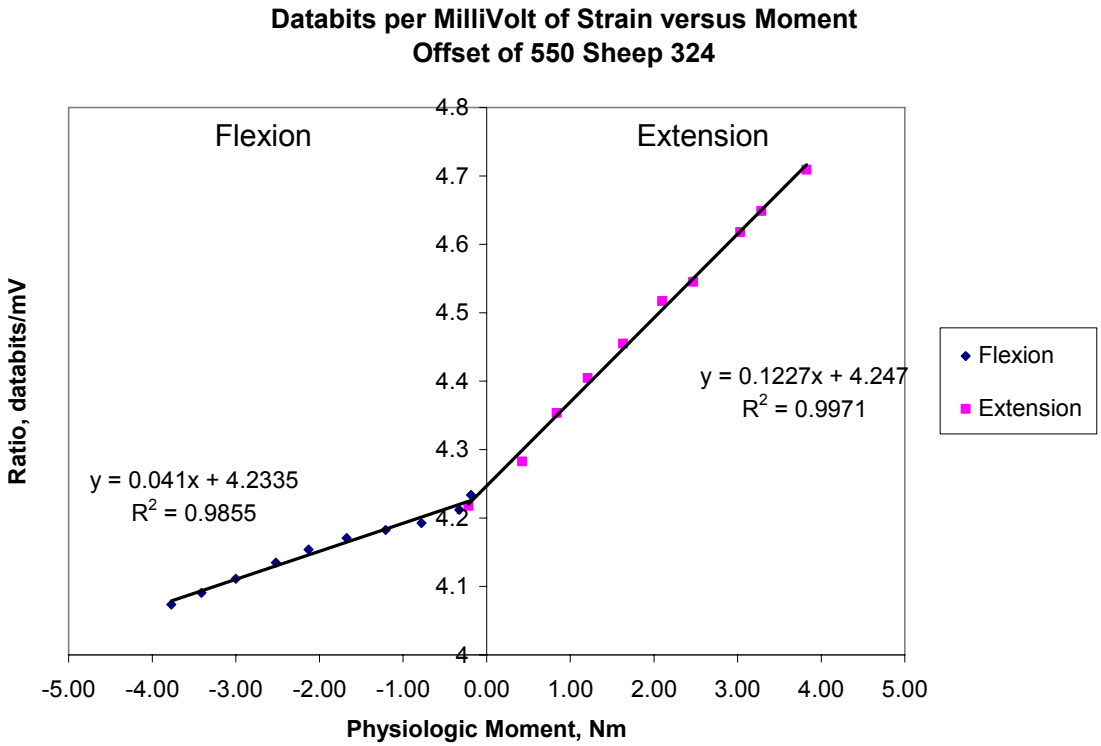

Figure 23, Ratio of Databits per Millivolt vs. Moment

(This should have been a constant value)

Based on these results, the researchers could not create a calibration equation and apply it to the data from Sheep 324 (Node 12) as hoped. Since it would be impossible to know the true physiological conditions, it would be pure conjecture to try and apply the above calibration equation to the data.

B. Second Sheep Spine *in vitro* Study

i. Study overview

The purpose of this second sheep spine study was to determine if a decrease in strain was correlated with an increase in stiffness of the fusion mass. This study then purchased two additional lumbar sheep spines and implanted pedicle screws for spinal fusion on each of them. Each spine was then potted them in PMMA and outfitted with the strain gage instrumented spinal plates. The potted spines were mounted in the test stand and loaded through a physiological range in both flexion and extension (Figure 24). Next, the spinal plates were removed to compare the stiffness of the spine without any stiffness provided by the spinal plates. Fusion was then simulated by adding a small quantity of PMMA (15gm) and allowing it to cure (Figure 25). The researchers then repeated the load cycle both with and without the spinal plates. This pattern of testing was repeated until the volume of PMMA no longer greatly influenced the stiffness or strain output (60gm). This corresponded to a

“solid bony fusion” that could be compared to previous studies, such as Kanayama [2]. The loading was repeated at seven levels for six trials at each loading level.

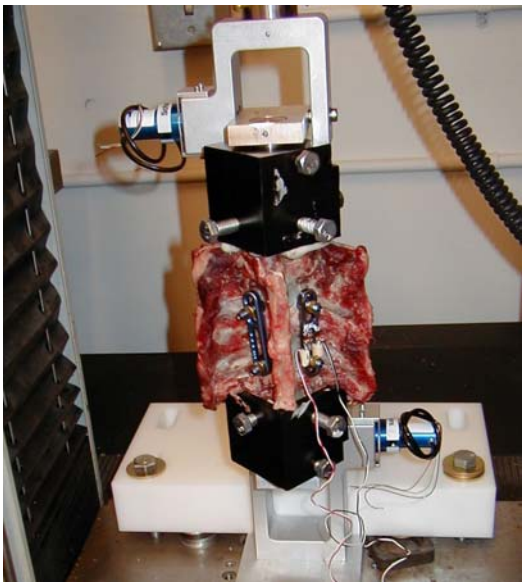

Figure 24, Sheep Spine on Test Stand Prior to Simulated Fusion

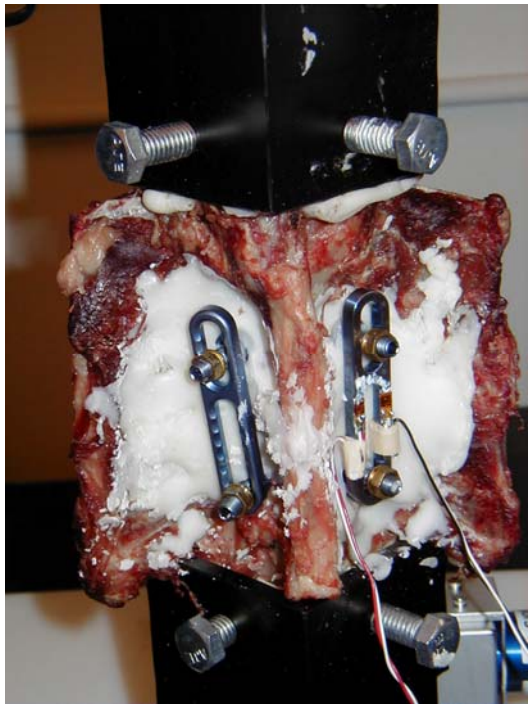

Figure 25, Sheep Spine on Test Stand with 60gm Simulated Fusion

ii. Results

As expected, strain correlated directly with the load applied (Figure 26), showing that strain is linearly related to load and moment.

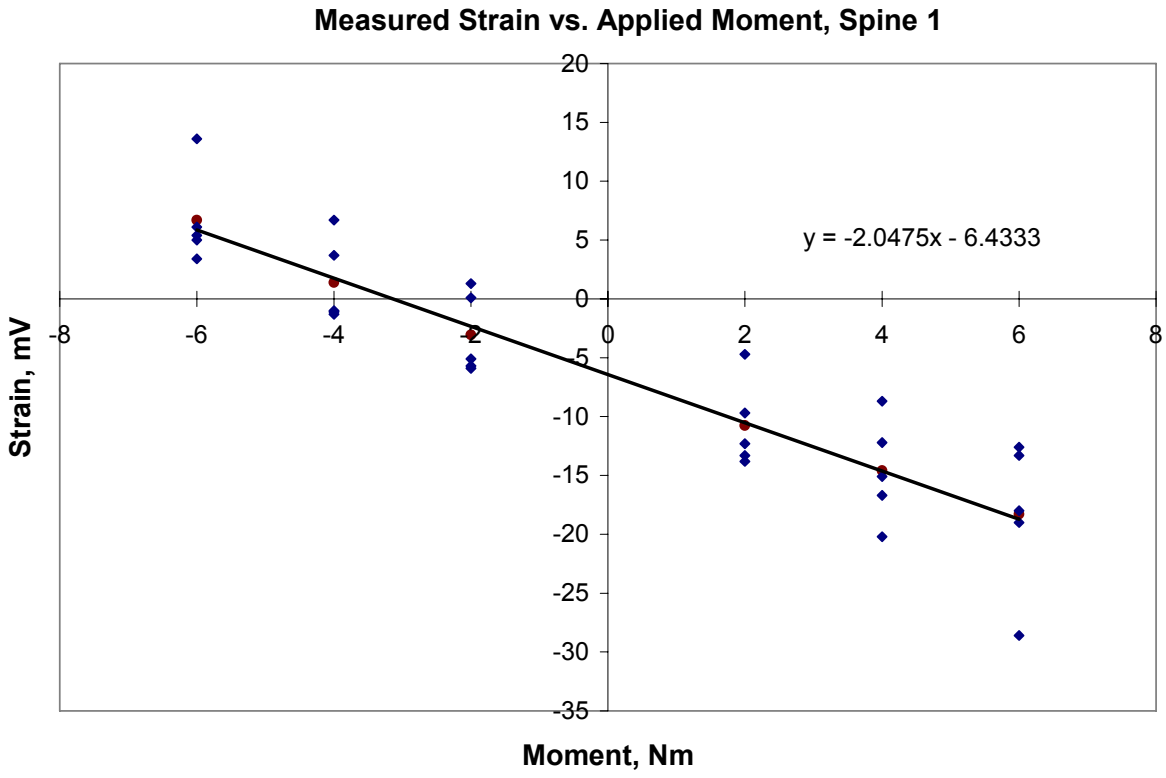

Figure 26, Measured Strain vs. Applied Moment

The stiffness of the spinal plate, also as expected, did not vary with load. As this plate was solid titanium, the stiffness should have been constant regardless of the applied moment or simulated fusion volume, and it was (Figure 27).

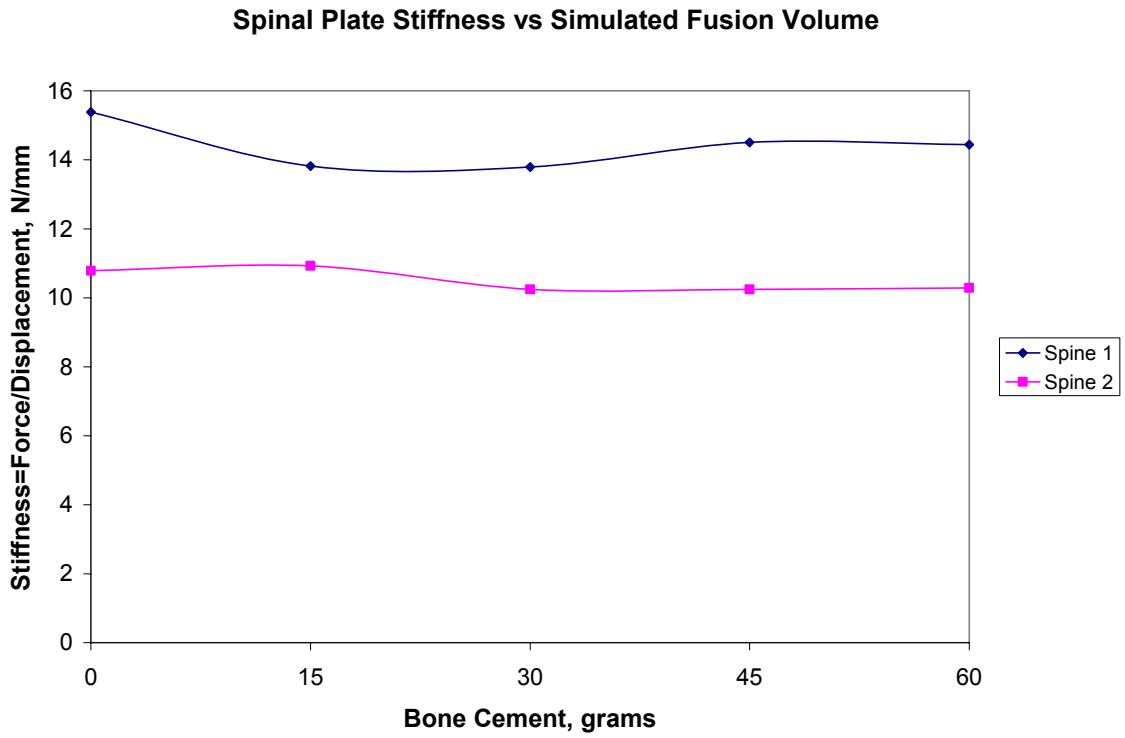

Figure 27, Stiffness of Spinal Plates vs. Simulated Fusion

The strain did vary with simulated fusion, initially increasing slightly for flexion and then stabilizing at a minimal plateau. For extension, the strain began at a large negative value and again plateaued at minimal value (Figures 28 and 29). Figure 29 has been inverted, eliminating the negative sign for clarity of comparison between flexion and extension, showing that the spine is stiffer in extension than in flexion for all loading and fusion levels. Both flexion and extension on both spines increased in strain at 15 grams of simulated fusion, which surprisingly corresponded to an increase in strain seen on the output of Sheep 324 around ten weeks (Figure 16).

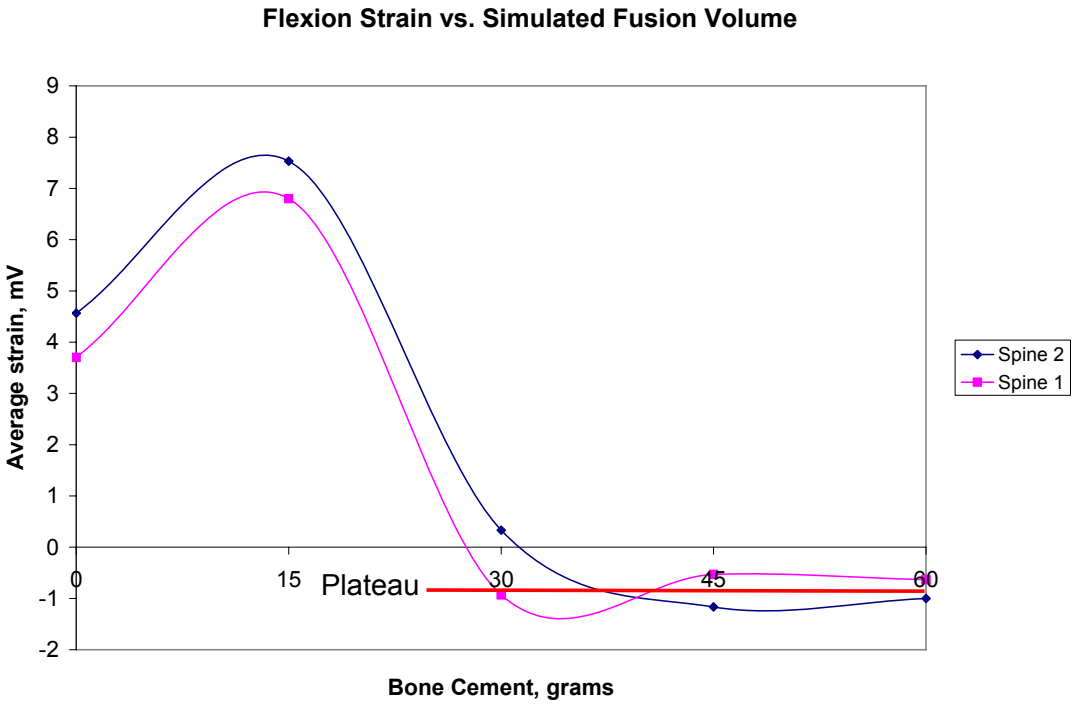

Figure 28, Flexion Strain vs. Simulated Fusion

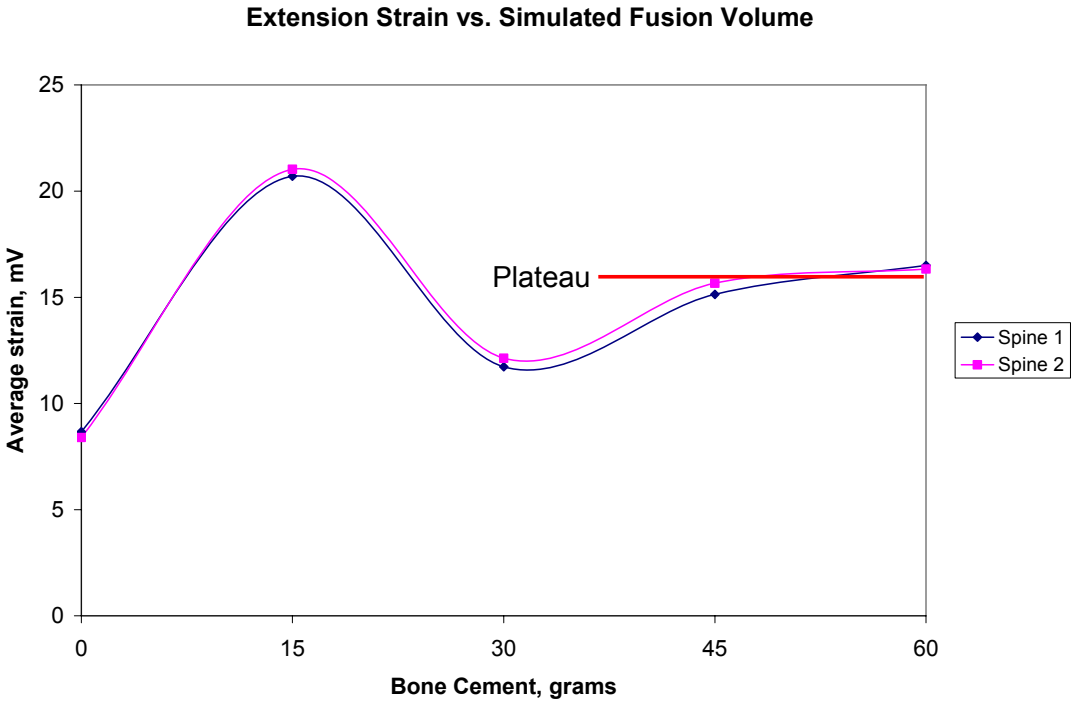

Figure 29, Extension Strain vs. Simulated Fusion

The flexion curve decreases in strain as the simulated fusion increases and replicates the shape of the output from the Kanayama study fairly well (Figure 4), indicating the test was a reasonable method for simulating fusion.

The other parameter this study decided to compare against the Kanayama study was stiffness of the fusion (Figure 5). Again the trend is similar, with the stiffness of the fusion mass increasing with increased simulated fusion mass. Below shows the resulting stiffness for each spine at each applied bending moment, with Spine 1 being stiffer in flexion than Spine 2 due to the manner in which the researcher arbitrarily applied the bone cement (Figure 30).

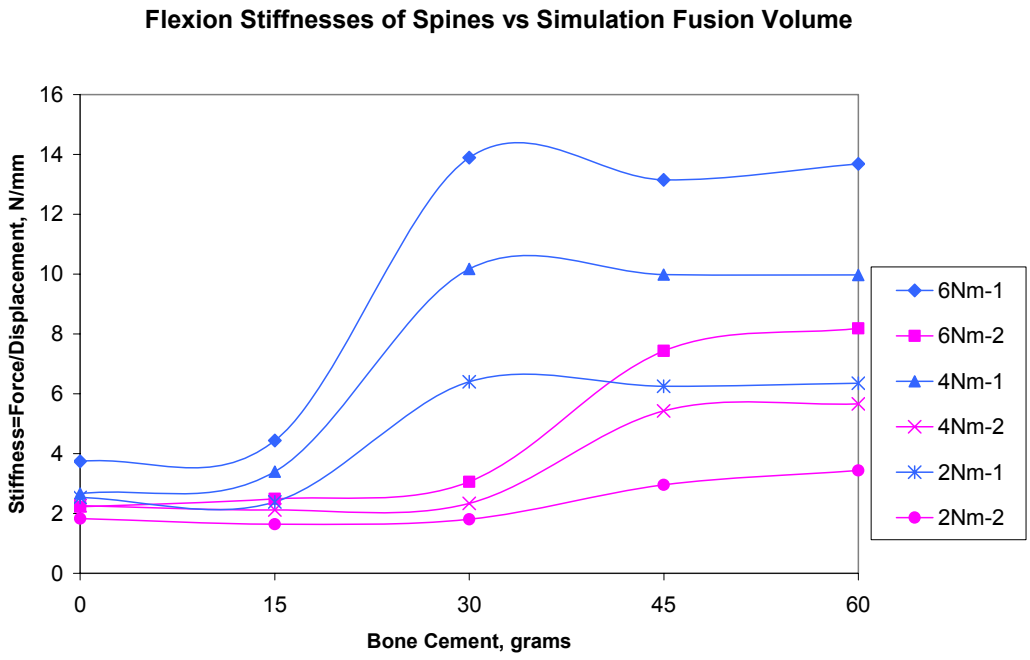

Figure 30, Flexion Stiffnesses of Spines vs. Simulated Fusion

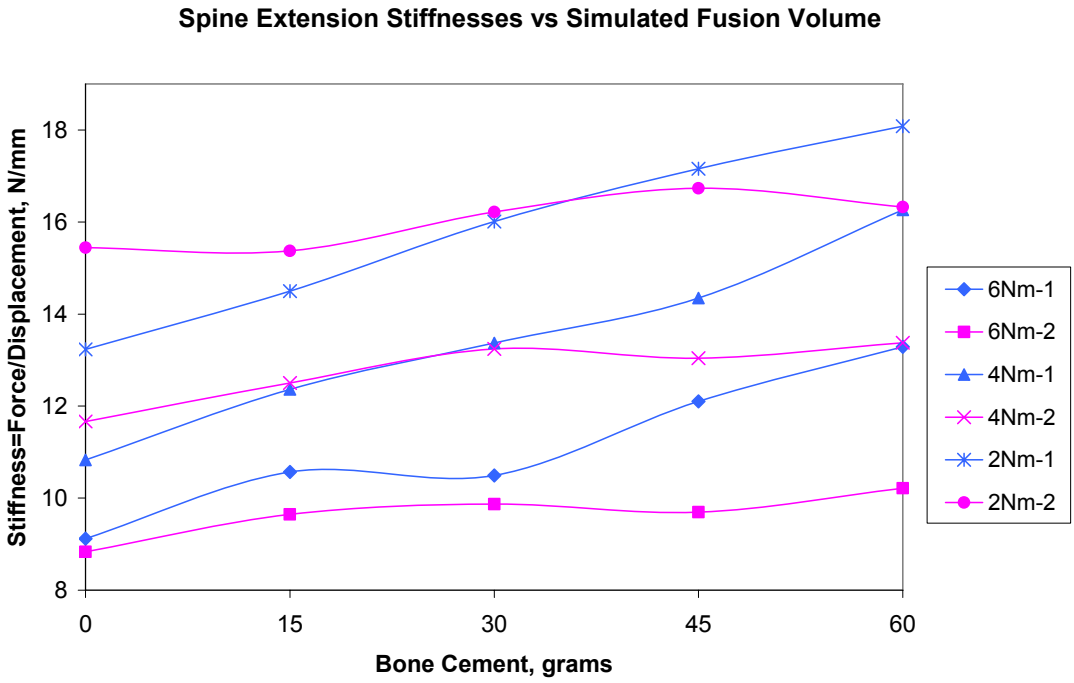

Figure 31, Spine Extension Stiffnesses vs. Simulated Fusion

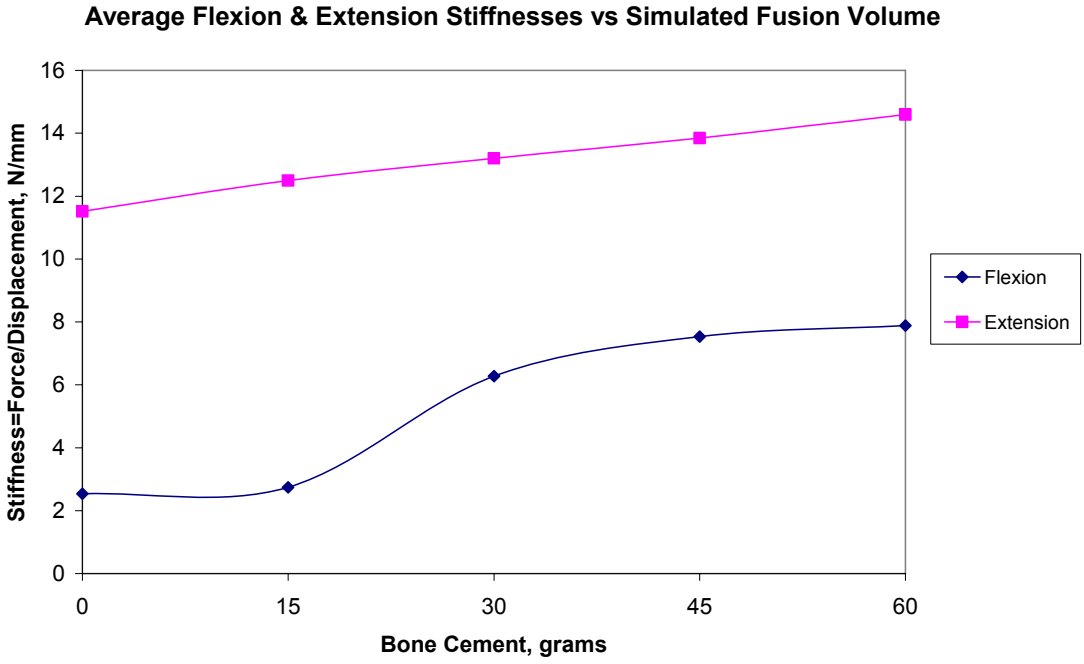

Figure 32, Combined Average Stiffness vs. Simulated Fusion

Like the strain versus simulated fusion results, the stiffness versus simulated fusion compared well with the Kanayama study for flexion. In extension, the spines were considerably stiffer, and the stiffness appears to be controlled by the spine anatomy and the intervertebral disc, not the spinal fusion for extension loading (Figure 31). In flexion, Spine 1 was stable at 30 grams of bone cement and Spine 2 was stable at 45 grams. The combined results show the general trend (Figure 32).

Another question of this study, however, was to see if there was a relationship between strain and stiffness. In other words, one of the goals was to determine if strain varied with the onset of fusion and eventually would plateau when solid fusion was achieved. The results were encouraging. By combining all the data from both spines and looking at both extension and compression, the strain did trend toward a plateau with increasing stiffness. Also, the magnitude was similar for both sheep spines and clustered into two groups, one for extension and one for flexion (Figure 33). A two degree polynomial trend line was added to show the trend of the data. Like actual fusion, the simulated fusion results varied based on the fusion's development, the orientation of the pedicle screws, and the preload in the spinal plate. Initially, there was considerable disparity between readings, but after 30 grams of simulated fusion, the results stabilized at a constant value. The resulting plateau was much more consistent for flexion than for extension.

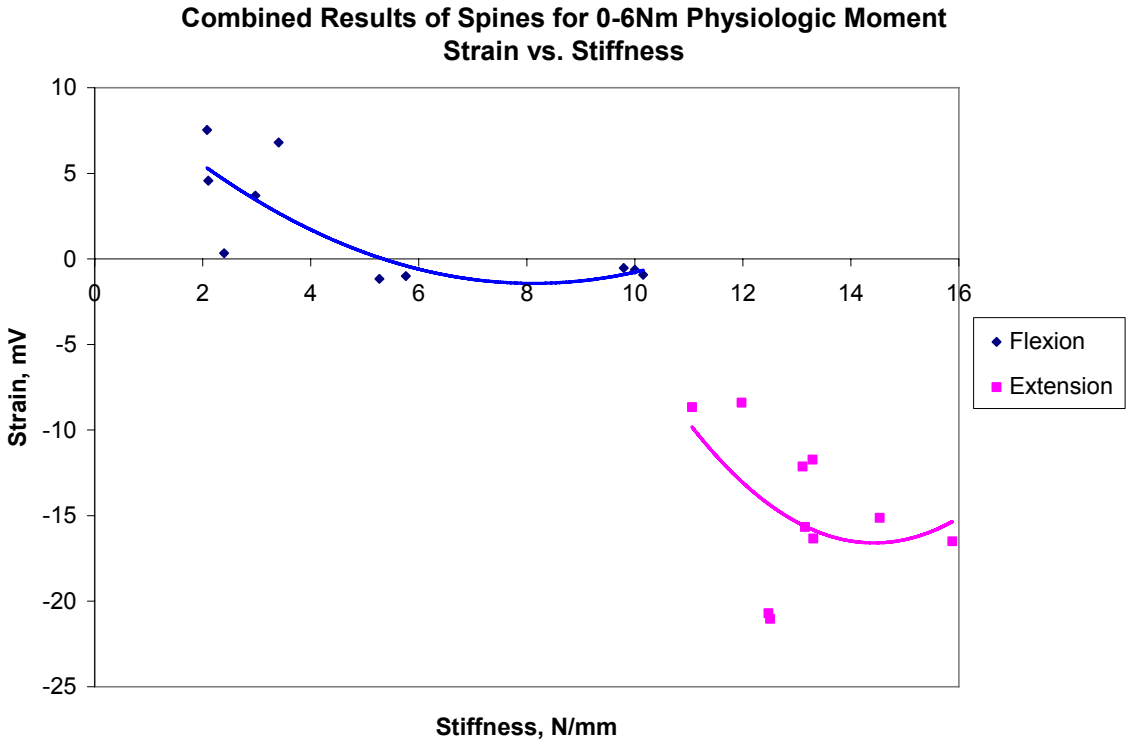

Figure 33, Comparison of Measured Strain vs. Fusion Mass Stiffness

iii. Cadaveric Study

From an early laboratory study with a mounted, instrumented cadaveric sheep spine in a universal test machine (Instron 1120), this study calculated a strain of about 25-50με when under a 5-6 Nm moment (Figures 34-36).

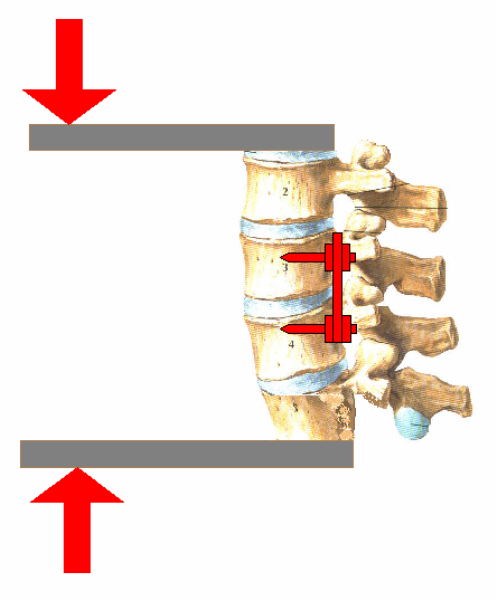

Figure 34, Lumbar Spine on Cantilevered Mounting Plates

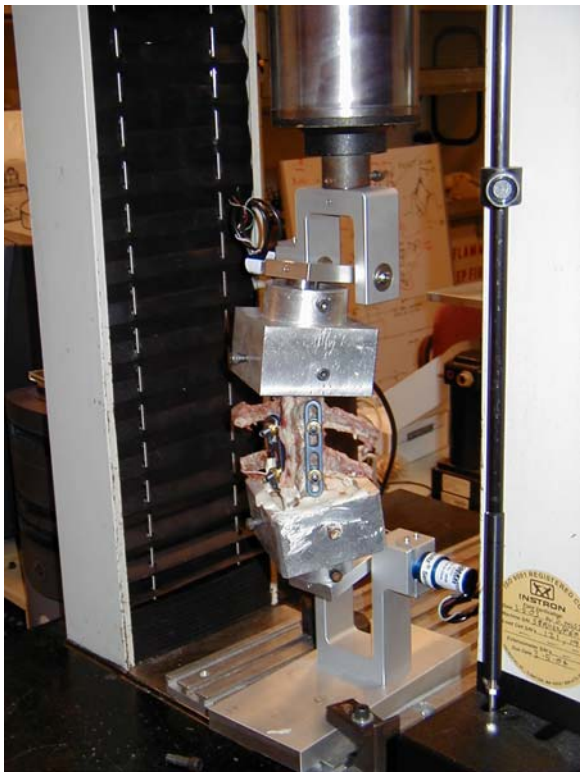

Figure 35, Cadaveric Sheep Spine in Test Stand on UTM

The test stand designed and built by this researcher was based on an earlier test stand constructed by Scott Yerby [121], specifically for this research project. Yerby's test stand allowed for measurement of the rotation at the two cantilevered plate ends for future measurement of the exact lever arm length and rotation angle, however, this study measured the lever arm manually.

Using a Micro Measurement CEA-series copper foil strain gage in a Wheatstone bridge with a calculated applied load of 43N for 5 Nm bending moment (the actual moment was closer to 3Nm due to a shortened lever arm), the cadaveric spine was tested in both flexion and extension with a resulting linear nearly one-to-one output relationship between strain and applied moment (Figure 36). The signal was amplified and conditioned using an Iotech signal conditioning box and a shunt resistor of 59kΩ. The output shown is after the preload of approximately 150με was subtracted.

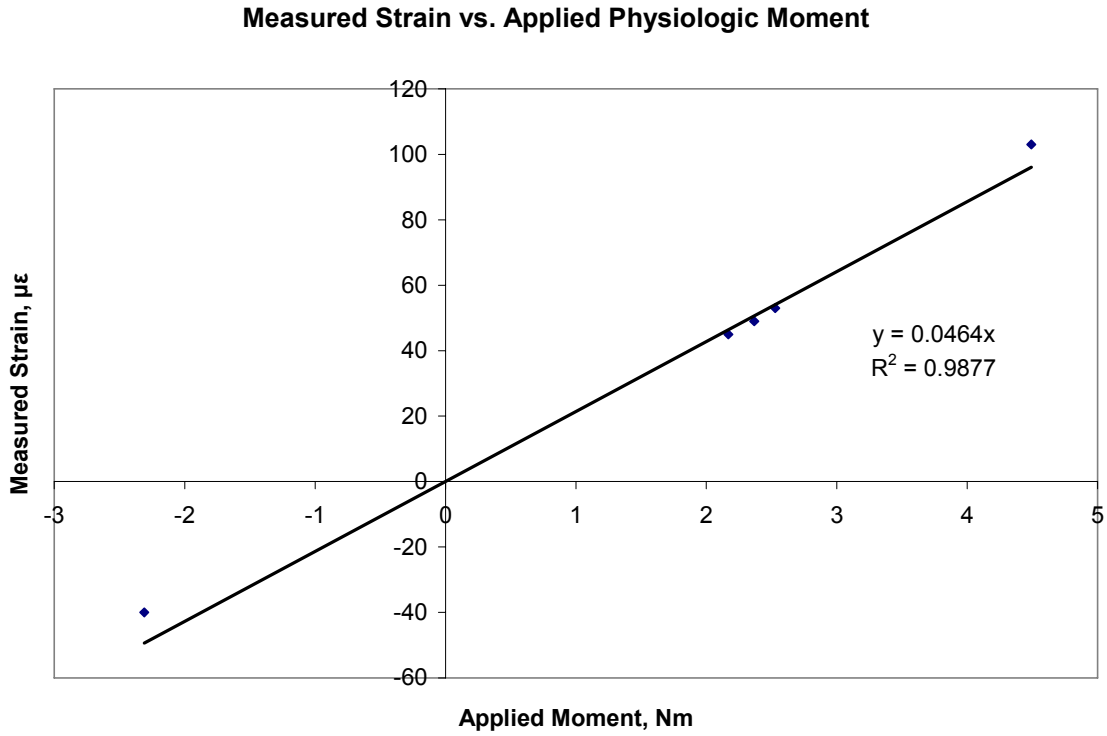

Figure 36, Measured Strain vs. Applied Moment

iv. Summary of MicroStrain device (sheep pilot study)

The system built by MicroStrain for the sheep pilot study (IACUC Protocol #10159) consisted of a spinal plate retrofitted with two semiconductor strain gages in a half bridge. The machined pocket containing the strain gages was hardwired to the transponder on pins 1 and 5. Inside the transponder, the half bridge was completed with 470Ω resistors in a Wheatstone bridge configuration (Figure 20).

Internal to the transponder, the MicroStrain device contained a 904MHz FM receiver. It also contained a Flash EEProm for storing the strain data over the four months. The base station on the laptop was

designed to interrogate the transponder every four hours for a total of six readings stored per day. Using AgileLink, a software based on LabView, the readings could be downloaded as often as desired onto the laptop for analysis (Figure 37).

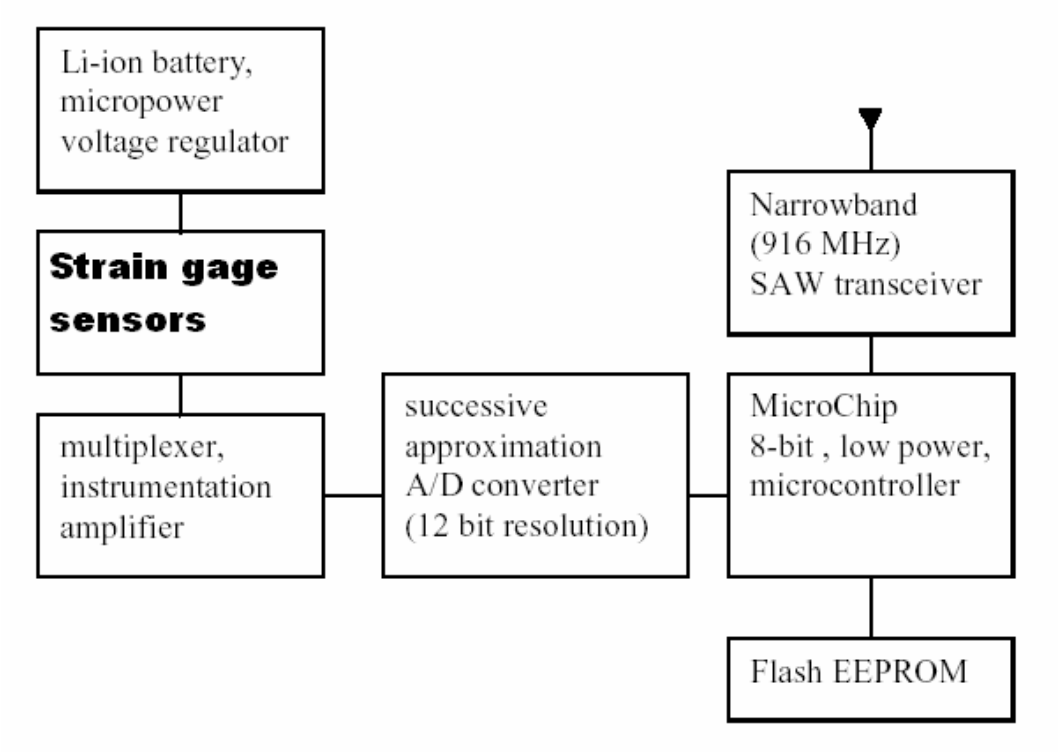

Figure 37, MicroStrain Standard Sensor System [118]

II. DISCUSSION

Based on the results of the sheep study using someone else's proprietary device, the researchers decided it was imperative to build their own sensor system in order to have full control over its design. Although the original goal of diagnosing the onset of spinal fusion using strain remained the same, the researchers had to step back from that goal and

prove that a sensor system could be built that functioned correctly every time.

Wireless transmission, although fraught with transmission range difficulties, still seemed like a promising method for transmitting the strain data to an external storage system. But most of the remaining components of the sensor system needed to be redesigned.

First, the strain gages were sensitive to temperature and the machined pocket contained three additional resistors for temperature compensation. In spite of that precaution, the four foot lead wires to the transponder definitely contributed some resistance and also temperature affects to the strain reading. Sheep 324 developed an infection and ran a fever for two weeks early in the study, which delayed the onset of fusion by at least those two weeks. How the fever affected the strain readings was unknown. The researchers felt it was thus important to consider sensors other than strain gages in their pursuit of the best method of measuring spinal fusion.

If the designed sensor could be made small enough, then it could also be retrofitted into existing spinal implants, allowing it to be used in all existing designs and increasing its popularity. MEMS is a well-established field for making other types of sensors, so the researchers wanted to incorporate microfabrication into their design if possible.

Finally, the entire MicroStrain system was dependent on batteries. It is unclear if the battery power affected the output in some kind of degrading pattern, perhaps explaining part of the slope in the databit output, but in a human application, batteries are difficult to get approved by the FDA. As they are filled with toxic substances, they are highly regulated, and necessarily limit the lifespan of the sensor. If the researchers were to design their own sensor system, they wanted to avoid the use of batteries. They also wanted to choose a transmission system that was safe for humans with minimal to no side effects of tissue heating, cell function altering, etc.

CHAPTER 3

Sensor System Design

I. INTRODUCTION

Rather than arbitrarily choose a design based on the preferences and experience of this researcher, a methodical approach for choosing each of the main subcomponents of the design was employed. Although many such methods exists, one that has been popular for twenty years is the Kepner Tregoe (KT) matrix system [122]. The KT Analysis is a well-orchestrated and documented root cause analysis and decision making method used by companies worldwide. The basic approach is as follows:

1. Prepare a decision statement (goal) for the design.
2. Establish requirements (musts), objectives (wants), and constraints (limits).
3. Rank the objectives and establish weights.
4. Generate alternatives that achieve the goal.
5. Assign a relative score for each alternative against the objectives.
6. Calculate the weighted score to select the top two or three best choices.
7. Evaluate the risk and probability of success for each top choice and select the best one.

II. DESIGN OPTION FEASIBILITY STUDY

As is commonly used in industry, this study has defined matrices of constraints and objectives and compared those with available design options. This researcher has modified the standard KT Analysis to allow for discussion of constraints rather than a “yes/no” check or weight for each constraint column. The design options are also further subdivided into three main subsystems rather than looking at the entire design as one, unified system. These subsystems are:

1. Sensing Options
2. Power Options
3. Communication Options

The constraints identified by this researcher are:

1. Lifespan of design option
2. Transmission range
3. Safety
4. Sensitivity to signal generated
5. Cost
6. Existing technologies available to test
7. Reliability of method
8. Noise sensitivity and what type(s) of noise
9. Accuracy
10. Repeatability of method

11. End user's usability
12. Operating conditions design option requires
13. Ancillary impacts on the patient

The full KT analysis is included below, "KT Analysis of Options vs. Constraints", (Table 1-3), and has been divided into three tables for legibility by subsystem. For legibility, each table has been divided between two pages.

This electronic strain measurement system is designed to replace clinical x-rays, as they are often inconclusive until the bone has completely mineralized. During surgery, one of the spinal plates would be replaced with an electronically instrumented spinal plate. For humans, the goal would be to have all the instrumentation hermetically embedded in an otherwise unaltered spinal plate.

A handheld unit would be brought into proximity of the sensor and an initial strain level would be recorded. Then, during routine office visits, the handheld sensor would again be brought into proximity of the sensor to get additional strain level recordings. Over time, the level of strain should decrease, if fusion is occurring, and eventually plateau at a lower level. This research study has shown that this will occur within eight to twelve weeks following surgery, at which time the fusion could be proclaimed solid and the patient's external bracing removed.

Sensing Options	Lifespan	Tx Range	Safety	Sensitivity	Cost	Existing Technologies
Piezoresistive strain gages	Unlimited	N/A	Materials limited to biocompatible choices, such as Si	Can be easily fabricated to the microstrain level, over 100x more sensitive than foil strain gages	Commercially available at low cost.	Readily available from multiple sources (ie Soltec, Micron)
Capacitive strain gages	Unlimited	N/A	Materials limited to biocompatible choices, such as Si	Can be easily fabricated to the microstrain level	Not commercially available. Needs to be custom made.	Not available
Photoelectric strain gages	Limited by visibility through optical window over time	Need to shine optical beam that penetrates tissue (short range)	Optical beams may adversely heat or excite tissue	Dependent on distance to source and resolution of imager	Not commercially available. Needs to be custom made.	Large version available for testing from FISO Technologies
Optical Fringes	Limited by exposed photolithographic layer	Need to shine optical beam that penetrates tissue (short range)	Optical beams may adversely heat or excite tissue	Dependent on distance to source and resolution of imager	Not commercially available. Needs to be custom made.	Not available
Spectroscopy	Limited by clarity of grating spacing over time	Need to shine optical beam that penetrates tissue (short range)	Optical beams may adversely heat or excite tissue	Dependent on distance to source, resolution of imager and wavelengths	Not commercially available. Needs to be custom made.	Not available
Acoustics of component	Unlimited	Need to apply range of acoustic waves. Short distances only.	Safe	Dependent on geometry of acoustic element (string)	Not commercially available. Needs to be custom made.	Not available

Table 1A Sensing Options vs. Constraints

Sensing Options	Reliability	Noise Sensitivity	Signal Strength	Accuracy	Repeatability	Operating Conditions	Ancillary Impacts to Patient
Piezoresistive strain gages	Must be used in a 4-arm bridge with redundancy	Sensitive to electric noise and thermal changes	Can be increased with 4-arm bridge and multiple bridges.	Highly dependent on gage placement. Perhaps rosette?	Highly dependent on gage placement. Perhaps rosette?	Uncertainty varies with temperature and implant placement	No impact. Biocompatible material
Capacitive strain gages	Redundancy is best choice.	Not sensitive to electrical noise. Can have parasitic capacitance	Can be increased by number of combs. Can be used in 4-arm bridge.	Gage placement important. Fabrication difficult.	Gage placement important.	Gage placement important.	No impact. Biocompatible material
Photoelectric strain gages	Unknown	Not sensitive to electrical noise.	Unknown	Unknown	Gage placement important.	Gage placement important.	May pick up stray infrared noise, causing heating of tissue.
Optical Fringes	Unknown	Not sensitive to electrical noise.	Unknown	Unknown	Gage placement important.	Gage placement important.	No impact. Biocompatible material
Spectroscopy	Unknown	Not sensitive to electrical noise.	Unknown	Unknown	Gage placement important.	Gage placement important.	No impact. Biocompatible material
Acoustics of component	Unknown	Not sensitive to electrical noise.	Unknown	Unknown	Independent of placement, but dependent on geometry of string	Independent of placement, but dependent on geometry of string	May pick up stray acoustic vibrations from environment similar to dental work.

Table 1B Sensing Options vs. Constraints

Power Options	Lifespan	Tx Range	Safety	Cost	Existing Technologies	Reliability
Battery	Limited to months for wireless transmission	Allows long distance transmission of signals	Difficult to get FDA approval. Toxic and best for short term only.	Commercially available at low cost.	Readily available from multiple sources.	Requires monitor of power remaining
Inductive coil	Unlimited	Need to power magnetic coil from short distances only.	Inductance and magnetism may adversely affect tissue	Commercially available at low cost.	Large version available for testing from Microstrain	Reliable
Fuel cell	Order of magnitude better life than batteries.	Allows long distance transmission of signals	Difficult to get FDA approval. Toxic and best for short term only.	Few sizes commercially available. High cost.	Large versions available for testing	Requires monitor of power remaining
Scavenged energy (solar, ionic, chemical)	Unlimited	Low level power source works best over short distances.	Uses conditions already present in body, so safe.	Not commercially available. Needs to be custom made.	Large versions available for testing solar. Others require lab work.	Unknown
Thermoelectric conversion	Unlimited	Low level power source works best over short distances.	Uses conditions already present in body, so safe.	Not commercially available. Needs to be custom made.	Not available	Unknown

Table 2A Power Options vs. Constraints

Power Options	Noise Sensitivity	Operating Conditions	Ancillary Impacts to Patient	End User Usability
Battery	N/A	Works well in human body conditions if hermetically sealed.	Could be mounted subcutaneously for replacement	Leakage from battery housing failure would be toxic.
Inductive coil	Sensitive to electrical noise and magnetic fields	Used in office setting in good conditions	Could be operated by end user to power circuit	Magnetic field might create inductive reaction, heating tissue.
Fuel cell	N/A	Works well in human body conditions if hermetically sealed.	Could be mounted subcutaneous for replacement	Leakage from fuel cell housing failure would be toxic.
Scavenged energy (solar, ionic, chemical)	Unknown	Uncertainty would vary with solar conditions, ionic conditions of patient, etc.	Solar would require end user education. Others would be N/A.	Unknown
Thermoelectric conversion	Unknown	Uncertainty would vary with body temperature and placement.	N/A	Unknown

Table 2B Power Options vs. Constraints

Communication Options	Lifespan	Tx Range	Safety	Sensitivity	Cost	Existing Technologies
RF transmission	Unlimited	Power decreases by square of distance, so short distances best.	Limited to FCC spectrum and frequencies safe for humans.	Sensitive to stray signal interference and magnetic fields	Commercially available at low cost.	Large versions available for testing
Microwave transmission	Unlimited	Power decreases by square of distance, so short distances best.	Limited to FCC spectrum and frequencies (if any) safe for humans.	Sensitive to stray signal interference and magnetic fields	Not commercially available. Needs to be custom made.	Not available
Hardwired	Limited by feasibility of leaving wires passing through tissue	Allows long distance transmission of signals	Prone to infection and damage of hardware. Materials need to be biocompatible.	Can be easily fabricated to be highly sensitive	Commercially available at low cost.	Readily available from multiple sources
Optical	Unlimited	Very fast. Requires line-of-sight conditions, mid-range.	External optics prone to infection and damage of hardware.	Can be easily fabricated to be highly sensitive	Commercially available at low cost.	Readily available from multiple sources
Acoustic	Unlimited	Very fast. Best with line-of-sight conditions, short range if internal.	Internal acoustics limited to biocompatible choices. May adversely affect tissues.	Limited by transmission through tissues and acoustic noise in office.	Not commercially available. Needs to be custom made.	Large versions available for testing
Passive RF	Unlimited	Short range	Safe. Materials limited to biocompatible choices, such as Si	Dependent on distance to source	Commercially available at low cost.	Readily available from multiple sources

Table 3A Communication Options vs. Constraints

Communication Options	Reliability	Noise Sensitivity	Accuracy	Repeatability	Operating Conditions	Ancillary Impacts to Patient	End User Usability
RF transmission	Sensitive to electrical noise and magnetic fields	Sensitive to electrical noise and magnetic fields	Subject to interference.	Subject to interference.	Used in office setting in good conditions	RF would require end user education	May pick up stray acoustic vibrations from environment.
Microwave transmission	Unknown	Sensitive to electrical noise and magnetic fields	Subject to interference.	Subject to interference.	Used in office setting in good conditions	Microwave would require end user education	May pick up stray acoustic vibrations from environment.
Hardwired	Reliable	Somewhat sensitive to electrical noise, but can be filtered.	Accurate	Repeatable	End user would need education on keeping site clean and dry.	End user would need education on keeping site clean and dry.	Possibility of infection.
Optical	Reliable over short distances in office setting.	Not sensitive to electrical noise.	Accurate	Repeatable	Optical port would have to be exposed to operate properly.	End user would need education on keeping site clean and dry.	May pick up stray infrared noise, causing heating of tissue.
Acoustic	Unknown	Not sensitive to electrical noise.	Unknown	Unknown	May need acoustically silent environment to operate properly.	N/A	May pick up stray acoustic vibrations from environment.
Passive RF	Dependent on distance to source	Sensitive to electrical noise and magnetic fields	Unknown for varying output	Repeatable	Used in office setting in good conditions	Easy to use	May pick up stray acoustic vibrations from environment.

Table 3B Communication Options vs. Constraints

Based on the above analysis and what this researcher learned from the literature review and pilot sheep study, the most feasible sensing options are piezoresistive strain, capacitive strain, or acoustic ‘ring down” with an embedded wire. Feasibility is based on the design option having the fewest unknowns, most literature on the topic, and highest safety for the patient. The most feasible power options are battery, supplied RF power from the receiver, inductive coil, and fuel cell. And the most feasible transmission options are RF transmission, passive RF transmission, or hardwiring. Using the above set of identified most feasible design options for each subsystem, a second KT analysis matrix compares each feasible design option with weighted design objectives. Some objectives are more necessary for a successful, safe design than others and are thus weighted more heavily than those objectives that would just be nice features. The weighting factors of 1 through 5 are applied to each objective based mainly on safety for the patient. If a factor is critical for patient safety, it receives a weight of 5. The identified objectives are:

1. Battery-free operation with power supplied by the external receiver.
2. Small form factor for entire system so it can be embedded in the spinal implant without sacrificing structural integrity of the implant.

3. Encapsulated, hermetically sealed environment to avoid fluid issues.
4. Unlimited lifespan for lifetime monitoring of spinal fusion.
5. Low manufacturing cost to enhance acceptance and thus market share.
6. Utilization of off-the-shelf components to decrease cost and increase reliability.
7. Low noise and low impedance to maximize signal strength and integrity.
8. Patentability to provide protection for design approach and add value for potential investors.
9. All biocompatible materials to minimize complications for patient and with FDA.
10. Insensitivity to environmental changes, such as body temperature, chemical changes, magnetic fields, and human activity (self or externally applied forces, vibrations, etc).
11. Insensitivity to installment in implant and implantation in patient, such as to orientation, preload, and rough handling.
12. No ancillary effects on patient.

	Battery-free Operation	Small Form Factor	Hermetically Encapsulated	Unlimited Lifespan	Low Cost	Off-the-Shelf Technologies	Low Noise & Impedance Issues	Patentability	Biocompatible Materials	Insensitivity to Environment	Insensitivity to Installation	No Ancillary Effects	Score (out of 330 maximum)
Weight for Objective:	2	5	5	2	1	1	2	1	5	5	3	1	33
Sensing Options													
Piezoresistive strain gages	10	10	10	10	10	10	3	1	10	5	5	10	267
Capacitive strain gages	10	10	10	10	6	3	6	7	10	9	7	10	294
Acoustic "ring down"	10	10	10	10	10	5	5	7	10	9	10	8	305
Power Options													
Battery	0	1	5	0	10	10	10	1	1	10	10	5	161
Fuel cell	0	1	5	0	8	10	10	1	1	10	10	5	159
Inductive coil	10	7	10	10	10	5	3	7	8	5	7	2	241
Supplied RF power	10	10	10	10	6	8	4	6	10	5	7	5	269
Communication Options													
RF transmission	10	10	10	10	8	8	5	5	10	5	7	10	277
Passive RF	10	10	10	10	10	10	5	1	10	5	7	10	277
Hardwired	1	5	3	4	10	10	10	1	5	10	10	2	198

Table 4 Feasible Design Options vs. Weighted Constraints

From this analysis, this design study reduced the feasible design options for each subsystem to the one or two options that would best meet the design constraints and objectives. For this design, it was concluded that:

1. For sensing the offloading of the spinal plate as the bony fusion forms, the best option appears to be acoustic “ring down”, followed closely by capacitive strain gage sensors. As acoustic “ring down” had a higher risk of failure, the design for this study will be a capacitive sensor.

2. The best option for powering the sensor is supplied RF power from the external system, followed by an inductive coil. As radio frequency transponders are a well-developed market for RFID, this design will use supplied RF power from the external handheld device.

3. The best means of communicating the information is either RF transmission with an active transponder or with a passive RF transponder. For ease of use and design simplicity, this design will use a passive RF transponder.

III. DESIGN OPTION ANALYSIS SUMMARY

Based on the results of the KT Analysis and the objectives for this design, the following system will be designed:

1. Capacitive sensor for measuring the strain in the spinal plate.
2. Radio frequency wireless transmission of the strain data to an external receiver.

3. Battery-free operation powered by the RF signal coming from the external receiver.

IV. SENSOR SUBSYSTEMS

A. Capacitive Sensors

When using capacitance as a MEMS sensor, two choices are available. The first flexes a membrane, thus changing the gap of the dielectric medium, usually air. This in turn alters the capacitance, but it is a complex, nonlinear relationship. The second choice is to use plates with a constant gap and change their overlapping area. The advantages of this alternative are many. First, the amount of overlapping area can be easily changed by adding more plates, the relationship between area and capacitance is linear, and this is a well understood MEMS fabrication process. The design of this study's MEMS interdigitated capacitive sensor is described later in this report.

B. Wireless Transmission Subsystem

i. Safety

The controlling factor in the design of the RF system was the frequency at which the carrier signal would be transmitted, as this frequency controls the dimensions of components in the RF system such as the antenna. For the purpose of the design, a frequency of between 900 MHz and 1 GHz was chosen to be transmitted out of the implanted system. The high frequency had better propagation characteristics, larger

available bandwidth [123], was safe for human exposure for durations up to six minutes [124], and was needed to reduce the size of the antenna. Patient safety concerns determined the choice to use frequency modulation for signal transmission. There are three types of signal modulation; frequency modulation (FM), amplitude modulation (AM), and pulse modulation (PM). PM has the most damage to biological tissues due to the high energy release during short time periods. On the other hand, AM is more susceptible to noise while being transmitted through biological tissue and that can cause false data readings. Consequently, frequency modulation (FM) was chosen because its amplitude is not relevant to the data transmitted and is safer than PM. Additional advantage of FM is the ability to have greater noise immunity at greater bandwidths [125].

FDA approval is also required for all biomedical devices. Wireless transmission was approved for pacemakers back in 2001 and thus serves as a standard for all other wireless devices [126]. According to the article, this new pacemaker “contains a tiny transmitter that automatically sends data on the patient's heart condition to the doctor between office visits [and] is the first implanted medical device to be approved that is capable of automatic, remote data transmission.” Since the spinal fusion sensor would not automatically transmit, its approval would be much simpler.

ii. Tissue heating

Tissue heating is of great concern in all wireless transmission through the body. To be safe, this design chose a frequency below that used by approved medical devices for pain management. These generally operate in the infrared region at high frequencies above 6GHz, where tissue heating dominates [127]. In the Ultra High Frequency range this design selected, 300MHz to 3GHz, the frequency is low enough to avoid tissue heating for short duration exposures, but high enough to avoid interacting with the tissue biologically through its magnetic field [128].

According to Gregory Lapin, “other biological processes have been shown to be affected by levels of RF energy that do not produce significant amounts of heat in tissue. These are all reversible effects (they go away when the RF energy is removed) and include change of operation of the calcium channels in cells, stimulation of the retina and optical nervous system to produce false perception of light, stimulation of the cochlea and auditory nervous system to produce false perception of sound, stimulation of nerve ending to produce a tingling sensation, and others.” Fortunately, there is no indication that any of these effects are harmful to humans [128].

iii. Range for radio frequency transmission

According to Vaughn, radio frequency power attenuates each time the distance is doubled in free space, but the behavior through salt water is much less predictable, because the resistive loss behavior is a complicated function of frequency. “There are resistive losses in the water, and the inverse square law,

which appears much more strongly than in the free space case because for a given distance, there are many more wavelengths that the wave propagates. ”For fresh water, the wavelength is about one ninth the length of the wavelength in free space [129].

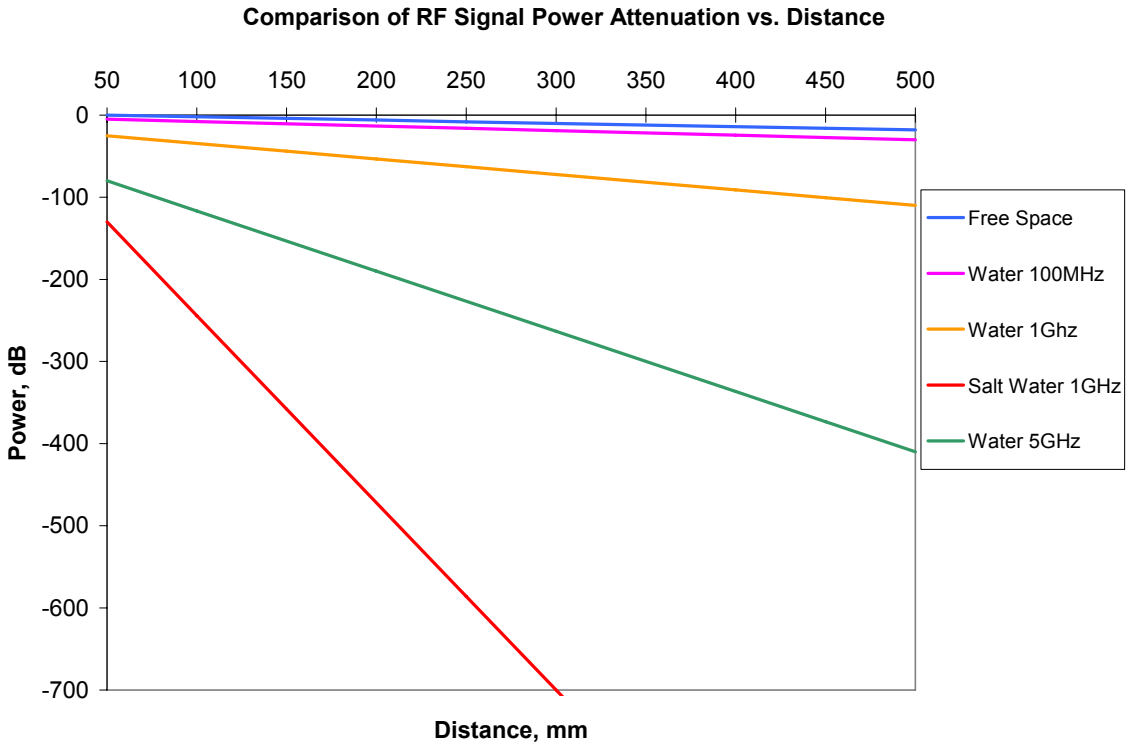

Figure 38, Radio Frequency Signal Attenuation vs. Distance [129]

The graph above (Figure 38) from Vaughn helps explain signal attenuation in free space, fresh water, and salt water. The x-axis is distance in millimeters. The y-scale is in dB. At the top of the graph, the blue line is the average power loss with distance in free space at 1GHz. As the frequency goes up, the loss increases for a given distance. For example, at a distance of 500mm, a frequency of 10GHz would drop its power by about 50dB on this scale. The

inverse square law states that the power loss is proportional to the inverse of the distance (in wavelengths) squared. “Each time the distance is doubled, the inverse square power law means that another 6dB of power is lost. For radio frequency in fresh water, the power loss is shown for four frequencies, 100MHz, 1GHz, 5GHz, and 10GHz. Salt water is shown at the frequency of interest, 1GHz. Muscle tissue is more dense than salt water, so its attenuation will be even greater, thus increasing the power requirement of the transponder.

From the pilot sheep study, this study learned that the signal transmission distance degraded from over 20m in free space to only 1m after implantation subcutaneously about 2cm. As this study’s design intends to implant the sensor within the spinal implant hardware, placement of the antenna will be deeper.

To simulated a worst case scenario, the MicroStrain transponder was buried within 15cm of bovine muscle tissue and covered with clothing to represent a very large, clothed human, and was then queried wirelessly at increasing distances until the data no longer streamed. The maximum distance was 0.5m, proving that wireless transmission would work without the need for the patient to undress. For this design, instructions will be included, showing that the handheld receiver should be held against the patient for best results.

iv. Battery-free operation

Many options exist for battery-free operation, but the simplest is to use the carrier frequency as the power source for a passive sensor, like a radio frequency identification device (RFID) [130]. The available power from the transponder is reduced rapidly with distance, resulting in a limited

communication distance. Typical reading distances are zero to 5m for 860 MHz to 930 MHz, which correlates well with the pilot sheep study. Also, passive sensors have an unlimited lifespan, as they require no batteries and thus can be made from biocompatible materials.

v. Posture

As is easily seen from the strain vs. moment studies, posture will have a profound effect on the measure strain prior to solid fusion. Thus, a controlled posture prior to measurement will be outlined in the surgeon's instructions. The best posture will probably be standing in a neutral upright erect posture against a wall with arms at side.

C. Assembly of System

The sensor system will consist of several parts, the capacitive sensor, the integrated circuit to amplify and transmit the output, the antenna, the handheld receiver, and the software. All of these components can be purchased off-the-shelf except the sensor itself, so they will not be developed further in this design report.

Chapter 4

Design and Testing of Interdigitated Capacitive Sensor

I. INTRODUCTION

To reiterate, this design used an area variation capacitive sensor because it was insensitive to temperature and provided a linear output with change in strain. The following chapter is the design of an interdigitated capacitive sensor of the appropriate geometry to meet the size and resolution requirements to detect the onset of spinal fusion.

II. THEORY

Based on earlier testing, the minimum distinguishable strain reading was set at 25 με. The sheep study showed that the actual strain ranged over 100 με, so this value is a conservative low value of resolution.

After deciding on an area variation sensor (Figure 39a), calculations revealed that a capacitance change due to 25μm of strain is on the scale of 10^{-16} F and therefore, too small of a change to measure accurately. To resolve this issue, an interdigitated capacitor design (Figure 39b) was implemented as the most effective way to maximize the capacitance measurement. A design using fifty-one free-standing, interdigitated fingers results in fifty parallel plate capacitors adding to the total capacitance measurement. As a result, the designed sensor will be able to sense a capacitance on the order of 10^{-14} F. The capacitance sensing relies on the lateral movement of the interdigitated fingers. The change in area between

the fingers due to the lateral movement results in a change of capacitance. The basic equation for parallel-plate capacitance is

$$C = \frac{\{\varepsilon_o \varepsilon_r A(n-1)\}}{d} = \frac{\varepsilon_o \varepsilon_r (wl)(n-1)}{d} \qquad [120]$$

where ε_o= 8.85x10^{-12} F/m is the permittivity of free space, ε_r = 1 is the permittivity of air, "A" is the area of the plates, "d" is the gap between the plates, "w" is the width of the plates, "l" is the length of the plates, and "n" is the number of interdigitated fingers.

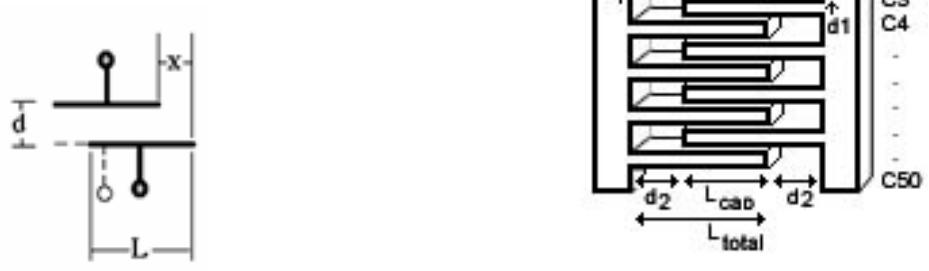

Figure 39: (a) Area Variation Motion Sensor (b) Spinal Fusion Micro-sensor

Images from http://design.stanford.edu/Courses/me220/list.html#notes

Before spinal fusion occurs, there will be a strain induced from the bending of the vertebrate. By placing the capacitance sensor in the direction of this strain, a lateral movement of the plates will cause the area

of the capacitor to change (Figure 39a, 39b). The capacitance can then be calculated using

$$C = \frac{\varepsilon_o \varepsilon_r w(l-x)(n-1)}{d} \qquad [120]$$

where "x" is the amount of displacement due to the strain (25 μm).

In addition to the capacitance created between each of the fingers, there is also a capacitance created between the tip of each finger and the opposing base. This capacitance changes as the gap between the finger and the base varies. Because the desired overall capacitance needed to be a function of only the lateral variation capacitance between the fingers, the sensor was designed to minimize any capacitances that might result from tip of each finger and the opposite base. As a result, the gap, "d_2", was set to be 50μm.

The capacitor dimensions were chosen such that maximum displacement due to strain could be sensed. According to Tang [131], interdigitated fingers remain free standing and function properly as long as the length of each finger does not exceed 200μm. For this reason, the total length of each finger, L_{Total}, was 200μm. The remaining 150μm was assigned to the capacitance length, L_{Cap} (Figure 39b). By using the relationship between capacitance, length, width, and gap, a large length and large width and a small gap are desired for a large capacitance value. Consequently, the chosen dimensions were length "L_{Cap}" of 150μm, width

"W_{Cap}" of 20μm, gap "d_1" of 5μm, and height "h" of 20μm. Using 51 interdigitated fingers, the resulting capacitance under no strain was

$$C_{NoStrain} = \frac{\varepsilon_o \varepsilon_r (wl)}{d}(n-1) = \frac{\left(8.85x10^{-12}\frac{F}{m}\right)(1)(5x10^{-6}m)(150x10^{-6}m)}{10x10^{-6}m}(50)$$

$$C_{NoStrain} = 3.34x10^{-14}F$$

During a strain of 25μm, the capacitance would be

$$C_{25\mu\varepsilon} = \frac{\varepsilon_o \varepsilon_r (wl)}{d}(n-1) = \frac{\left(8.85x10^{-12}\frac{F}{m}\right)(1)(5x10^{-6}m)(150x10^{-6}m - 25x10^{-6}m)}{10x10^{-6}m}(50)$$

$$C_{25\mu\varepsilon} = 2.60x10^{-14}F$$

By carefully choosing these dimensions, the design should maximize the capacitance measurement of the sensor.

Since capacitance and motion are linearly related for an area variation sensor, the capacitance can be measured directly [51]. However, a transducer is needed to translate the capacitance change response to an electrical output signal [132]. Capacitance bridges are commonly used as transducers to convert the capacitance changes into an electrical voltage output, so a capacitance bridge was used for this design [51].

The designed capacitance bridge combined the capacitances of all fifty capacitors as one of the four legs, C_T, of the capacitance bridge (Figure 40). The other three legs (C_{ref1}, C_{ref2}, and C_{ref3}) were set as

reference capacitors. The reference capacitors being equal to C_T during no strain:

$$C_{ref1} = C_{ref2} = C_{ref3} = C_{T\_\text{No Strain}} = 3.34\text{x}10^{-14}\ \text{F}$$

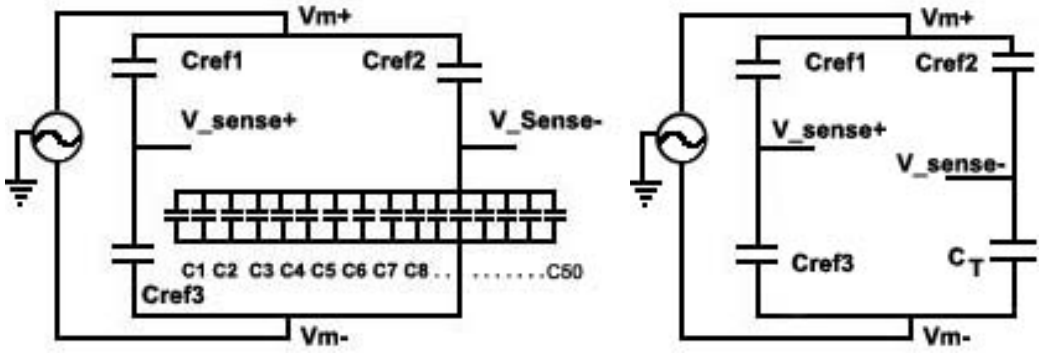

Figure 40: (a) (b)

Figure 40, Capacitive Bridge Circuit Diagram

When spinal fusion has occurred, and if no strain were present, the expected voltage output at Vsense+ would be equal to the voltage output at Vsense-.

$$V_{sense+} = \frac{C_{ref1}(2V_m)}{C_{ref1}+C_{ref3}} - V_m = \frac{C_{ref1}(2V_m) - (C_{ref1}+C_{ref3})V_m}{C_{ref1}+C_{ref3}} = \frac{(C_{ref1}-C_{ref3})V_m}{C_{ref1}+C_{ref3}}$$

$$V_{sense-} = \frac{C_{ref2}(2V_m)}{C_{ref2}+C_T} - V_m = \frac{C_{ref2}(2V_m) - (C_{ref2}+C_T)V_m}{C_{ref2}+C_T} = \frac{(C_{ref2}-C_T)V_m}{C_{ref2}+C_T}$$

However, before spinal fusion has occurred, strain would be induced due to the bending of the vertebrate. During this time, there would be a

difference between the output voltages, V_{sense+} and V_{sense-}. This could then be amplified and transmitted with a difference amplifier [133].

Rather than design a new circuit to meet the needs of this sensor, the researchers would adapt an Analog Devices capacitance-to-digital converter, similar to the one shown in Figure 41 below to amplify and convert the signal to a digital voltage output.

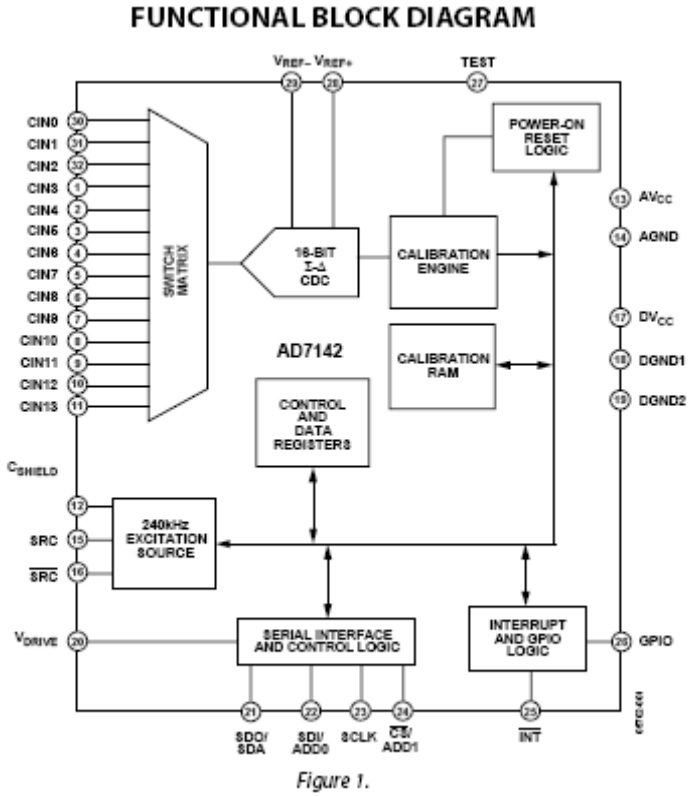

Figure 41, Analog Devices AD7142 Capacitance to Digital Converter

Finally, the transducer output voltage, Vo, could be calculated using:

$$V_o = a_{cm}\left(\frac{V_{sense+} + V_{sense-}}{2}\right) - a_{dm}\left(\frac{V_{sense+} - V_{sense-}}{2}\right) \qquad [10]$$

where a_{cm} and a_{dm} are the amplifying common mode and differential mode gains.

III. PROTOTYPE TESTING

Using the equations for capacitance, this study designed a large scale prototype capacitor out of 0.5mm stainless steel sheet. As shown in Figures 42 and 43, the prototype had 20 interdigitated fingers with the following dimensions:

$$w = 0.5mm$$
$$l_o = 3.8mm$$
$$A = wl_o = (0.0005m)(0.0038m) = 1.90x10^{-6}\,m^2$$
$$d = 0.15mm$$

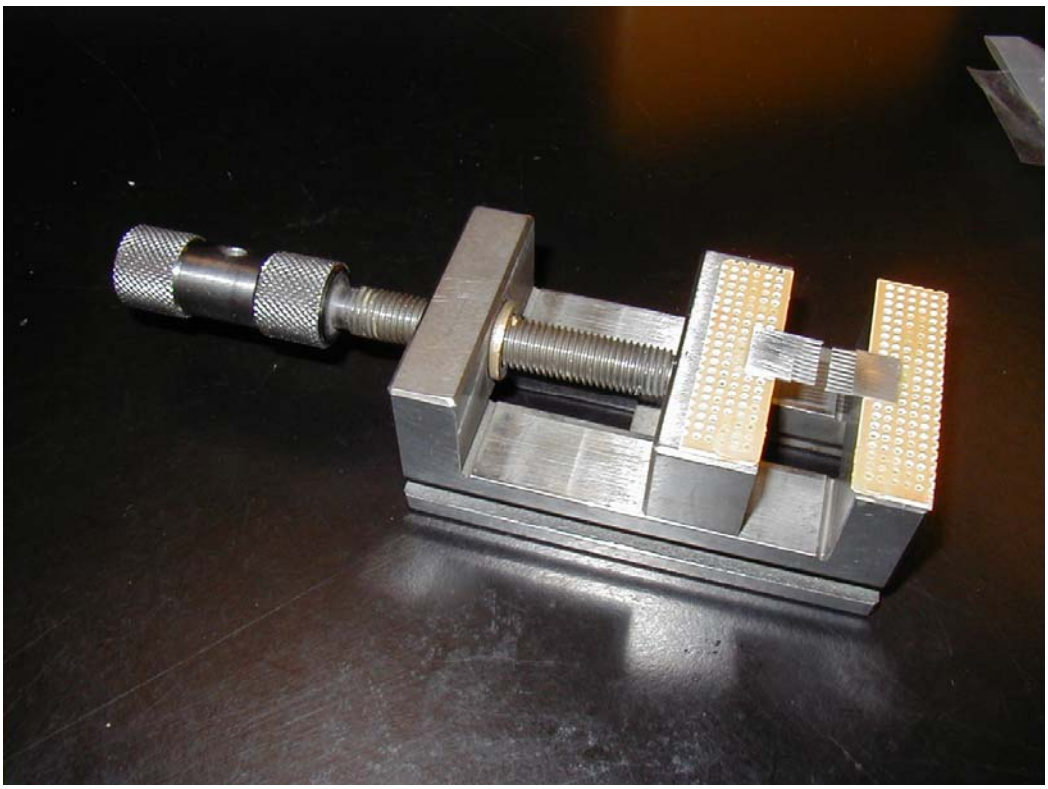

Figure 42, Interdigitated Capacitor Prototype on Vise

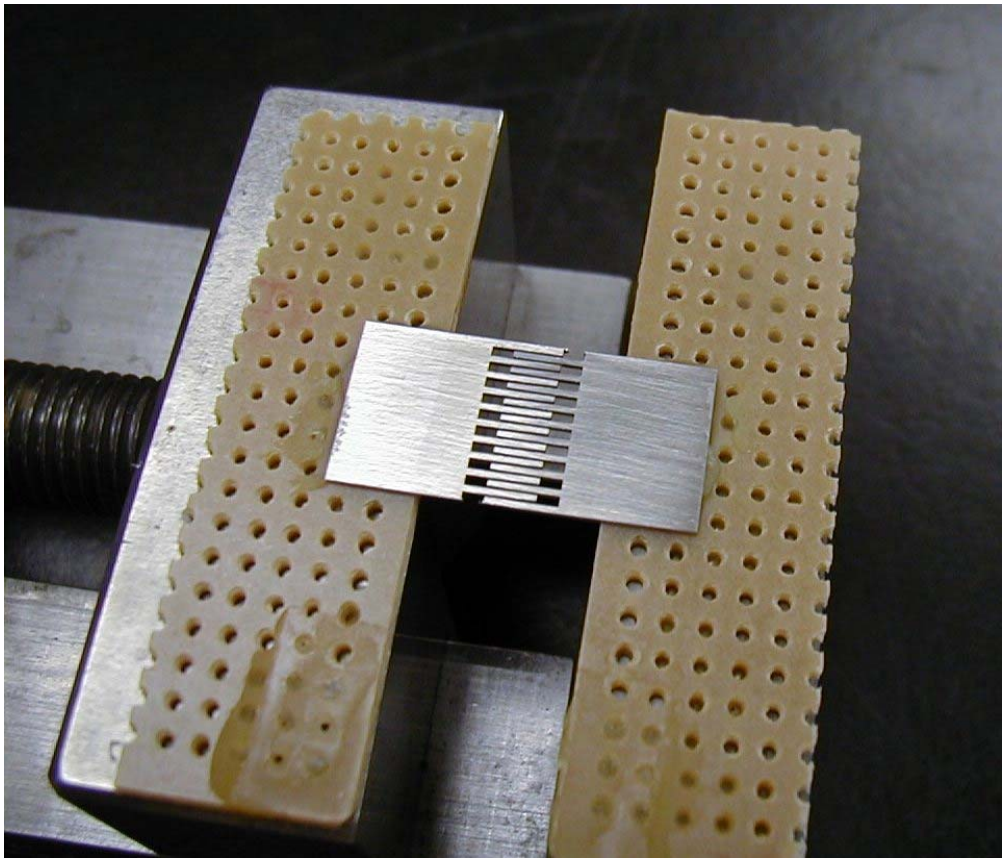

Figure 43, Close-up of prototype capacitor on fiberglass base

With these dimensions, the capacitance could be calculated for any overlap, from zero to 5mm. The nominal overlap value of 3.8mm gave a resulting theoretical capacitance of 2.13pF as shown below:

$$C = \frac{\varepsilon_o \varepsilon_r A}{d}(n-1) = \frac{\left(8.8541x10^{-12}\,\frac{F}{m}\right)(1)\left(1.90x10^{-6}\,m^2\right)}{0.00015m}(19) = 2.13\,pF$$

This result was then verified with laboratory testing. As shown in Figure 43 above, the capacitor was electrically isolated from the test vice with a piece of 1mm fiberglass board. Using a digital multimeter capable of measuring capacitance to 0.001nF (Fluke 189 True RMS), the researchers

adjusted the overlap from its minimal to maximal overlap and obtained the graph in Figure 44. Also shown on the graph is the theoretical expected capacitance from the calculations.

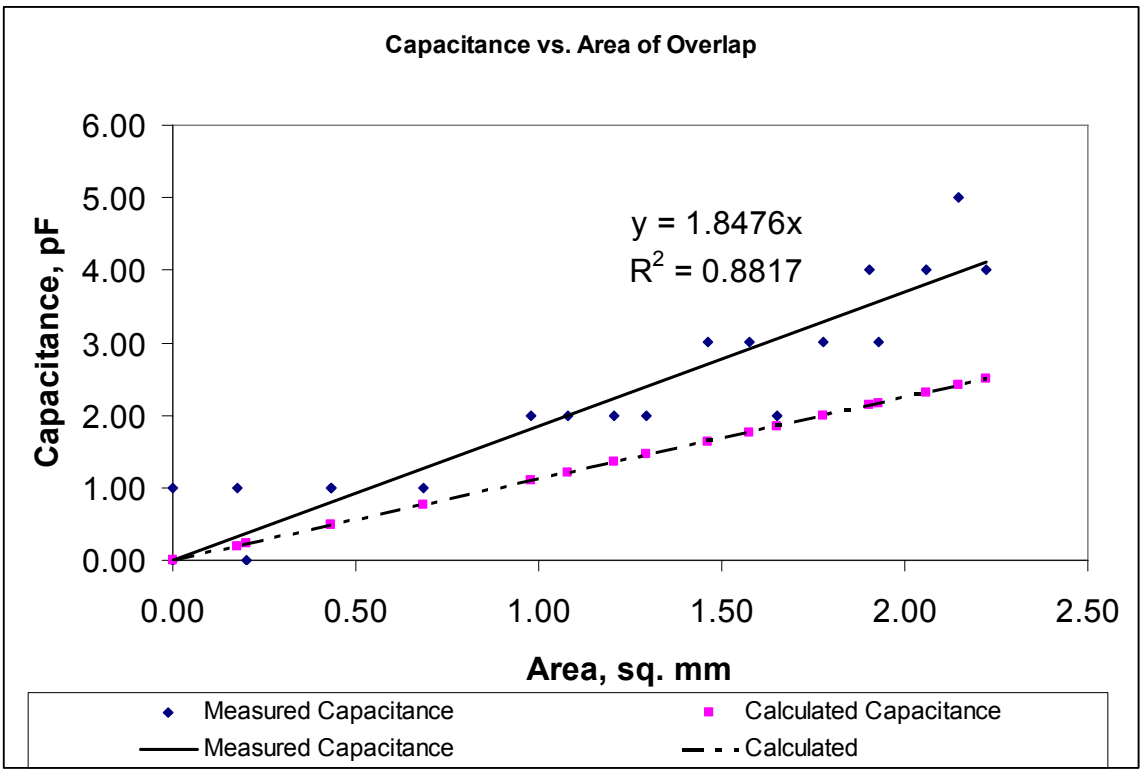

Figure 44, Capacitance vs. Area of Overlap for Prototype

Although the measured values were slightly larger than expected from the calculations, the agreement was reasonable. The experimental output was linear and of the same order of magnitude as the calculations. Some uncontrolled sources of error from theoretical included the permittivity constants for the lab room, the temperature variation in the room throughout the experiment, and the resolution of the multimeter.

Since the multimeter had resolution to only 0.001nF, it had to be adjusted until the overlap caused the least significant digit to change.

IV. DISCUSSION

Use of an interdigitated capacitor works in practice as well as in theory and can be verified with a large scale prototype. With an Analog Devices 1742 capacitance to digital converter, an even smaller prototype could be tested, even one at the proper microfabricated size. Thus, this design concept is a success at generating a measurable signal.

CHAPTER 5

Microfabrication of Interdigitated Capacitive Sensor

I. INTRODUCTION

Micro Electronic Mechanical fabricated Systems, or MEMS devices have been fabricated for over twenty years. MEMS devices have at least some of their dimensions in the micrometer range. Historically, they have been used to create sensors, such as accelerometers and pressure transducers, but now they have various uses. Automobiles contain dozens of MEMS devices, such as gyroscopes, tire pressure sensors, air bag sensors, Manifold Absolute Pressure sensors (MAPS), brake sensors, and emission sensors.

More recently, MEMS mechanical devices with motion have been incorporated into extremely successful products, such as digital projectors ink jet printer heads, biomedical cameras, optical switching (fiber optics for telecommunications industry).

Based on the integrated circuit (IC) photolithographic process using silicon, the technology was invented in 1958 by Jack Kilby who created the first integrated circuit on a silicon wafer. He received the Nobel Prize in 2000 for this work [134]. The process of creating an integrated circuit is outlined below:

1. Create a pattern mask at large scale.
2. Focus UV light through a series of lenses to reproduce the reduced image on a silcon wafer.
3. Step over to the next location and continue until the entire wafer is exposed.
4. Chemically wet etch the wafer to create the desired pattern of “wires”, transistors, and other circuits.

The process for MEMS is very similar, but the objective is to create mechanical beams and membranes that generate a signal when their geometry changes. Since silicon can be easily doped to make it into a piezoresistive or piezoelectric material, a change in geometry, such as deflection of a beam, will generate a change in resistance, much like a copper foil strain gage. However, silicon-based materials are much more sensitive to change in geometry and will therefore a piezoresistive strain gage, for instance, will generate a 100-fold change as compared to copper foil for the same strain. Below are the basic steps for creating a microfabricated structure:

1. Spin a photoresist polymer onto the silicon wafer.
2. Softbake the photoresist.
3. Expose the photoresist to UV light through a mask.

4. Develop the image and dissolve the photoresist in all the undeveloped regions.
5. Apply other oxides or metals to the entire surface.
6. Wash in acid to dissolve any areas without photoresist. This builds the first layer of a structure, such as the beam standoff.
7. Repeat this process to create the desired finished geometry.
8. Release from the silicon wafer substrate or flip over to etch the other side.

Silicon is a cubic centered diamond lattice crystal, not an amorphous solid like glass, so the crystal can be oriented to behave in a specific manner upon etching. For instance, on a (100) wafer, a diagonal (111) plane intersects a (100) plane at 54.7°, giving a pyramidal etch. The (100) crystal orientation is the most common wafer. It is used to create the square membranes of pressure transducers and other such sensors. For a (110) wafer, the z-axis of the (111) planes are at 90°, giving a vertical etch. This configuration is used for beams, such as in accelerometers and gyroscopes.

Silicon is a readily available, proven technology, and can be done at low cost. In addition, it is very possible to integrate the sensor with the IC, allowing the entire sensor system to be of compact size and with “built-in” wiring connections.

Although the material properties of silicon can be used to one's advantage, this is also a very brittle material, and has no yield region (Table 5). As compared to stainless steel, silicon has four times the yield strength, one third the weight, but only 1/20th the shear modulus.

Since silicon wafer fabrication came from the IC industry, the high cost of small production runs is often prohibitive for MEMS applications. Several companies have formed what they call multiuser MEMS processing services, or MUMPS, and will batch several MEMS devices on one wafer, reducing the setup cost for all the users. In general terms, one wafer setup is about $5000-$8000 at a MUMPS facility, but will yield hundreds of prototypes for testing.

Although great in theory integration with the IC often poses problems, because the microfabrication processes are incompatible. MEMS sensors often need metals, such as aluminum, for strength, and these will contaminate an IC wafer fabrication facility. Also, MEMS devices are often low yield and are made on smaller diameter wafers, about 4-6 inches, whereas ICs are now all made on 12 inch wafers.

Silicon is extremely sensitive to temperature (and thus makes a great temperature sensor even if that is not the intention) but can also only be used over a small temperature range (-50°C to 150°C).

Optically, silicon is opaque, so alignment of MEMS structures can be very challenging, and packaging can also be very difficult and costly. In

general, the largest cost of any MEMS device is the packaging, accounting for about 4/5th of the overall cost of the finished device.

MATERIAL	Density g/cm^3	Young's Modulus GPa	Shear Modulus GPa	Poisson Ratio	Yield Stress MPa	Specific Strength MPa/ρ	Fracture Toughness MPa-m^0.5	Thermal Expansion 10^-6/C
Bone (compact)	1.95	14	3.5	0.43	100	50	4.9	20
Concrete	2.45	48	20	0.2	25	10	0.7	11
Diamond	3.5	1035				15000		1.0
Glass (soda, SiO_2)	2.39	63	26	0.23	1500	700	0.7	8.8
Silicon	**2.32**	**110**	**44**	**0.24**	**3200**	**3040**	**1.5**	**2.6**
Silicon Carbide (SiC)	2.85	430	190	0.15	9800	6560	4.2	4.2
Steel, carbon	7.85	210	76	0.29	590	75	49.5	13.5
Steel, stainless	7.85	210	786	0.28	870	110	49.5	16.6

Table 5, Material Properties of Various Materials [135]

II. MICROFABRICATION TECHNIQUE AND STEPS

The fabrication of this microfabricated MEMS sensor will involve forty-nine steps and nine masks. The interdigitated fingers are formed using poly-silicon and released by wet etching sacrificial phososilicate glass (PSG).

In order to maximize the amount of strain sensed by the sensor, the design needed to minimize any adhesive, transitional material used between the sensor and the spinal plate. Such materials would attenuate the strain sensed by the sensor. As a result, a technique called “gold bump compression bonding” [136]. This technique allowed the sensor to be

placed directly on the spinal plate by patterning small, gold bumps on the sensor and the target spinal plate, aligning the two surfaces together, compressing them together at room temperature, and releasing the sensor from its substrate by severing its fragile, break-away tethers.

To eliminate parasitic capacitance from contributing to the signal from between the base of the fingers and the surface of the titanium spinal plate, the entire sensor would be fitted into a well of polyimide, a flexible yet insulating plastic commonly used in the circuit industry.

Below is a step-by-step description of the microfabrication process for the designed sensor.

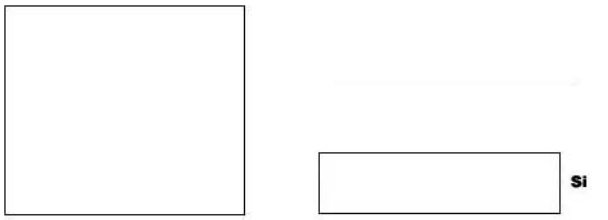

(1) Begin with a silicon wafer.

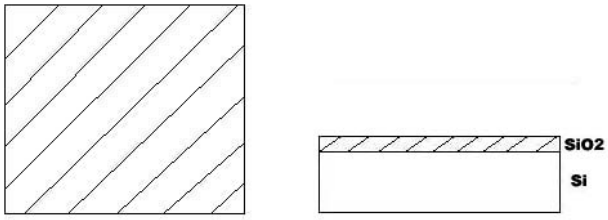

(2) Thermal Oxidation (2μm)
Passivates the silicon surface.

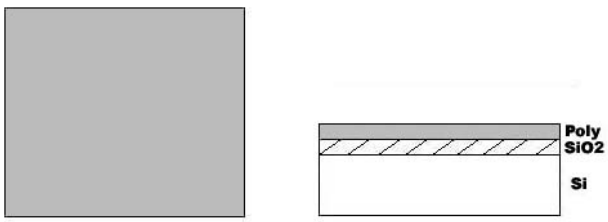

(3) LPCVD Polysilicon (0.5μm)
Creates the break-away tethers for the final release of the structure.

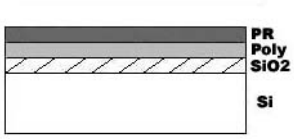

(4) Spin on photo-resist (PR).

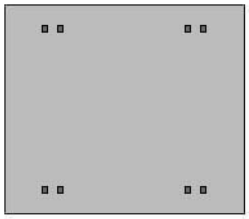

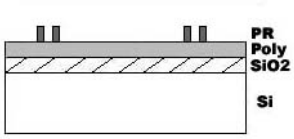

(5) Mask 1: Pattern Polysilicon break-away tethers, expose, and develop photo-resist.

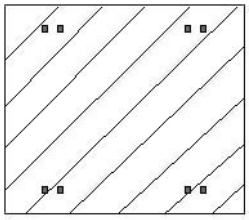

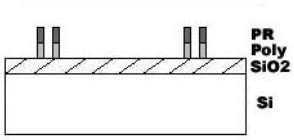

(6) Etch Polysilicon using reactive ion etching (RIE).

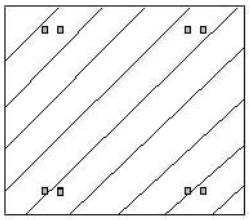

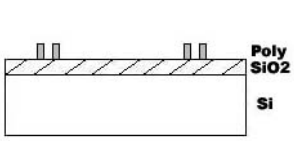

(7) Remove PR using acetone.

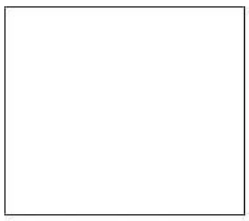

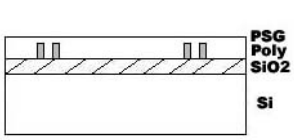

(8) Deposit sacrificial phosphosilicate glass (PSG 1μm) and provide some degree of planarization.

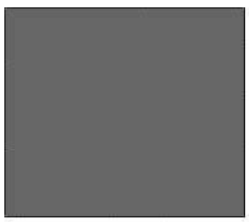

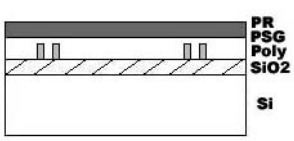

(9) Spin on photo-resist.

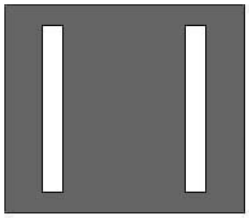

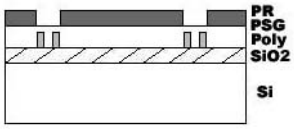

(10) Mask 2: Make anchor windows between the 1st and 2nd layers of Polysilicon.

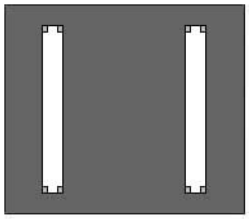

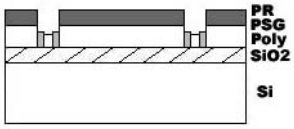

(11) Partially etch PSG in 10:1 Hydrofluoric acid (HF) to create connections to the break-away tethers

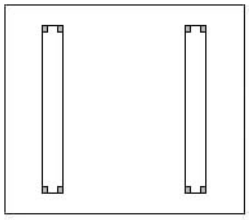

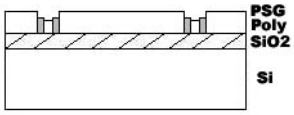

(12) Remove PR with acetone.

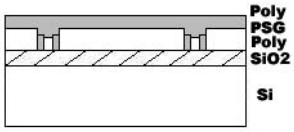

(13) LPCVD 2nd layer of poly-silicon (2μm).

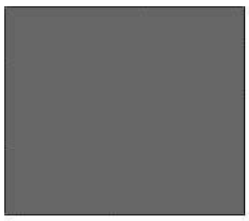

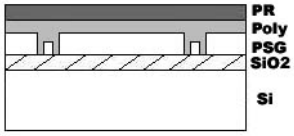

(14) Spin on photo-resist.

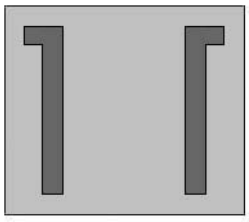

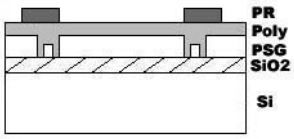

(15) Mask 3: Pattern anchors, expose, and develop PR.

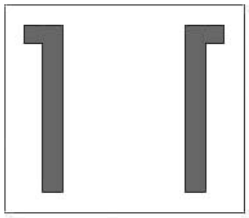

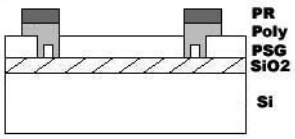

(16) Etch polysilicon using RIE.

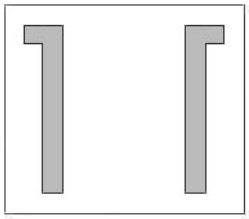

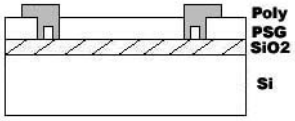

(17) Remove PR using acetone.

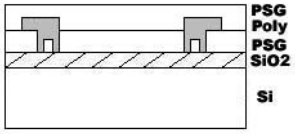

(18) Deposit 2nd sacrificial PSG (3μm) and provide some degree of planarization

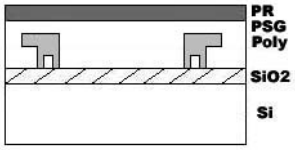

(19) Spin on photo-resist.

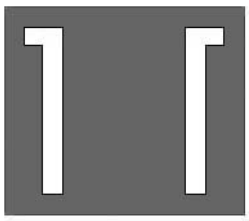

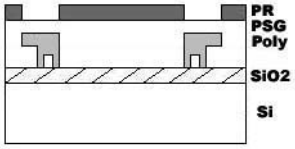

(20) Mask 4: Make anchor windows between the 2nd and 3rd polysilicon layer, expose, and develop PR.

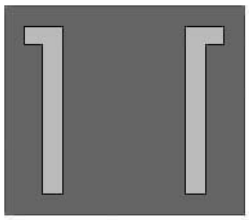

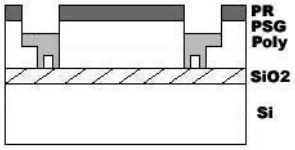

(21) Etch PSG in 10:1 HF.

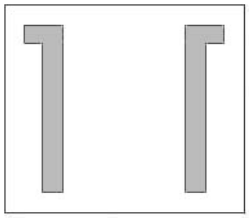

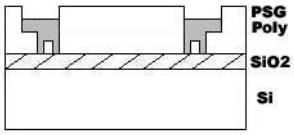

(22) Remove photo-resist with acetone.

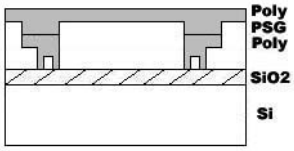

(23) LPCVD 3rd layer of polysilicon (20μm) to create the interdigitated fingers.

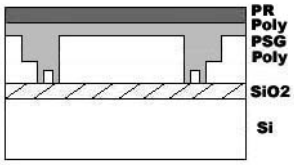

(24) Spin on photo-resist.

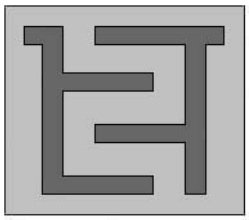

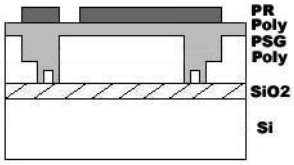

(25) Mask 5: Pattern interdigitated fingers, expose, and develop PR.

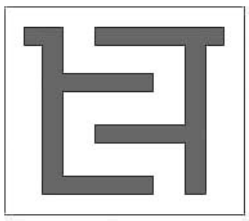

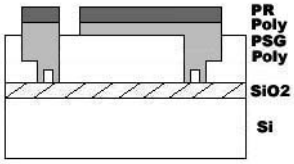

(26) Etch poly-silicon using RIE.

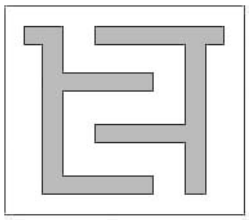

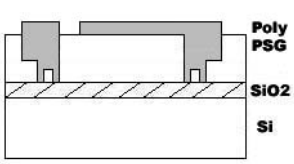

(27) Remove PR with acetone.

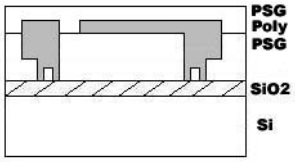

(28) Deposit sacrificial PSG (22μm) and provide some degree of planarization.

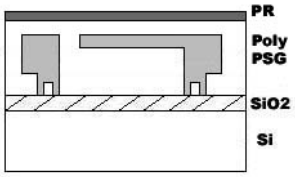

(29) Spin on photo-resist.

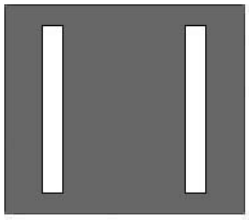

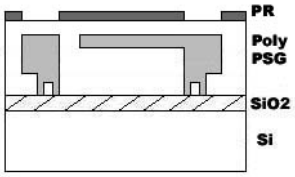

(30) Mask 6: Make anchor windows between the 3rd and 4th Polysilicon layer, expose, and develop PR.

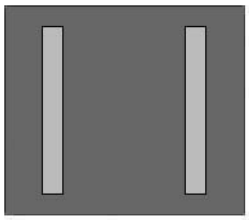

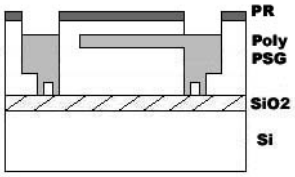

(31) Etch PSG using 10:1 HF.

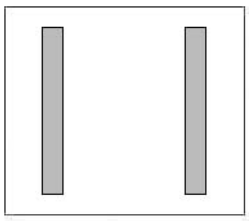

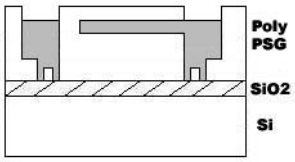

(32) Remove PR using acetone.

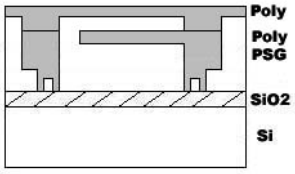

(33) LPCVD 4nd layer of Polysilicon (2μm)

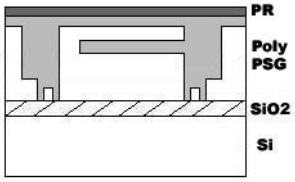

(34) Spin on photo-resist.

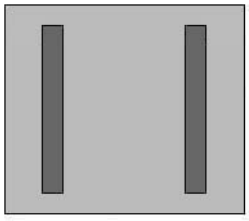

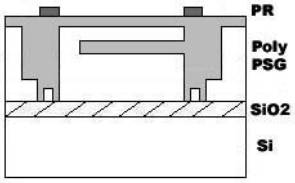

(35) Mask 7: Pattern anchors, expose, and develop PR.

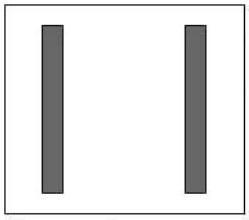

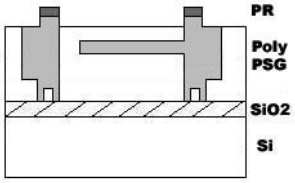

(36) Etch Polysilicon using RIE.

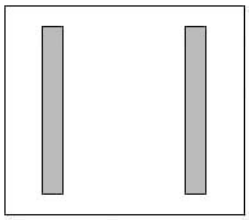

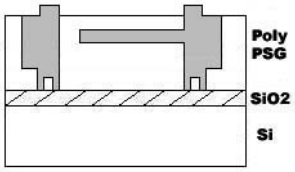

(37) Remove photo-resist.

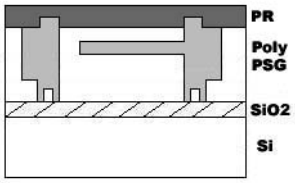

(38) Spin on photo-resist.

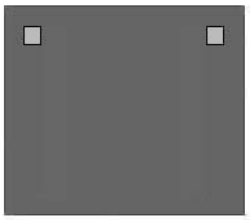

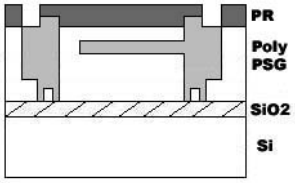

(39) Mask 8: Make contact holes, expose, and develop photo-resist.

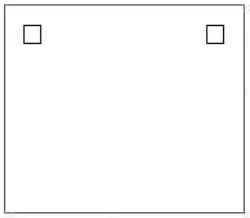

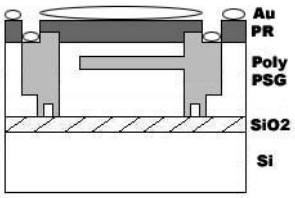

(40) Sputter gold to create contacts (10μm).

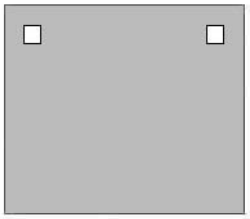

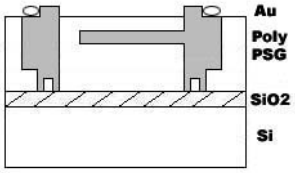

(41) Lift-Off excess gold using acetone.

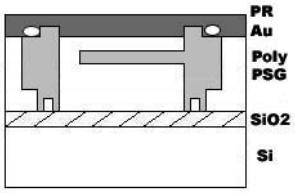

(42) Spin on photo-resist.

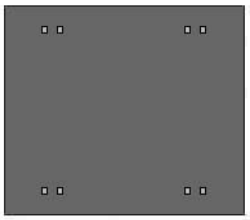

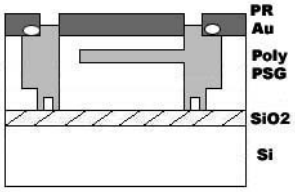

(43) Mask 9: Pattern for “gold bump compression bonding.”

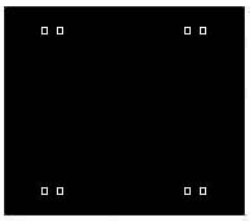

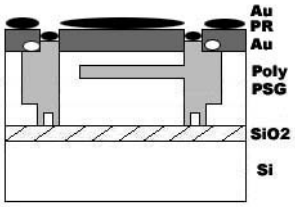

(44) Sputter gold to create gold bumps.

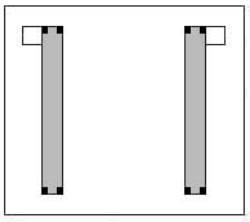

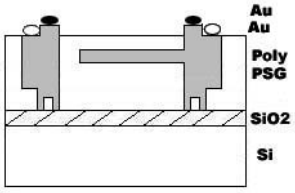

(45) Lift-Off excess gold using acetone.

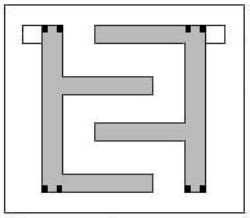

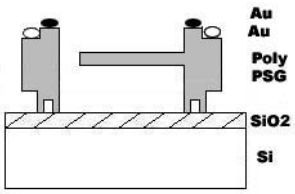

(46) Release Structure: Etch the sacrificial PSG in 10:1 HF.

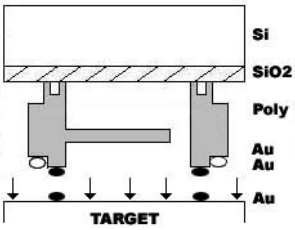

(47) Flip, place in polyimide well, and align with target spinal plate (target also has gold bumps).

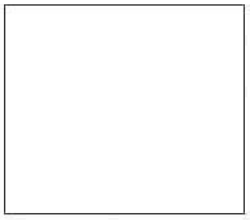

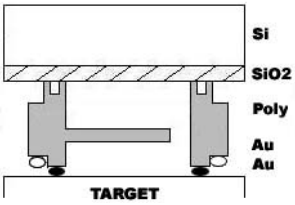

(48) Compress at room temperature.

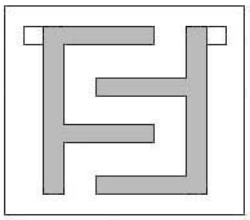

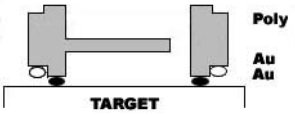

(49) Release structure from the original substrate using breakaway tethers.

III. DISCUSSION

The researchers envision the completed sensor system as a diagnostic tool to aid surgeons and researchers. Having continual feedback as the fusion progresses will allow surgeons and researchers to provide better care to their patients, make decisions sooner about the necessity for secondary surgical intervention, and study the effects of new spinal implant designs in terms of the speed of bony fusion.

The design outlined in this report has several potential limits, mainly in the interface between the sensor and implant. It is not clear that the sensor can be successfully incorporated into all implant designs or that it can be sealed against moisture indefinitely. If the sensor is secured into the implant and covered by a soldered, hermetically sealed plate, it is unclear if the heat introduced by the soldering will affect the electronic components of the sensor.

The researcher has considered solutions to these limitations. By attaching the sensor directly to the surface of the implant and not having an intervening layer of silicon, the sensor should detect the exact motion of the implant. The polyimide serves as an insulating layer, but is free floating and sandwiched between the sensor and the implant by the gold compression bonding bumps.

Experience with the design may illustrate the need to press-fit the sensor system, in its own separate titanium housing, into the implant. The advantage of this method is the ability to assemble the sensor, its electronics, and the antenna bracket on the bench top. With sufficient press-fit of the housing into the implant, the housing will become load-sharing with the implant. Hermetic sealing can then be accomplished by soldering around the interface of the housing and the implant. The solder sealing would no longer be structural, and the amount of soldering would

be considerably less. This would lead to less heat introduction, perhaps providing better protection to the electronics of the sensor system.

CHAPTER 6

Patent Summary

I. INTRODUCTION

The following section is selected sections of this study's patent application taken directly from utility patent application UC04-400-2, based on a provisional patent filed one year prior, 60/586,593.

Included sections highlight the additional potential uses for this technology and better describe how a signal would be generated, amplified, received, and processed by the end user. Anything already described in detail elsewhere in this report was omitted to avoid redundancy.

II. PATENT APPLICATION

STRAIN MONITORING SYSTEM AND APPARATUS

CROSS-REFERENCE TO RELATED APPLICATIONS

[0001] This application claims priority from U.S. provisional application serial number 60/586,593 filed on July 8, 2005, incorporated herein by reference in its entirety.

STATEMENT REGARDING FEDERALLY SPONSORED RESEARCH OR DEVELOPMENT

[0002] Not Applicable

INCORPORATION-BY-REFERENCE OF MATERIAL SUBMITTED ON A COMPACT DISC

[0003] Not Applicable

NOTICE OF MATERIAL SUBJECT TO COPYRIGHT PROTECTION

[0004] A portion of the material in this patent document is subject to copyright protection under the copyright laws of the United States and of other countries. The owner of the copyright rights has no objection to the facsimile reproduction by anyone of the patent document or the patent disclosure, as it appears in the United States Patent and Trademark Office publicly available file or records, but otherwise reserves all copyright rights whatsoever. The copyright owner does not hereby waive any of its rights to have this patent document maintained in secrecy, including without limitation its rights pursuant to 37 C.F.R. § 1.14.

[0005] A portion of the material in this patent document is also subject to protection under the maskwork registration laws of the United States and of other countries. The owner of the maskwork rights has no objection to the facsimile reproduction by anyone of the patent document or the patent disclosure, as it appears in the United States Patent and Trademark Office publicly available file or records, but otherwise reserves all maskwork rights whatsoever. The maskwork owner does not hereby

waive any of its rights to have this patent document maintained in secrecy, including without limitation its rights pursuant to 37 C.F.R. § 1.14.

BRIEF SUMMARY OF THE INVENTION

[0006] The present invention takes a systematic approach to satisfying the foregoing needs through the use of four main features: strain sensing, integrated microfabricated circuitry, RF signal transmission, and data collection. According to an aspect of the invention, the sensor comprises an inter-digitated capacitor. Another aspect of the invention is the microminiaturization of a strain sensing system. Using the techniques of the present invention, a strain sensing system can be microscopic in size. The resultant miniaturization allows the system to be incorporated or integrated into an implant or other device. Another aspect of the invention is the elimination of the need for an internal battery power supply or external leads connecting the system to an external power supply. This is accomplished through the use of an inductively coupled power supply.

[0007] According to another aspect of the invention, strain monitoring is used as an indicator of medical conditions including monitoring the progress of spinal fusion, monitoring glucose levels, measuring spinal loading, and monitoring heart rate.

[0008] For example, for monitoring spinal fusion, the inventive strain sensor system can be bonded to the implant, which will be load sharing with the bone. Thus, as the spine heals, the implant strain will diminish. In

this embodiment, the invention comprises an implantable strain transduction system for humans for determining when fusion has occurred.

[0009] Accordingly, the present invention generally comprises an implantable capacitive strain sensor system that can produce a reliable, reproducible signal that will indicate via a radio telemetry signal when strain has changed.

[0010] To address the need to detect spinal fusion more rapidly, the invention comprises an electronic solution for detecting spinal fusion. The invention takes into account that the spinal instrumentation will not be rigid when initially implanted. There will be minor gaps between the pedicle screws and spinal plate that will allow for some movement. The screws will also move slightly until bone grows into the threads to hold them rigidly fixed. The anterior sides of the vertebrae are not fixed, and because the two vertebrae are separated by the cushioning intervertebral disc, there will always be some movement from this source. We propose that the spinal plate anchored to the two pedicle screws will act like a beam with a moment applied at both ends. The moment will induce bending in the spinal plate that could be measured as a strain.

[0011] This strain would initially be large, but it would decrease over time as the bone growth provided additional fixation. After some period of time, the strain would minimize at a lower value and remain relatively constant. By periodically sampling the strain electronically, a curve could

be generated, showing the onset of rigid fixation.

[0012] There is time dependent relationship between strain and fusion that can be detected by measuring strain in the spinal instrumentation. If spinal fusion can be detected by a radio telemetry system much earlier than a traditional radiograph, then time spent in bracing or modified activities for spine surgery patients can be minimized. Accordingly, an aspect of the invention is to reduce the amount of time patients must remain in a brace in order to avoid other complications, such as disuse atrophy, and that the patients' recovery and eventual outcome is thus improved.

[0013] In order to make the inventive strain measurement system implantable in humans, the entire system is encapsulated using a novel approach whereby the spinal hardware contains a strain sensor. In one embodiment, the invention contains a strain sensor that will accurately measure low levels of strain and transmit the data using an RF antenna and transceiver. In another embodiment, the entire system is powered by radio frequency to avoid the complications of implanting batteries within humans. Otherwise, batteries will be mounted subcutaneously and removed once fusion has been determined.

[0014] Further aspects of the invention will be brought out in the following portions of the specification, wherein the detailed description is for the purpose of fully disclosing preferred embodiments of the invention

without placing limitations thereon.

[0015] Prior to implantation, the inter-digitated capacitor sensor is preferably set to a “neutral” baseline. For example, this may be accomplished using the above-described operational amplifiers with a 12-bit A/D resolution that creates 4096 databits. The databits would be subdivided so that a percentage of the databits represents an equivalent range of the known values of strain for the area of interest. If, for example, a spinal implant experiences 1000με (microstrain) when implanted, each 1με would correspond to approximately 4 databits. Therefore, a neutral baseline value would be 2048 databits prior to implantation.

[0016] Amplifier 64 should never saturate; if it does, the output data becomes unusable. The system may still output a databit value, but it will be a constant value, virtually unvarying over the entire measurement period. The external receiver subsystem is preferably configured to detect this failure mode. This can be corrected by resetting the neutral baseline to a new value until it is within range.

[0017] The second amplifier 66 is employed to set the operating range of the device. For example, in spinal implants a normal range of strain is approximately 100με. The second amplifier 66 is thus preset to represent +/- 100 με or a range of 200 με. In a 12-bit A/D, this corresponds to 1 με change for every 20 databits of change in the strain.

[0018] Note also that, in some applications, the inter-digitated

capacitor sensor and implant hardware is subjected to an initial strain by the surgeon. For example, in spine surgery, the torque applied to the pedicle screws induces approximately 600 με in the spinal hardware. Thus, the inter-digitated capacitor sensor is preferably adjustable to recenter its value at the example 2048 databits. As the exact amount of induced strain cannot be predetermined, this adjustability is important for good performance of the sensor system.

[0019] Depending on the application, the strain after insertion or implantation will either increase, decrease, or oscillate with time and conditions. In a spinal fusion application, the spinal implant hardware may initially be in flexion or extension, depending on the completely variable orientation of the pedicle screws, plates, rods, or cages. For example, databit values below 2048 may indicate extension and values above 2048 may indicate flexion. Thus, the external receiver subsystem that communicates with the inter-digitated capacitor sensor should be able to analyze the initial change in strain from baseline and deduce the initial orientation of the spinal hardware. This information would then be stored in the external receiver subsystem for use in an algorithm that calculates the actual change in strain. Over time, the overall strain may decrease towards a plateau value, but the “sign” of this change is dependent on the initial orientation.

[0020] It will be appreciated that, although the system has been

described above in the context of detecting spinal fusion, strain can be used as an indicator of other biomedical conditions as well. Using MEMS transduction, the system allows for the implantation or insertion of an inter-digitated capacitor strain sensor into area of interest. Advantageously, the system employs a sensitive inter-digitated capacitive strain sensor and RF transmitter subsystem are microscopic in size, temperature-independent, use no batteries, use biocompatible materials, are sealed from the environment, and can easily be integrated into an implant or used as part of a self-contained transponder unit. Preferably, RF frequencies are used which fall within publicly available bands and which are safe to biological tissues. In essence, the system can be considered a lifetime implant.

[0021] As described above, the RF transmitter subsystem communicates sensor information to an external receiver subsystem, which may, for example, comprise a commercial RF ID tag type receiver. The receiver subsystem may be embodied in many forms such as a handheld unit, portable unit, or wristwatch-style unit, and even contain data processing capabilities or capabilities to interface with a computer.

[0022] Preferably, algorithmic information used for data processing can be stored, processed, and analyzed externally thus keeping the system small in size and allowing for use of an inductive power subsystem. In an alternative embodiment, the system may include memory or the like for storing databit information from the sensor. This will provide the option

of recording periodic or random time points for later analysis, and can provide for short-term or long-term storage. A healthcare professional, for example, would later query the device with a transmitter and signal it to download its stored data. The device could optionally be erased after download for long term studies. This configuration would require use of an external transceiver for bidirectional communication as an alternative to the receiver subsystem previously described. In addition, since data would be stored, this enhanced embodiment of the system would likely require a replaceable and/or rechargeable power source subcutaneous to the skin.

[0023] In addition, the external wireless transceiver can be configured to process the databit information received if desired. For example, the transceiver could include a processor and associated software that subtracts the databit information from the carrier RF wave, averages the databits into a single value, and applies the appropriate algorithms to convert the databit reading into a useable number. A 1000 Hz transceiver gathering strain information for one second would generate 1000 databits for each reading. If the averaged value were 2500 databits, the output strain would be 12.5 με. This would be added to the baseline value of perhaps 600 με and give a reading to the surgeon of 612.5 με. Each of these averaged values could be recorded over time to show trends in the strain, such as a slow decline and eventual plateau in spinal strain such as illustrated in the example shown in Figure 45-46. In some applications,

user education may be needed if the user or patient can influence the sensor reading by, for instance, body position. If necessary, an operating protocol might be needed to inform the user how to orient the patient for consistent readings over a long term study.

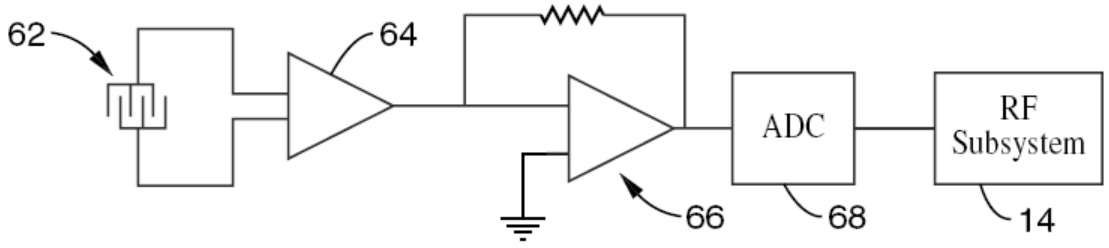

Figure 45, Capacitive Sensor with Two Amplifiers

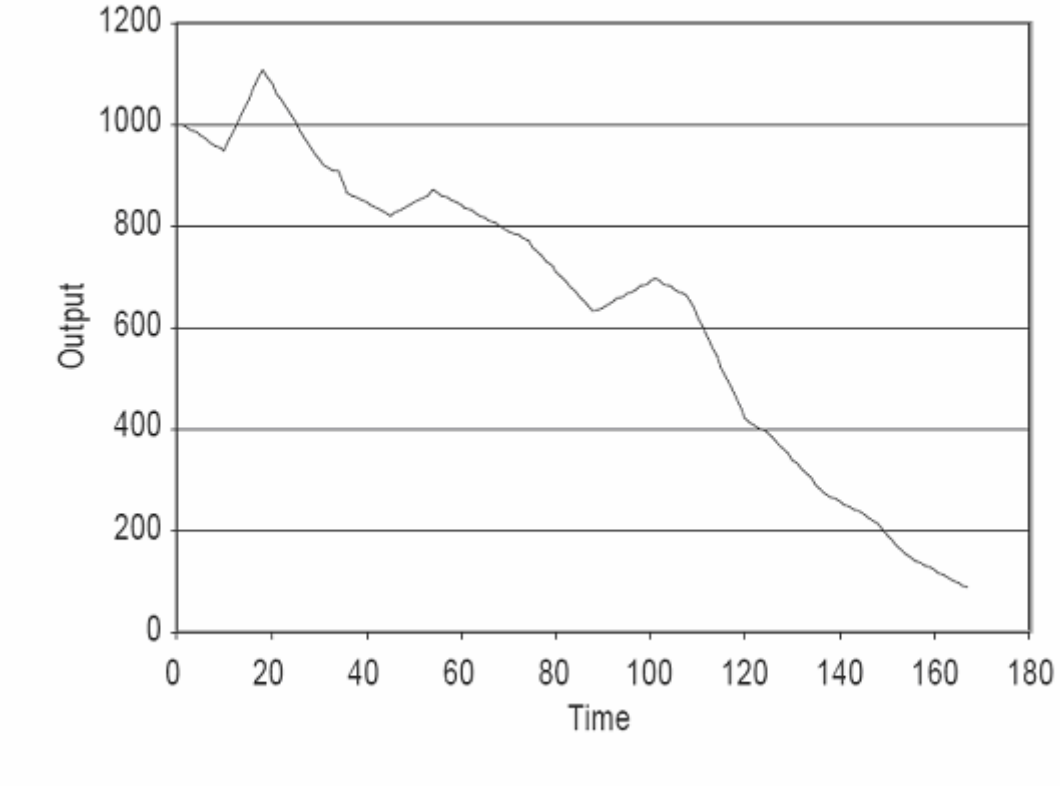

Figure 46, Sensor Output in Databits vs. Time in Days

[0024] As indicated above, the system is applicable to detecting biomedical conditions in general and has far reaching application. For example, referring to Figure 47, the system can be used for measurement of blood chemicals, factors, and minerals using MEMS. In this embodiment, the inter-digitated capacitor sensor would, for example, be inserted into the forearm with a syringe into forearm, or tethered inside a vein as needed to expose sensor to blood stream. The sensor would be mounted on a housing 302 that includes a chamber 304 containing a hydrogel, hydrophilic polymer, or other biocompatible material 306 that dynamically and reversibly swells when exposed to specific chemicals. High selectivity would be a crucial characteristic of the hydrogel. For example, glucose and lactate are both found in the blood, and have similar affinities in many hydrogels. It is important to thus test the marker of interest against potential competitive markers. Figure 47 illustrates one configuration for a blood chemical sensor with a disc of polymer 306 swelling to induce a strain.

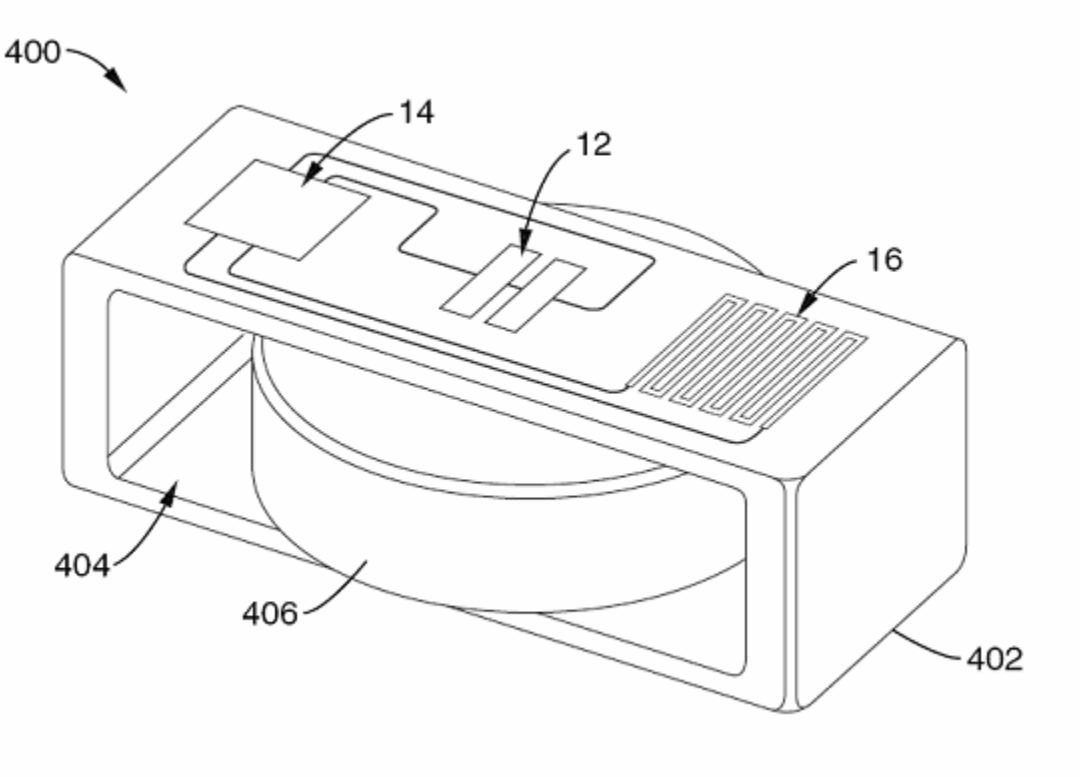

Figure 47, Sensor around Hydrogel Chamber

[0025] Swelling of the hydrogel, polymer or other material would induce a strain in the inter-digitated capacitor sensor that would be transmitted by its corresponding transponder. This strain would corresponds to a specific concentration of specific marker within the blood and bodily fluids, such as glucose, electrolytes, sodium, hydration level, pH, toxic chemicals, or heavy metals (lead, mercury, chromium, etc). Thus, the strain can inform the user of a high or low level of a specific marker of interest. This would be of extreme interest to diabetics, endurance athletes, and military personnel in the field.

[0026] In this embodiment, an external wireless transceiver, most

likely a wristwatch-style device, would analyze the strain information and process it with an algorithm to display glucose level, electrolyte levels (perhaps several key variables on one unit), etc. in terms commonly used for that application. Potentially, the wristwatch-style transceiver could communicate with a remote location for monitoring and advice by a professional, such as the user's physician or a military person's superior officers. The wristwatch style unit could also be configured to provide alerts or alarms to tell the user to take a specific action, such as replenish electrolyte levels, seek immediate medical attention, or inject insulin.

[0027] Similarly, the system could be configured for measurement of heart rate. Similar to the application described above with reference to Figure 47, the heart rate monitor inter-digitated capacitor sensor could be simply injected by syringe beneath the skin, since the entire body "pulses" upon each beat of the heart. For an injected version, the sensor would have a sealed chamber that would flex under the pressure of each pulse and induce a strain that would be transmitted wirelessly to a wristwatch-style unit to give the user continuous heart rate monitoring.

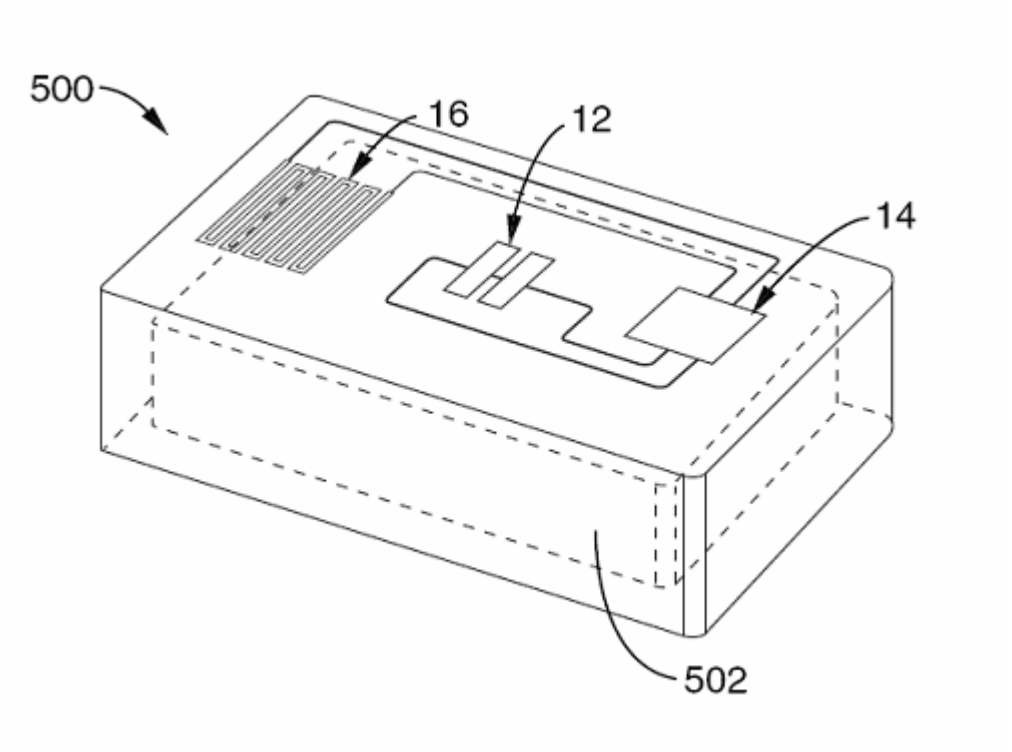

Figure 48, Sensor on Sealed Chamber

[0028] Figure 48 illustrates a sealed chamber version of a heart rate monitor. Alternatively, the inter-digitated capacitor sensor could be adhered to a blood vessel of the forearm (or other desirable region of the body) for larger strain potentials as illustrated in Figure 49. If needed to achieve a strain above the background noise of the body, the sensor could be designed to cuff the external surface of blood vessel. This would induce a hoop stress and would maximize the strain potential from the blood vessel.

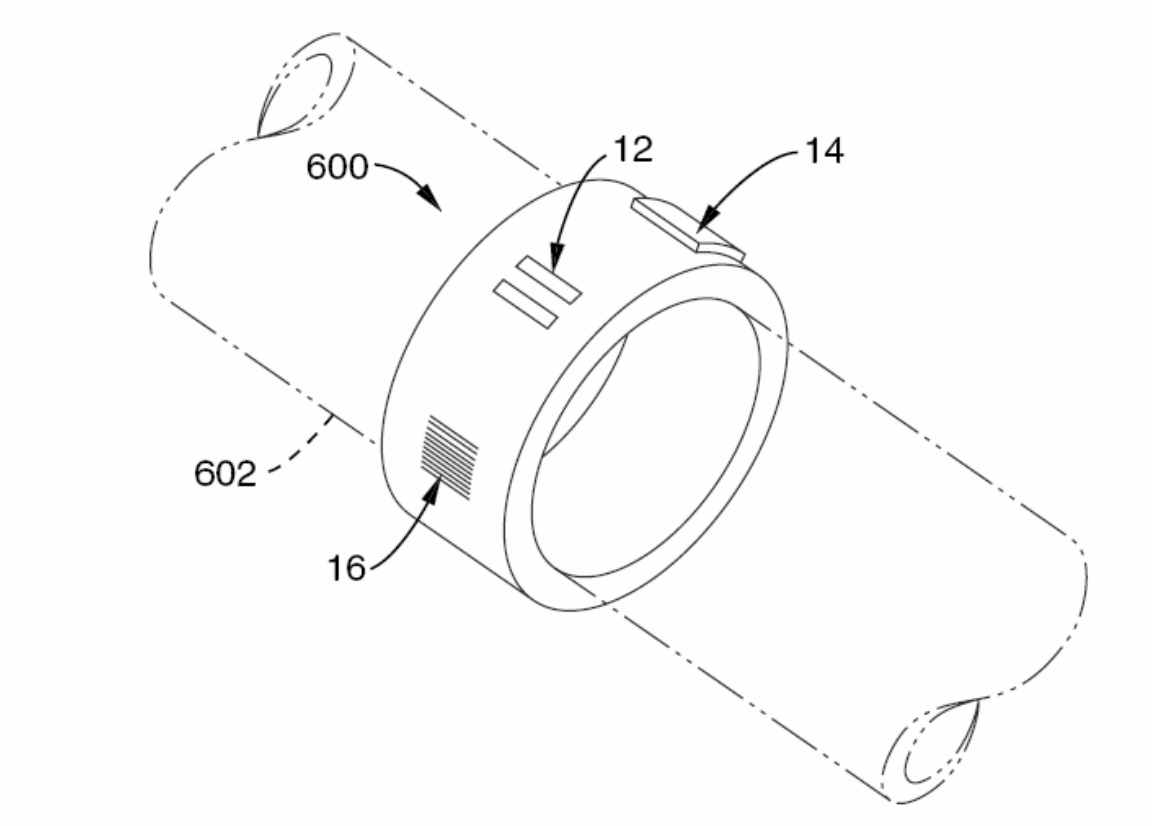

Figure 49, Sensor on Blood Vessel

[0029] As described above, the preferred sensor configuration comprises an inter-digitated capacitor sensor. It will be appreciated that other types of sensors could be used, but that an inter-digitated capacitor sensor is clearly advantageous. Other types of sensors, although inferior to the inter-digitated capacitor sensor, include microfabricated pies-resistive strain gages configured in a Wheatstone bridge. In this configuration, change in resistance of the bridge is monitored as a voltage, converted to a digital signal, and transmitted to a handheld receiver.

[0030] Also as described above, in order to create a successful data acquisition system, several technologies must be integrated together that

are driven by the microsensor design. The quantity to be measured and the environment that the sensor will reside in will determine the type of sensor, and the packaging needed to protect it from the potentially harsh surroundings. Although the description above contains many details, these should not be construed as limiting the scope of the invention but as merely providing illustrations of some of the presently preferred embodiments of this invention. Therefore, it will be appreciated that the scope of the present invention fully encompasses other embodiments which may become obvious to those skilled in the art, and that the scope of the present invention is accordingly to be limited by nothing other than the appended claims, in which reference to an element in the singular is not intended to mean "one and only one" unless explicitly so stated, but rather "one or more." All structural, chemical, and functional equivalents to the elements of the above-described preferred embodiment that are known to those of ordinary skill in the art are expressly incorporated herein by reference and are intended to be encompassed by the present claims. Moreover, it is not necessary for a device or method to address each and every problem sought to be solved by the present invention, for it to be encompassed by the present claims. Furthermore, no element, component, or method step in the present disclosure is intended to be dedicated to the public regardless of whether the element, component, or method step is explicitly recited in the claims. No claim element herein is

to be construed under the provisions of 35 U.S.C. 112, sixth paragraph, unless the element is expressly recited using the phrase "means for."

III. DISCUSSION

Because numerous marketable opportunities exist for this technology, the researchers invested in patenting this idea with the hopes of later converting the results of this research into a marketable product. Potentially, being able to diagnose solid bony fusion early would be of interest to orthopaedic implant manufacturers, as they could then claim “smart implants”. Use of their “smart implant” product would allow patients to return to work months earlier as compared to traditional implants.

Obviously, spinal fusion is not the only potential market for this technology. All orthopaedic implants have a measurable strain that could be tracked over time. In addition, many other medical phenomena could be measured with strain, as discussed in the patent application above, so this one patent does provide enough intellectual property to found an entrepreneurial enterprise.

CHAPTER 7

Market Analysis and Cost Estimates

I. INTRODUCTION

As the researchers are interested in using this technology for founding a new business, a complete Executive Summary, market analysis, and cost estimation were performed prior to speaking with two different venture capitalists. To date, no funding has been received, and further research is probably warranted, but included below is the data prepared for the formation of a new business.

II. EXECUTIVE SUMMARY

Deborah Schenberger

Measurement of Spinal Fusion Using MEMS Transduction

Executive Summary

May 11, 2005

A. Overview Summary Statement

I intend to start a new business manufacturing and selling an implantable bio-MEMS device measure the onset of spinal fusion. Over 300,000 spinal fusion surgeries are performed in the United States every year, but little is known about the process of spinal fusion, especially in its early stages. Surgeons still rely on x-ray radiographs to determine whether or not the spine has fused, and this cannot be seen by x-ray until the fusion process has completed and mineralized, causing a delay of two

months to a year. Because of this delay, patients are forced to remain immobilized in a body brace, limiting their ability to return to the work force and seriously atrophying the core muscles of the trunk. With this device implanted in each spinal implant, surgeons would be able to bring a handheld radio transceiver up to the skin, measure the amount of strain in the implant using this MEMS, battery-free device, and thus deduce whether or not the spine has fused without the use of x-rays. In addition to allowing the patient a quicker return to a normal life and limited muscle atrophy, this device would allow lifetime monitoring of the fusion, giving invaluable information to the surgeon in case of later loosening.

B. Market Need

This idea for measuring spinal fusion was conceived by Dr. Munish Gupta, Lead Orthopaedic Spine Surgeon at the UC Davis Medical Center. He is interested in developing this device for use in his own practice and is a strong advocate for using this technology to revolutionize the practice of spinal fusion. We received funding from DePuy Spine, a Johnson & Johnson company, to get proof this concept would work, and our sixteen week sheep study showed that strain did have a measurable trend as fusion progressed. The sheep study, however, was done with a private company's proprietary device using strain gages, batteries, and long wire leads that would not be acceptable in a human application.

C. Market Size & Addressable Market Segment

Although the current concept involves only spinal fusion, this same technology would be of great interest to the entire orthopaedic field, especially hips and knees. Patients often complain of pain, but nothing can be seen from conventional imaging methods. Using a wireless, implanted, solution, any implant could be retrofitted or designed to incorporate this device, a mere one millimeter square. Unfortunately, with at least 500,000 hip surgeries, 350,000 knee surgeries, and 300,000 spine surgeries performed in the United States every year, the potential market size is over one million units per year.

D. Customers

The orthopaedic industry is controlled by a few consolidated giants. The main customer would be DePuy, the second largest orthopaedic conglomerate in the world. Other interested players would be Howmedica Osteonics Stryker, Smith & Nephew, and Synthes. As a private company, this new business enterprise could work with each company individually to retrofit their implant designs with this technology. They could then incorporate their complimentary technologies, such as the popular triangulation systems for improving placement of orthopaedic implants with the wireless system of this device to assist during surgery as well as afterwards.

E. Competition

There is a company in Kentucky that is developing a battery-operated copper strain gage housing of about an inch in size that attaches to a scoliosis rod to measure fusion. They are also applying for a patent on their concept, which is inferior to this one. John O'Banion, patent attorney for O'Banion and Ritchey, states that our design for spinal fusion is by far "the best and most thorough research of a design" he has every seen. Unlike the one known competitor, this device is microscopic and battery-free. It can thus be incorporated into virtually any existing biomedical system, and will operate indefinitely.

Other researchers have modified orthopaedic implants for the hip and knee to include hollow centers where strain gages or other tension devices are mounted. These papers have reviewed, and all of them were in a temporary, research setting. None were designed to be commercialized, but that could change in the future as these papers were funded by the aforementioned orthopaedic giants.

F. Management

President: Deborah Schenberger, 40. Deborah has sixteen years of engineering experience, mainly in mechanical engineering design and robotics. Over the past ten years, she has worked for both an orthopaedic implant manufacturer, Ortho Development Corporation, in Utah, and a medical device manufacturer for the orthopaedic industry, Synvasive

Technology in El Dorado Hills, California. She has a Master's degree in Mechanical Engineering from Stanford University and is in the final stages of receiving her Ph.D. in Biological Systems Engineering from U.C. Davis. She will work full-time on this business in her role as president, hiring staff as needed to assist with marketing, finance, and research and development. She has business contacts at all of the major orthopaedic companies.

Surgeon Advisor: Dr. Munish Gupta, 49. Munish is an Associate Professor, Department of Orthopaedic Surgery, School of Medicine, University of California, Davis (2001-Present). He is also a Consulting Orthopaedist, Shriners Hospital for Children, Sacramento, California (1997–Present) and has served as a Clinical Instructor at both the University of California, Irvine, and the University of Louisville, College of Medicine. He has published numerous peer-reviewed articles and has contributed chapters on spinal surgery to over five books. Munish will be an advisor on this business, providing access to the orthopaedic giants at the very top levels of the potential companies. He will also personally invest in the start-up of this business, provide free clinical testing of devices, and provide feedback on the needs of the market.

G. Financial Projections

This device has a large market potential. Once commercialized, each device would sell for $1000, and the handheld unit for transceiving

the signal from the device would sell for $10,000. This is comparable to the cost of implants at the OEM level of $2500 to $4000 and surgical saw handheld units of $15,000 to $25,000. If 10% of the market was interested in this device, that would be 100,000 devices a year at $1000 each, plus handheld units, a one time cost per surgeon of $15,000 to $25,000. Thus, the potential is for $100 Million in sales per year.

H. Funding Stages & Milestones

This business is at its earliest stages of start-up. So far, the researchers received $65,000 for the pilot sheep study from DePuy Spine. To develop the first prototypes will take two years to microfabricate, thoroughly test on the bench top and in animal models, and then test in humans in clinical trials. Setting up an office and laboratory space for continued testing and development of this device are the most urgent priorities.

Phase 1: $765,000 for year one to launch this business, develop implantable device, and test in large scale sheep study.

Phase 2: $2,030,000 for years two and three to develop human implantable device, test in human clinical trials, and fabricate devices for commercial sale.

Phase 3: Company will cover its own expenses after year three and will become profitable by year six.

I. Capital Required, Uses of Capital and Exit Strategy

Below is a summary of capital requirements for year one. This level of funding will be sufficient for the first two years, after which clinical trials in humans will increase the funding needs by $500,000 in year three. Year four and beyond, sale of the product will cover expenses, and the company should be profitable by the close of year five. The exit strategy is to sell the company after year five with at least one marketed, profitable product.

Expenses Year One	Amount
1. Office and laboratory space ($2/ft^2 x 10,000ft x 12 mo)	$240,000
2. Salaries for personnel	$400,000
3. Microfabrication costs ($10,000 per prototype)	$20,000
4. Capitol and computer equipment	$20,000
5. Animal study (35 sheep over 16 weeks)	$40,000
6. Marketing and travel expenses	$15,000
7. Patent expenses	$30,000
TOTAL	**$765,000**

III. DISCUSSION

According to the venture capitalists consulted for this business, start-up funding is difficult to receive, but ranges between $300,000 and $600,000. Entrepreneurs relinquish a percentage of their stock in exchange for funding. The exact amount relinquished is negotiable, but is

based on the future sale value of the business. For a business worth $50M at sale (five times yearly product sales of $10M), typically venture capitalists require 25-30% of the company stock. In this way, if the company is successful, they at least double their initial investment. The second round of funding, although for more money, is lower risk for investors because the product is closer to marketability, so the stock required is a lower percentage, another 20% on average. In general, investors do not want to take a controlling interest away from the entrepreneur, because it discourages the entrepreneur from working as hard.

Several forums exist for presenting new business ideas to potential investors, but the easiest method to find potential investors is to work with a venture capitol firm. The firm has a pool of investors to which they present various opportunities, and they will also seek new investors on exciting investment opportunities.

The advice I received from the venture capitalists I consulted was to protect my intellectual property by not hiring on to an existing company that may want to develop my device. In general, companies use this strategy to obtain intellectual property at low cost, often firing the inventor after a year or so of employment. Universities, in contrast, are good for invention protection, as they will allow inventors to use their intellectual property attorneys as needed to fight patent infringements and do not assume

ownership of patents developed prior to employment at the university. After employment, they share in the profit of any intellectual property, usually about 50% of any royalties going to the inventor.

As this technology is still in its early stages and is more than a year from being marketable, the advice was to continue developing the device in a university research environment, wait for the patent to issue, and look for research funding to further develop the device as much as possible before seeking venture capital funding.

CHAPTER 8

Conclusions

I. LIMITATIONS

The capacitance of this design is limited in resolution to 1pF; thus, to be able to measure a significant difference, the strain must change by at least 5pF over the course of the analysis. Also, this design can only be used if the capacitance can be isolated from parasitic capacitances, such as the base plate to which the sensor is attached.

Also, this design must be isolated from moisture, thus increasing the difficulty of packaging. If hermetically sealed, the isolated components will contain a volume of air, so this design cannot be used in environments with pressures considerably higher or lower than one atmosphere, such as in ocean or outer space applications.

For capacitance, the sensor needs to be stimulated by a time varying source, such as radio frequency. For human safety, this signal must be higher than 100MHz and lower than 3GHz; however, signal attenuation is associated with higher frequencies. Thus, the source signal needs to have considerable power to excite the capacitive sensor.

All of the work on this study was with very limited numbers of sheep spines, and was intended to show if there might be a relationship between strain and spinal fusion. Human studies will be required to confirm any

findings in a full-scale sheep study, and this will take considerable funding and time.

In addition, there is no evidence that early fusion detection will mean an earlier recovery. The muscles play a crucial role in a full, functional recovery, and this research has not established if the current method of bracing is too short or too long a time period. It may be discovered that the muscle needs at least sixteen weeks to achieve optimal strength, or it may instead be learned that optimal strength would be achieved in the muscle by removing the brace after only one or two weeks. This could be confirmed through studies in human patients using the LMM to show muscle strength as a function of time.

This leads to another issue, quality of life improvements for patients who remove the brace early versus those that wait the current sixteen weeks or longer. Is their functional outcome improved? Is the muscle atrophy significantly different between the two groups after one year or more? Also, is there a greater recurrence of injury in either group? All of these issues would need to be addressed through long term studies in human patients using a combination of range of motion and strength testing.

Long term studies are also needed to characterize the strain “plateau” due to spinal fusion. A computer algorithm needs to be developed to recognize the pattern of the onset of spinal fusion at the very

beginning of the strain versus time curve's inflection. This way, the amount of time the patient spends in bracing could be optimized without a lag period while the surgeon tries to interpret a trend in the results.

II. FUTURE WORK

Again, this research was performed on only two spines. There were no repeatability measures and no statistical measures, but the results from the two spines were very similar, indicating a promising trend. Future work will provide the necessary validation. These studies are not yet defined in detail, other than the full scale sheep study outlined below.

The next step for this research project is to build a microfabricated interdigitated capacitive sensor for laboratory testing. Once calibrated, this sensor needs to be incorporated in an electronic circuit with amplifiers and signal transponders to test the system under *in vitro* conditions. This will reveal inadequacies in the design that must be addressed prior to a full scale sheep study. This may include signal attenuation, noise, tissue heating, or moisture influx.

In addition to the stated results in the summarized animal protocol below, the prior in vitro study will also be used to test for unexpected problems with this method of measuring spinal fusion, such as creep or drift of the signal over time. Such creep would falsely indicated the onset of fusion, so the entire system needs to be put in a container under constant load for several months to ensure that the output remains the same.

The sheep study will need to include a minimum of 35 sheep in five groups of seven. These groups will be sacrificed at four, eight, twelve, and sixteen weeks to correlate the sensor output with mechanical testing of the spines. Each group will contain seven animals. The sixteen week time frame will have two groups, one control with no bone growth factor added to the spinal fusion site (resulting in a nonunion) and one with bone growth factor. This was approved in an animal use and care protocol by the university as described below. Some of the text is now outdated, as the study evolved over time to test capacitive rather than resistive strain, and the finite element analysis was dropped, but the surgical procedure is accurate.

Layman's Summary:

In layman's terms, "Sheep will undergo spinal fusion with strain gage instrumentation. The strain gage instrumentation will be read bi-weekly, and the sheep will be radiographed weekly. The spines will be harvested at 4, 8, 12, and 16 weeks." This statement would have been placed on the sheep pens for the benefit of all people entering the Animal Research Facility at the University of California at Davis.

Purpose of Study and Expected Outcomes:

The aim of this study is to develop an implantable strain gage system for humans for determining when spinal fusion has occurred.

Currently, this can only be determined through radiographs, which significantly underestimate the presence of a spinal fusion. The hope is that the amount of time patients must remain in a brace can be minimized following spinal fusion surgery in the lumbar spine in order to avoid other complications, such as disuse atrophy, and that the patients' recovery and eventual outcome is thus improved.

The study has several steps to achieve its end goal, the first being a finite element model of the lumbar vertebrae with spinal hardware. The second step is bench top testing of the strain gage and telemetry systems to ensure they work as predicted by the finite element model and that all of the electronics can be sealed against moisture in vivo. The third step will be to implant the system in sheep to determine if strain gage output will correlate with fusion. This protocol is for the third stage of the study.

Thirty-five skeletally mature sheep will be required for this study to be euthanized at each of four, eight, twelve, and sixteen weeks. Seven sheep will be euthanized at each of the intervals. All the sheep will be quarantined for two weeks at the UC Davis Animal Resource Services facility. For all sheep, a two-vertebrae spinal fusion surgery will be performed by an orthopedic surgeon. The spinal fusion surgery will be using commercially available spinal instrumentation system across two vertebrae.

The spinal instrumentation will have previously been fitted with strain gage telemetry systems. The radio telemetry device will be implanted subcutaneously near the spinal fusion site, and data from the radio telemetry systems will be recorded for analysis. Radiographs will also be taken weekly to attempt to detect the presence of a spinal fusion.

After four weeks, seven sheep will be sacrificed and the spines analyzed. Analysis will include:

- Manual testing
- Plane radiographs
- CT scan
- Nondestructive mechanical testing
- Removal of spinal instrumentation
- Mechanical testing of the spine to yield
- Histology

This sequence will be repeated at eight weeks, twelve weeks, and sixteen weeks. Control animals that received no bone graft after spinal surgery will be euthanized at sixteen weeks for comparison. It is expected that complete spinal fusion will have occurred prior to sixteen weeks, and that it will be indicated through all means, including radiograph.

Summary of Surgical Procedure:

All sheep will undergo general anesthesia with Pentothal 20 mg/kg as the inducing agent for anesthesia and will be maintained with Halothane 1-3% inhalation anesthesia and a constant rate infusion of fentanyl intraoperatively. This combination provides a more balanced anesthesia and avoids some of the side effects of halothane, such as hypotension. To reduce pain from procedure, sheep will be pretreated with a preemptive analgesia of an opiod, such as buprenorphine or butorphenol. Postoperatively, pain control will be managed by Buprenorphine 0.01 mg/kg IM as needed. Animals will be given Cephazolin antibiotic perioperatively for two days. The sheep will have a posterior procedure performed on their spine. Seven sheep representing each interval will undergo the surgical procedure each week. Thus, five weeks of surgical sessions will be required to perform all the spinal fusion surgeries. The longest interval groups will be performed first to minimize the length of the research study.

To assess the adequacy of anesthesia during spinal fusion surgery, the animals' heart rate will be monitored via EKG. Pain is usually accompanied by an increase in heart rate. The technician in the room is responsible for monitoring heart rate and administering additional anesthesia as needed to alleviate pain. Jaw tone will be also be monitored, and if tone is found, the inhalation anesthesia can be increased. In

addition, the animals' vital signs for respiratory rate, oxygen saturation, and body temperature will be monitored. Mechanical ventilation and a source of heat will be available in case they are needed during the procedure. Fluids will be provided to the sheep during the procedure.

All thirty-five animals will undergo general anesthesia. A mid-line incision will be made over the lumbosacral junction in the lumbar spine. All thirty-five animals will undergo a two-vertebrae fusion using spinal plates provided by DePuy Acromed Corporation. To facilitate a union, the orthopedic surgeon adds a bone growth factor around the spinal hardware. This is a granular substance in a liquid paste added only at the time of surgery. Seven of the thirty-five animals will not receive bone growth factor and will serve as controls. The remaining 24 animals will receive bone growth factor. All thirty-five animals will have a radio transmitter attached to the spinal plates by wires implanted just beneath the skin.

Post-operatively, the Lab Animal Health Clinic's assistance will be enlisted for post-operative care. Eating habits of the sheep will be monitored, and if anorexia or other indications of pain are noted, the sheep will be given analgesics to alleviate suffering. Other indications of pain include malaise, reluctance to move, and teeth grinding.

The sheep will be corralled and restrained twice weekly in order to scan the skin for a signal from the subcutaneously implanted radio

transmitter. At weekly intervals, the sheep will undergo x-rays from lateral and AP directions. For the x-ray procedure, the animals will be anesthetized with a short-acting barbituate, either sodium pentathol by IV or an intubation of Ketamine and Valium.

At four weeks post-surgery, seven of the sheep will be euthanized with an IV injection of pentobarbital. The spines will then be harvested for radiographic, biomechanical, and histological studies.

This process will be repeated for seven sheep at eight and twelve weeks. At sixteen weeks, the remaining seven sheep and seven controls will be euthanized according to the method described above. The study groups and numbers are summarized in Table 5 below.

Study Groups and Numbers:

Group	Procedures / Drugs	Qty.	Cat.
16wc	Control Group will be maintained for 16 weeks and receive the same spinal surgery, but they do not receive the bone growth factor during spinal fusion surgery. This results in a non-union condition. Week 1—Spinal fusion surgery using general anesthesia with Pentothal 20 mg/kg. Maintained with Halothane 1-3 mg/kg. Given Cephazolin antibiotic perioperatively for two days. Week 17—euthanized using pentathol in anesthetizing dose followed by a saturate KCL 15ml injection and bilateral pneumothoraces.	7	3
16w	16 Week Group Week 2—Spinal fusion surgery using general anesthesia with Pentothal 20 mg/kg. Maintained	7	3

	with Halothane 1-3 mg/kg. Given Cephazolin antibiotic perioperatively for two days. Week 18—euthanized using pentathol in anesthetizing dose followed by a saturate KCL 15ml injection and bilateral pneumothoraces.		
12w	12 Week Group Week 3—Spinal fusion surgery using general anesthesia with Pentothal 20 mg/kg. Maintained with Halothane 1-3 mg/kg. Given Cephazolin antibiotic perioperatively for two days. Week 15—euthanized using pentathol in anesthetizing dose followed by a saturate KCL 15ml injection and bilateral pneumothoraces.	7	3
8w	8 Week Group Week 4—Spinal fusion surgery using general anesthesia with Pentothal 20 mg/kg. Maintained with Halothane 1-3 mg/kg. Given Cephazolin antibiotic perioperatively for two days. Week 12—euthanized using pentathol in anesthetizing dose followed by a saturate KCL 15ml injection and bilateral pneumothoraces.	7	3
4w	4 Week Group Week 5—Spinal fusion surgery using general anesthesia with Pentothal 20 mg/kg. Maintained with Halothane 1-3 mg/kg. Given Cephazolin antibiotic perioperatively for two days. Week 9—euthanized using pentathol in anesthetizing dose followed by a saturate KCL 15ml injection and bilateral pneumothoraces.	7	3

Table 5, Summary of Groups and Numbers for Animal Study

The above sheep study was approved in Animal Protocol #10159 by the university's ethics committee. Category 3 "Moderate to Severe Distress" refers to discomfort to the animal, such as a major surgical procedures conducted under general anesthesia, with subsequent

recovery; prolonged (several hours or more) periods of physical restraint; or induction of behavioral stresses such as maternal deprivation.

III. CONCLUSIONS

The goals of this design were met as follows.

1. The researcher tested the hypothesis that strain is related to the onset of spinal fusion using an *in vivo* sheep model for a period of seventeen weeks. Although inconclusive, further laboratory testing on additional sheep spines proved that strain does decrease and eventually plateau with the onset of spinal fusion.

2. An interdigitated capacitive sensor was designed to detect strain in spinal hardware and an approach was discussed on how to transmit that information through the body to an external receiver.

3. A large scale interdigitated capacitive sensor was prototyped and successfully tested.

4. The intellectual property was patented for later use in starting a business.

5. A rudimentary business was plan presented for seeking funding for this enterprise.

All the goals of this design study have been successfully met, and the researcher looks forward to continuing with the development of the final product.

Works Cited

1. Heerkens, Y.F., et al., *Passive Resistance of the Human Knee: the Effect of Immobilization.* Journal of Biomedical Engineering, 1986. **8** (2): p. 95-104.
2. Kanayama, M., et al., *Maturation of the posterolateral spinal fusion and its effect on load- sharing of spinal instrumentation. An in vivo sheep model.* J Bone Joint Surg Am, 1997. **79**(11): p. 1710-20.
3. Cowen_&_Company, *Medical Devices and Supplies: Spine*. 2005. p. 36-49.
4. Credit-Suisse-First-Boston, *Orthopaedics 2005: The Spine*. 2005. p. 38-50.
5. Deyo, R.A., Daniel Cherkin, Douglas Conrad, and Ernest Volinn, *"COST, CONTROVERSY, CRISIS" :LOW BACK PAIN AND THE HEALTH OF THE PUBLIC*, in *Annual Review of Public Health*. 1991, Annual Review of Public Health. p. 141-156.
6. Kuntz, K., *Cost-Effectiveness of Fusion With and Without Instrumentation for Patients With Degenerative Spondylolisthesis and Spinal Stenosis.* SPINE 2000. **25**(9): p. 1132-1139.
7. Tinkleman, D., *The Impact of Chronic Obstructive Pulmonary Disease on Long-term Disability Costs.* Journal of Managed Care Pharmacy, 2005. **11**(1).
8. Moore, K.L., *Essential Clinical Anatomy.* 1st ed. 1995, Maryland: Lippincott Williams & Wilkins. 510.
9. Fathallah, F.A., W.S. Marras, and M. Parnianpour, *An assessment of complex spinal loads during dynamic lifting tasks.* Spine, 1998. **23**(6): p. 706-16.
10. Marras, W.S., et al., *Prospective validation of a low-back disorder risk model and assessment of ergonomic interventions associated with manual materials handling tasks.* Ergonomics, 2000. **43**(11): p. 1866-86.
11. Marras, W.S., et al., *Biomechanical risk factors for occupationally related low back disorders.* Ergonomics, 1995. **38**(2): p. 377-410.
12. Marras, W.S., et al., *The role of dynamic three-dimensional trunk motion in occupationally-related low back disorders. The effects of workplace factors, trunk position, and trunk motion characteristics on risk of injury.* Spine, 1993. **18**(5): p. 617-28.
13. Luo, Z.P., G.R. Buttermann, and J.L. Lewis, *Determination of spinal facet joint loads from extra articular strains-- a theoretical validation.* J Biomech, 1996. **29**(6): p. 785-90.
14. Sharma, M., N.A. Langrana, and J. Rodriguez, *Role of ligaments and facets in lumbar spinal stability.* Spine, 1995. **20**(8): p. 887-900.
15. Wood, K.B., et al., *In vivo analysis of canine intervertebral and facet motion.* Spine, 1992. **17**(10): p. 1180-6.
16. Slosar, P.J., *Indications and outcomes of reconstructive surgery in chronic pain of spinal origin.* Spine, 2002. **27**(22): p. 2555-62; discussion 2563.
17. Selby, D.K., *When to operate and what to operate upon.* Orthop Clin North Am, 1983. **14**(3): p. 577-88.
18. Anract, P., *[Indications and limitations of surgery of common low back pain].* Rev Prat, 2000. **50**(16): p. 1793-6.

19. Chen, Q., et al., *Postoperative bone re-growth in lumbar spinal stenosis. A multivariate analysis of 48 patients.* Spine, 1994. **19**(19): p. 2144-9.
20. Hall, H., et al., *Outcomes of surgeons who have undergone spine surgery.* J Spinal Disord, 1997. **10**(6): p. 518-21; discussion 522.
21. Katz, J.N., *Lumbar spinal fusion. Surgical rates, costs, and complications.* Spine, 1995. **20**(24 Suppl): p. 78S-83S.
22. Kuslich, S.D., et al., *Four-year follow-up results of lumbar spine arthrodesis using the Bagby and Kuslich lumbar fusion cage.* Spine, 2000. **25**(20): p. 2656-62.
23. Little, D.G. and D. MacDonald, *The use of the percentage change in Oswestry Disability Index score as an outcome measure in lumbar spinal surgery.* Spine, 1994. **19**(19): p. 2139-43.
24. Mayer, H.M., *[Discogenic low back pain and degenerative lumbar spinal stenosis - how appropriate is surgical treatment?].* Schmerz, 2001. **15**(6): p. 484-91.
25. Netter, F.H., *Atlas of Human Anatomy*. 2nd ed, ed. A.F.D. II. 2001, New Jersey: Vivendi Universal Publishing Co. 525.
26. Pitzen, T., et al., *Motion of threaded cages in posterior lumbar interbody fusion.* Eur Spine J, 2000. **9**(6): p. 571-6.
27. Puttlitz, C.M., V.K. Goel, and M.H. Pope, *Biomechanical testing sequelae relevant to spinal fusion and instrumentation.* Orthop Clin North Am, 1998. **29**(4): p. 571-89.
28. Iatridis, J.C., et al., *Shear mechanical properties of human lumbar annulus fibrosus.* J Orthop Res, 1999. **17**(5): p. 732-7.
29. Parente, E.J. and D.M. Nunamaker, *Stress protection afforded by a cast on plate fixation of the distal forelimb in the horse in vitro.* Vet Surg, 1995. **24**(1): p. 49-54.
30. Szivek, J.A. and F.P. Magee, *A long-term in vivo bone strain measurement device.* J Invest Surg, 1989. **2**(2): p. 195-206.
31. Szivek, J.A., et al., *An implantable strain measurement system designed to detect spine fusion: preliminary results from a biomechanical in vivo study.* Spine, 2002. **27**(5): p. 487-97.
32. Boden, S., JH Schimandle, WC Hutton, *An experimental lumbar intertransverse process spinal fusion model: Radiographic, histologic, and biomechanical healing characteristics.* . Spine, 1995(20): p. 410-420.
33. Martin, R.B., David B. Burr, and Neil A. Sharkey, *Skeletal Tissue Mechanics*. 1st ed. 1998, New York: Springer-Verlag. 392.
34. Foster, M.R., Matthew J. Allen, et. al., *Characterization of a developing lumbar arthrodesis in a sheep model with quantitative instability.* The Spine Journal, 2002. **2**(4): p. 244-250.
35. Abbs, J.H. and B.N. Gilbert, *A strain gage transduction system for lip and jaw motion in two dimensions: design criteria and calibration data.* J Speech Hear Res, 1973. **16**(2): p. 248-56.
36. Bessman, E.S., et al., *Accuracy enhancement of in-vivo bone strain measurements and analysis.* J Biomech Eng, 1982. **104**(3): p. 226-31.
37. Buttermann, G.R., et al., *Description and application of instrumented staples for measuring in vivo bone strain.* J Biomech, 1994. **27**(8): p. 1087-94.

38. Caler, W.E., D.R. Carter, and W.H. Harris, *Techniques for implementing an in vivo bone strain gage system.* J Biomech, 1981. **14**(7): p. 503-7.
39. da Fonseca, J.C. and O.L. da Silva, *Measurements of stress and strain in live bone by electrical strain gage method.* Rev Bras Pesqui Med Biol, 1975. **8**(5-6): p. 469-74.
40. Gross, T.S., K.J. McLeod, and C.T. Rubin, *Characterizing bone strain distributions in vivo using three triple rosette strain gages.* J Biomech, 1992. **25**(9): p. 1081-7.
41. Hoshaw, S.J., et al., *A method suitable for in vivo measurement of bone strain in humans.* J Biomech, 1997. **30**(5): p. 521-4.
42. Keller, T.S. and D.M. Spengler, *In vivo strain gage implantation in rats.* J Biomech, 1982. **15**(12): p. 911-7.
43. Maliniak, M.M., et al., *Hydroxyapatite-coated strain gauges for long-term in vivo bone strain measurements.* J Appl Biomater, 1993. **4**(2): p. 143-52.
44. Rabkin, B.A., et al., *Long-term measurement of bone strain in vivo: the rat tibia.* J Biomed Mater Res, 2001. **58**(3): p. 277-81.
45. Szivek, J.A., et al., *Preliminary development of a hydroxyapatite-backed strain gauge.* J Appl Biomater, 1990. **1**(3): p. 241-8.
46. Perusek, G.P., et al., *An extensometer for global measurement of bone strain suitable for use in vivo in humans.* J Biomech, 2001. **34**(3): p. 385-91.
47. Szivek, J.A., et al., *Technical note: development of a model for study of in vivo bone strains in normal and microgravity environments.* J Appl Biomater, 1995. **6**(3): p. 203-8.
48. Zadler, B.J., *PROPERTIES OF ELASTIC MATERIALS USING CONTACTING AND NON-CONTACTING ACOUSTIC SPECTROSCOPY*, in *Applied Physics*. 2003, Colorado School of Mines. p. 176.
49. Globalspec.com, *http://strain-gauges.globalspec.com/Specifications/Test_Measurement/Product_Material_Testing/Strain_Gauges*, in *Optical: Photoelastic Strain Gauges, Moire Interferometry Strain Gauges, and Holographic Interferometry Strain Gauges* 2005.
50. GreenMed, *http://www.greenmed.co.jp/lpl/E/flat10_E.htm*.
51. Baxter, L.K., *Capacitive Sensors--Design and Application*. 1997: IEEE Press.
52. Doebelin, E.O., *Measurement Systems: Application and Design*. 5th ed. 2004, Boston: Mc Graw Hill Higher Education. 1061.
53. Meckes, R.A., G. Dorfinger, G. Wachutka. *Capacitive Silicon Microsensor for Force and Torque Measurement.* in *Transducers '00, The 11th International Conference on Solid-State Sensors and Actuators*. 2001. Munich, Germany.
54. Suster, M., Jun Guo, Nattapon Chaimanonart, Wen H. Ko, and Darrin J. Young, *A High-Performance MEMS Capacitive Strain Sensing System*. 2004, EECS Department, Case Western Reserve University: Cleveland.
55. FilancBowen, T.R., Geun Hyung Kim, and Yuri M. Shkel, *Novel Sensor Technology for Shear and Normal Strain Detection with Generalized Electrostriction.* IEEE, 2002. **0-7803-7454-1**: p. 1648-1653.
56. Pallas-Areny, J.G.W., *Sensors and Signal Conditioning.* 2nd ed. 2001, New York: John Wiley and Sons.

57. McLain, F., S.A. Yerby, and T.A. Moseley, *Comparative morphometry of L4 vertebrae: comparison of large animal models for the human lumbar spine.* Spine, 2002. **27**(8): p. E200-6.
58. Wilke, H.J., et al., *Anatomy of the sheep spine and its comparison to the human spine.* Anat Rec, 1997. **247**(4): p. 542-55.
59. Cotterill, P.C., et al., *An anatomical comparison of the human and bovine thoracolumbar spine.* J Orthop Res, 1986. **4**(3): p. 298-303.
60. Lebwohl, N.H., et al., *Biomechanical comparison of lumbosacral fixation techniques in a calf spine model.* Spine, 2002. **27**(21): p. 2312-20.
61. Minamide, A., *An experimental approach to spinal fusion using sintered bovine bone in a pig model.* J Spinal Disord, 2000. **13**(2): p. 156-64.
62. Swartz, D.E., et al., *Physical and mechanical properties of calf lumbosacral trabecular bone.* J Biomech, 1991. **24**(11): p. 1059-68.
63. Cavanaugh, J.M., et al., *Lumbar facet pain: biomechanics, neuroanatomy and neurophysiology.* J Biomech, 1996. **29**(9): p. 1117-29.
64. Erulkar, J.S., Jonathan Grauer, et. al., *Flexibility Analysis of Posterolateral Fusions in a New Zealand White Rabbit Model.* Spine, 2001. **26**(10): p. 1125-1130.
65. Xue, M., *[In vivo radiotelemetric study of strain on the rabbit mandible].* Zhonghua Kou Qiang Yi Xue Za Zhi, 1990. **25**(1): p. 27-8, 61-2.
66. Rohlmann, A., et al., *2000 Volvo Award winner in biomechanical studies: Monitoring in vivo implant loads with a telemeterized internal spinal fixation device.* Spine, 2000. **25**(23): p. 2981-6.
67. Wilke, H.J., et al., *New in vivo measurements of pressures in the intervertebral disc in daily life.* Spine, 1999. **24**(8): p. 755-62.
68. Abe, E., et al., *The effect of spinal instrumentation on lumbar intradiscal pressure.* Tohoku J Exp Med, 1999. **187**(3): p. 237-47.
69. Bay, B.K., et al., *Measurement of strain distributions within vertebral body sections by texture correlation.* Spine, 1999. **24**(1): p. 10-7.
70. Buttermann, G.R., et al., *An experimental method for measuring force on the spinal facet joint: description and application of the method.* J Biomech Eng, 1991. **113**(4): p. 375-86.
71. Cao, K.D., M.J. Grimm, and K.H. Yang, *Load sharing within a human lumbar vertebral body using the finite element method.* Spine, 2001. **26**(12): p. E253-60.
72. Chosa, E., et al., *Analysis of the effect of lumbar spine fusion on the superior adjacent intervertebral disk in the presence of disk degeneration, using the three-dimensional finite element method.* J Spinal Disord, 2004. **17**(2): p. 134-9.
73. Gedalia, U., et al., *Biomechanics of increased exposure to lumbar injury caused by cyclic loading. Part 2. Recovery of reflexive muscular stability with rest.* Spine, 1999. **24**(23): p. 2461-7.
74. Kobayashi, K., et al., *Healing of full-thickness tears of avian supracoracoid tendons: in situ hybridization of alpha1(I) and alpha1(III) procollagen mRNA.* J Orthop Res, 2001. **19**(5): p. 862-8.
75. Natarajan, R.N. and G.B. Andersson, *The influence of lumbar disc height and cross-sectional area on the mechanical response of the disc to physiologic loading.* Spine, 1999. **24**(18): p. 1873-81.

76. Yerby, S.A., J.R. Ehteshami, and R.F. McLain, *Loading of pedicle screws within the vertebra.* J Biomech, 1997. **30**(9): p. 951-4.
77. Kawaguchi, Y., H. Matsui, and H. Tsuji, *Back muscle injury after posterior lumbar spine surgery. Part 1: Histologic and histochemical analyses in rats.* Spine, 1994. **19**(22): p. 2590-7.
78. Solomonow, M., et al., *Neuromuscular disorders associated with static lumbar flexion: a feline model.* J Electromyogr Kinesiol, 2002. **12**(2): p. 81-90.
79. Kong, W.Z., V.K. Goel, and L.G. Gilbertson, *Prediction of biomechanical parameters in the lumbar spine during static sagittal plane lifting.* J Biomech Eng, 1998. **120**(2): p. 273-80.
80. Lim, T.H., et al., *Effect of endplate conditions and bone mineral density on the compressive strength of the graft-endplate interface in anterior cervical spine fusion.* Spine, 2001. **26**(8): p. 951-6.
81. Ledet, E.H., et al., *Real-time in vivo loading in the lumbar spine: part 1. Interbody implant: load cell design and preliminary results.* Spine, 2000. **25**(20): p. 2595-600.
82. Lieber, R.L., *Skeletal Muscle, Structure, Function, & Plasticity: The Physiological Basis of Rehabilitation*. 2nd ed. 2002, Baltimore: Lippincott, Williams, & Wilkins. 342.
83. Garrett, W.E., Jr., et al., *Recovery of skeletal muscle after laceration and repair.* J Hand Surg [Am], 1984. **9**(5): p. 683-92.
84. Lehto, M.U. and M.J. Jarvinen, *Muscle injuries, their healing process and treatment.* Ann Chir Gynaecol, 1991. **80**(2): p. 102-8.
85. Urabe, T., *[An experimental study on recovery of lacerated muscles after repair]*. Nippon Seikeigeka Gakkai Zasshi, 1988. **62**(4): p. 415-25.
86. Gejo, R., et al., *Magnetic resonance imaging and histologic evidence of postoperative back muscle injury in rats.* Spine, 2000. **25**(8): p. 941-6.
87. Buckwalter, J.A., *Activity vs. rest in the treatment of bone, soft tissue and joint injuries.* Iowa Orthop J, 1995. **15**: p. 29-42.
88. Alba, C.D. and P. LaStayo, *Postoperative management of functionally restrictive muscular adherence, a corollary to surgical tenolysis: a case report.* J Hand Ther, 2001. **14**(1): p. 43-50.
89. Menetrey, J., et al., *Suturing versus immobilization of a muscle laceration. A morphological and functional study in a mouse model.* Am J Sports Med, 1999. **27**(2): p. 222-9.
90. Edgerton, V.R., et al., *Adaptations in skeletal muscle disuse or decreased-use atrophy.* Am J Phys Med Rehabil, 2002. **81**(11 Suppl): p. S127-47.
91. Phillips, L.G. and J.P. Heggers, *Layered closure of lacerations.* Postgrad Med, 1988. **83**(8): p. 142-8.
92. Chien, S.H., et al., *[Repair method and healing of skeletal muscle injury]*. Gaoxiong Yi Xue Ke Xue Za Zhi, 1991. **7**(9): p. 481-8.
93. Proske, U. and D.L. Morgan, *Muscle damage from eccentric exercise: mechanism, mechanical signs, adaptation and clinical applications.* J Physiol, 2001. **537**(Pt 2): p. 333-45.
94. Morgan, D.L. and U. Proske, *Popping sarcomere hypothesis explains stretch-induced muscle damage.* Clin Exp Pharmacol Physiol, 2004. **31**(8): p. 541-5.

95. Ferguson, S.A., W.S. Marras, and T.R. Waters, *Quantification of back motion during asymmetric lifting.* Ergonomics, 1992. **35**(7-8): p. 845-5.
96. Ferguson, S.A., W.S. Marras, and P. Gupta, *Longitudinal quantitative measures of the natural course of low back pain recovery.* Spine, 2000. **25**(15): p. 1950-6.
97. Ferguson, S.A., et al., *Spinal loading when lifting from industrial storage bins.* Ergonomics, 2002. **45**(6): p. 399-414.
98. Ferguson, S.A.a.W.S.M., *Revised protocol for the kinematic assessment of impairment.* Spine J, 2004. **4**(2): p. 163-9.
99. Marras, W.S., et al., *The classification of anatomic- and symptom-based low back disorders using motion measure models.* Spine, 1995. **20**(23): p. 2531-46.
100. Marras, W.S., et al., *The quantification of low back disorder using motion measures. Methodology and validation.* Spine, 1999. **24**(20): p. 2091-100.
101. Marras, W.S., et al., *Impairment magnification during dynamic trunk motions.* Spine, 2000. **25**(5): p. 587-95.
102. Marras, W.S., et al., *Spine loading characteristics of patients with low back pain compared with asymptomatic individuals.* Spine, 2001. **26**(23): p. 2566-74.
103. Marras, W.S., et al., *Spine loading in patients with low back pain during asymmetric lifting exertions.* Spine J, 2004. **4**(1): p. 64-75.
104. Mayer, T., *Comparison of CT scan muscle measurements and isokinetic trunk strength in postoperative patients.* Spine, 1989. **14**(1): p. 33-6.
105. Cholewicki, J. and J.J.t. VanVliet, *Relative contribution of trunk muscles to the stability of the lumbar spine during isometric exertions.* Clin Biomech (Bristol, Avon), 2002. **17**(2): p. 99-105.
106. Gracovetsky, S., *Function of the spine.* J Biomed Eng, 1986. **8**(3): p. 217-23.
107. Kong, W.Z., et al., *Effects of muscle dysfunction on lumbar spine mechanics. A finite element study based on a two motion segments model.* Spine, 1996. **21**(19): p. 2197-206; discussion 2206-7.
108. Williams, M., et al., *Multifidus spasms elicited by prolonged lumbar flexion.* Spine, 2000. **25**(22): p. 2916-24.
109. Wisleder, D., et al., *A method to study lumbar spine response to axial compression during magnetic resonance imaging: technical note.* Spine, 2001. **26**(18): p. E416-20.
110. Ferguson, S.A., et al., *Predicting recovery using continuous low back pain outcome measures.* Spine J, 2001. **1**(1): p. 57-65.
111. Kovacs, K.M., et al., *Localized oxygen use of healthy and low back pain individuals during controlled trunk movements.* J Spinal Disord, 2001. **14**(2): p. 150-8.
112. Hamel, T., and Arms, *6,433,629 Micropower differential sensor measurement*. 2001: USA.
113. Beacon, L., and Wadey, *5,935,086 Orthopaedic measurement and display system*. 1999.
114. Durdle, L., Raso, and Hill, *5,995,879 Method and device for monitoring the relative position of at least two freely movable points and provide feedback therefrom*. 1999.
115. Porat, P., and Doron, *6,432,050 Implantable acoustic bio-sensing system and method*. 2002.

116. Raffius, P., and Sonnenschein, *6,223,138 Carrier frequency measurement method and apparatus*. 2001.
117. Valdevit, K., Elster, and El-Said, *20020050174 (Patent Application) Displacement transducer*. 2001.
118. Townsend, C.P.a.S.W.A., *US 2002/0024450 A1 Data Collection and Storage Device. United States Patent Application Publication*. 2002.
119. Hnat, W.P., John F. Naber, and Kevin M. Walsh, *2004/001137 (Patent Application) Strain Sensing System*. 2004.
120. Kanayama, M., et al., *Does spinal instrumentation influence the healing process of posterolateral spinal fusion? An in vivo animal model.* Spine, 1999. **24**(11): p. 1058-65.
121. Yerby, S.A., et al., *The effect of boundary conditions on experimentally measured trabecular strain in the thoracic spine.* J Biomech, 1998. **31**(10): p. 891-7.
122. Kepner_Tregoe, *KT Analysis* www.kepner-tregoe.com.
123. Kinget, P.M.H., *Integrated GHz Voltage Controlled Oscillators*, Bell Labs-Lucent Technologies. p. 1-29.
124. Yao, J., *RF MEMS from a device prospective.* J. Micromech. Micoeng., 2000. **10**: p. R9-R38.
125. Bobrow, L.S., *Fundamentals of Electrical Engineering.* 2nd ed. 1996. 1163.
126. Snider, S., *FDA APPROVES NEW TYPE OF PACEMAKER* http://www.fda.gov/bbs/topics/ANSWERS/2001/ANS01108.html, in www.fda.gov. 2001.
127. (COMAR), I.C.o.M.a.R., *Human Exposure to Microwaves and Other Radio Frequency Electromagnetic Fields*, in *IEEE Engineering in Medicine and Biology Magazine*. 1995. p. 336-337.
128. Lapin, G.D., *RF Safety and Amateur Radio* http://home.comcast.net/~glapin1/RFSafetyHam.html. 2002.
129. Vaughan, R., Simon Fraser University, *How much will an RF signal will be antenuated traveling through water relative to the frequency (say 100MHz - 10 GHz)?*. http://www.science.ca/askascientist/viewquestion.php?qID=1767. 2004.
130. Joint_Automatic_Identification_Technology, *RFID Passive* http://www.eis.army.mil/AIT/technology/rfid_passive.asp. 2004.
131. W.C. Tang, T.H.N., R.T. Howe, *Laterally Driven Polysilicon Resonant Microstructures.* Sensors and Actuators, 1989. **20**: p. 25-32.
132. Howe, R.T., *Microelectronics--An Integrated Approach*. 1997.
133. Carr, J.J., *Sensors and Circuits*. 1993: PTR Prentice Hall, Inc.
134. Nobel_Prize_Organization, *History of the Integrated Circuit* http://nobelprize.org/physics/educational/integrated_circuit/history/.
135. www.mcelwee.net, *Properties of Various Materials* http://www.mcelwee.net/html/properties_of_various_material.html.
136. M.M. Marharbiz, M.B.C., R.T. Howe, R. Horowitz, A. P. Pisano. *Batch Micropackaging by Compression-Bonded Wafer-to-Wafer Transfer*. in *Micro Electro Mechanical Systems 12th IEEE International Conference*. 1999.